Functional Characterization of Nitrate Transporters in Maize

A thesis submitted for the degree of the Doctor of Philosophy

at

The University of Adelaide

Faculty of Sciences

School of Agriculture, Food and Wine

Submitted by

Zhengyu Wen

22nd July 2015

Table of Contents

List of Figures

List of Tables

I. Abstract

Nitrate is an essential nutrient for plant growth. Nitrate acquisition by roots and its intercellular translocation is mediated by nitrate permeable transport proteins. Nitrate transporters have been extensively studied in the model plant, *Arabidopsis thaliana*. Nitrate transporters belong to three protein families: NPF (Nitrate Transporter 1/Peptide Transporter), NRT2 (Nitrate Transporter 2) and CLC (Chloride Channel) (Miller et al., 2007; Wang et al., 2012). However, there is little known about how these proteins orchestrate nitrate transport in maize.

Four putative nitrate transporter genes (*ZmNPF6.4*, *ZmNPF6.5*, *ZmNPF6.6*, and *ZmNPF7.10*) were cloned from a maize root cDNA population. Preliminary localization studies using C-terminal YFP-fusions showed maize NPF proteins targeting to the plasma membrane, with the exception of ZmNPF7.10, where targeting could not be resolved. Gene expression studies indicated *ZmNPF6.6* was induced strongly in roots by nitrate. Its shoot expression was mostly absent. In contrast, *ZmNPF6.4* exhibited a constitutive expression pattern in both root and shoot tissues and was not sensitive to nitrate. Both ZmNPF6.5 and ZmNPF7.10 showed little expression in either root or shoot tissues.

Functional characterization studies were conducted on ZmNPF6.4 and ZmNPF6.6 as there was no nitrate transport activity measured with ZmNPF6.5 and ZmNPF7.10 using a preliminary screening experiment in *Xenopus laevis* oocytes. Combining electrophysiology and chemical flux analysis, ZmNPF6.4 was characterized as a pH-dependent, low-affinity, non-selective nitrate and chloride transporter. On the other hand, *ZmNPF6.6* encoded a pH-dependent, dual-affinity, nitrate specific transporter, which was also permeable to chloride in the absence of nitrate. The functional differences between ZmNPF6.4 and ZmNPF6.6 were explored using site-directed mutagenesis experiments. The “affinity switch” Thr101 within the nitrate transceptor, AtNPF6.3, is conserved in ZmNPF6.6

(Thr104) (Liu, 2003). However, mutating ZmNPF6.6:Thr104 to alanine or aspartate (dephosphorylation and phosphorylation mimics, respectively), did not transform the dual-affinity transporter into either a high- or low-affinity monophasic transporter. Instead, both HATS and, predominantly, the LATS activities of ZmNPF6.6 were repressed by both T104A and T104D mutations. The equivalent of the predicted nitrate-binding residue in AtNPF6.3 (His356) was investigated in ZmNPF6.4 and ZmNPF6.6. In ZmNPF6.4, a tyrosine residue (Tyr370) is present instead of a histidine. Replacement of Y370 with histidine (ZmNPF6.4:Y370H) conferred dual-affinity nitrate transport and enhanced nitrate specificity over chloride. However, replacing His362 in ZmNPF6.6 with Tyr362 made the transporter non-functional.

A preliminary analysis of the high-affinity nitrate transport system was conducted by functionally characterizing *ZmNRT2.1* and *ZmNRT3.1A*. The plasma membrane targeting of ZmNRT2.1 required the presence of ZmNRT3.1A. This was confirmed using a C-terminal fusion of NRT2.1 with YFP. Signal was only detected in onion epidermal cells that were co-transformed with both *ZmNRT2.1* and *ZmNRT3.1A*. Gene expression analysis identified both a N-starvation induced expression and a nitrate induced expression pattern for *ZmNRT2.1*. In contrast, *ZmNRT3.1A* exhibited a constitutive expression in both roots and shoots. When ZmNRT2.1 and ZmNRT3.1A were co-injected into *Xenopus laevis* oocytes, high-affinity nitrate transport activity was measured. Single injections of either cRNA failed to elicit a nitrate transport phenotype.

II. Declaration

I certify that this work contains no material which has been accepted for the award of any other degree or diploma in my name, in any university or other tertiary institution and, to the best of my knowledge and belief, contains no material previously published or written by another person, except where due reference has been made in the text. In addition, I certify that no part of this work will, in the future, be used in a submission in my name, for any other degree or diploma in any university or other tertiary institution without the prior approval of the University of Adelaide and where applicable, any partner institution responsible for the joint-award of this degree.

I give consent to this copy of my thesis, when deposited in the University Library, being made available for loan and photocopying, subject to the provisions of the Copyright Act 1968.

I also give permission for the digital version of my thesis to be made available on the web, via the University's digital research repository, the Library Search and also through web search engines, unless permission has been granted by the University to restrict access for a period of time.

Signature:_____

Zhengyu Wen

III. Acknowledgements

Finally, I am at the very end of my PhD journey. When I look back, I see a path full of joy and happiness blended with sorrow and sadness. It was not an easy way and I do not think I can make this far without help from people around me. Therefore, I would like to sincerely acknowledge them here.

Without a doubt, I must firstly acknowledge my supervisors, Assoc Prof. Brent Kaiser and Prof. Stephen Tyerman. In particular, I am very appreciated to Brent for securing me an Australian Postgraduate Award (Industry) and a full fee scholar scholarship from the University of Adelaide. I'm also grateful for his guidance, advice, encouragement and support during my bumpy PhD journey, which also makes him a good friend to me. For Steve, I feel so lucky to be one of his students and to get an opportunity to learn from him. He helped me with a better understanding of the complicated electrophysiology. I cannot thank my great supervisors enough but quoting a line from *The Dark Knight Rises* (Nolan, 2012) "A hero can be anyone. Even a man doing something as simple and reassuring as putting a coat around a young boy's shoulders to let him know that the world hadn't ended.". I felt the exactly same way in that cold rainy night back to July 2011, when I first met Brent and Steve in a science event in Lirra Lirra. It has been very empowering and life-changing. They have also set for me an excellent role model as hard-working and enthusiastic scientists. In many respects, Brent and Steve have inspired me like the Dark Knight influenced Robin.

I would also like to thank those who ever helped me during research. I would like to thank Professor Diane Mather for showing me a possible PhD pathway and introducing me to my supervisors. Dr. Julie Dechorgnat and Karen Francis, you are my Lucius Fox and Alfred Pennyworth. Thank you for the help with all the trivial things about my research. I would like to say thank you to Nenah MacKenzie for running the IRMS for my endless samples. I must thank Wendy Sullivan, Dr. Sunita

Ramesh and Dr. Manchun Zhao for providing me *Xenopus* oocytes and useful tips about voltage clamping technique. I would also like to recognize Dr. Bo Xu, Dr. Sam Henderson, Dr. Nannan Yang, Dr. Serik Eliby and the late Dr. Ainur Ismagul for helping me with YFP-fusion analysis and onion transformation. Additionally, I really appreciate all the friendly support from Apriadi Situmorang, Jonathan Alan Wignes, Dr. Evgenia Ovchinnikova, Yue Qu and Jiaen Qiu.

I would also like to acknowledge my family, especially my two grandmas for financially supporting my first year overseas study. I wish you were able to be in my graduation ceremony.

I would like tell my lovely wife “Butterfly”, thank you for being with me through the ups and downs of my PhD study. I don’t have the words to tell you how grateful I am for what you have sacrificed to support me. I am so lucky to have you in my life, and you know I will do the same thing to support you always and forever. Honey, if I could choose again, I would stay in Adelaide and let you pursue your career. For that, I am forever indebted to you.

In the end, I would like to acknowledge the generous support that I have received through scholarships from the University of Adelaide and DuPont Pioneer.

IV. Abbreviations

~	Approximately
3'	Three prime of nucleic acid sequence
ABA	Abscisic acid
BLAST	Basic Local Alignment Search Tool
C-terminal	Carboxyl terminal
CBL	Calcineurin B-like molecule
cDNA	Complementary deoxyribonucleic acid
cHATS	Constitutive HATS
CIPK	CBL interacting protein kinase
cLATS	Constitutive LATS
CLC	Chloride Channel
cm	Centimeter
CRISPR	Clustered regularly interspaced short palindromic repeats
cRNA	Capped RNA
Ct	Threshold cycle
DNA	Deoxyribonucleic acid
DW	Dry weight
ECFP	Enhanced Cyan Fluorescent Protein
g	Grams
GOGAT	Glutamate-oxoglutarate aminotransferase
GS	Glutamine synthetase

h	Hour
HATS	High-affinity transport system
HEPES	4-(2-Hydroxyethyl)piperazine-1-ethanesulfonic acid
iHATS	Inducible HATS
iLATS	Inducible LATS
IRMS	Isotope Ratio Mass Spectrometer
kg	kilogram
LATS	Low-affinity transport system
M	Molar
MES	2-(N-Morpholino) ethanesulfonic acid, 4-morpholineethanesulfonic acid
MFS	Major Facilitator
mg	Milligram
Min	Minute
mM	Millimolar
mmol	millimole
mRNA	messenger RNA
N	Nitrogen
NPF	Nitrate Transporter 1/Peptide Transporter
NRT	Nitrate Transporter
NUE	Nitrogen Use Efficiency
NUtE	Nitrogen Utilization Efficiency
PCR	Polymerase Chain Reaction

qPCR	Quantitative PCR
RNA	Ribonucleic acid
RNaseA	Ribonuclease A
SDS	Sodium Dodecyl Sulphate
SEM	Standard error of the mean
TALENs	Transcription activator-like effector nucleases
TM	Transmembrane Domain
UTR	Untranslated region
v/v	volume/volume
w/v	weight/volume
YFP	Yellow Fluorescent Protein
ZFNs	Zinc finger nucleases
µM	Micromolar
µmol	Micromole

Chapter 1: Literature Review

Nitrate Transporters in *Arabidopsis thaliana*: What may Lie ahead for Maize?

1.1 Introduction

Nitrate is the major nitrogen source for plants growing in warm, pH neutral aerobic soils. These soil environments facilitate microbial nitrification, which is a process converting urea and ammonia rapidly into nitrate. Nitrate can either accumulate in the soil solution, be accessed by plant and microbial organisms as a source of exogenous nitrogen or dissipate through leaching or volatilization (Glass, 2009). The 'plant nitrate journey' begins with its uptake from the soil solution by plant roots and root hairs. Once inside the plant, the bulk of absorbed nitrate will be assimilated, a process involving the reduction of nitrate to nitrite and then nitrite to ammonium by the enzymes, nitrate reductase and nitrite reductase, respectively. Generated ammonium is then assimilated by the GS/GOGAT (glutamine synthetase/glutamate-oxoglutarate aminotransferase) pathway into glutamine/glutamate, which serve as substrates for the synthesis of amino acids (Tischner and Kaiser, 2007). Apart from its nutritional value, nitrate and its derivatives can function in cellular osmoregulation (through storage in the vacuole), signaling pathways and a range of primary stress responses (Guo et al., 2003; Little et al., 2005; Chopin et al., 2007; Ho et al., 2009; Chen et al., 2012).

Nitrate uptake and assimilation takes place across a range of different organs and cellular locations across the plant. As nitrate is a negatively charged anion, its transport across hydrophobic cellular membranes will require nitrate permeable transport proteins (Glass, 2009; Dechorgnat et al., 2011). In higher plants, known

nitrate transporters (NRTs) belong to three different protein families, including NPF family (Nitrate Transporter 1/Peptide Transporter), NRT2 family (Nitrate Transporter 2) and CLC family (Chloride Channel). Significant advances have been made in understanding their role in plant nitrogen metabolism using the model plant system, *Arabidopsis thaliana.* Unfortunately, similar scope and understanding is limited in maize and other agriculturally important crop species.

Zea mays L. (maize), is a cereal crop predominantly cultivated in aerobic soils where nitrate is often the main nitrogen source available for growth. In general, maize production relies heavily on nitrogen fertilizer inputs to ensure growth and economic yields. This dependency of maize on nitrogen fertilizer inputs has been estimated at 10 million tons per annum globally (Moose and Below, 2009), a quantity required to meet the rapid expansion (30 to 165 million hectares) of planted maize over the last decade (FAO, 2012). Unfortunately like many cereal crops, maize has low NUE (Nitrogen Use Efficiency) where only 25-50% of applied nitrogen is actually being used by the crop (Moose and Below, 2009). This results in a significant amount of nitrogen fertilizer that is either lost to the environment or poorly utilized for its intended purpose. Loss of nitrogen to the environment can cause many negative impacts, some of which lead to eutrophication of water systems, increased emissions of nitrous oxide (a potent greenhouse gas), and the pollution of ground water used for human consumption (Ramos, 1996; Stulen et al., 1998; Giles, 2005). In addition, the price of nitrogen fertilizer continues to increase over the last three decades (USDA, 2012) directly resulting from the increasing cost of non-renewable fossil fuels, natural gas and petroleum, which are used as the main energy provider in the manufacture of nitrogen fertilizers. Even though maize is used to feed a large proportion of the worlds population, especially in sub-Saharan Africa and Latin America (more than 1.2 billion people) (IITA, 2009), the huge environmental and economical impact caused by maize production cannot be neglected. Improving maize NUE, linked to an appropriate

nitrogen fertilizer practice, will be an important platform in which to achieve greater sustainability for future agricultural practices.

This review aims to discuss recent studies on nitrate transport proteins with a focus on the model plant, *Arabidopsis thaliana*. The notable research gap in this field between Arabidopsis and maize, as well as other agriculturally important plant species, will be demonstrated.

1.2 Nitrate Acquisition

1.2.1 Nitrate uptake systems

Nitrate is a water soluble anion. In soil, nitrate heterogeneity (spatial and concentration) can be very high, varying by 2-3 orders of magnitude within the rhizosphere and across the soil profile (Jackson and Caldwell, 1993). In order to cope with such fluctuating soil environments, plants have evolved with two nitrate uptake systems, the high-affinity transport system (HATS) and the low-affinity transport system (LATS). Both systems contain inducible and constitutive components (Glass, 2009; Wang et al., 2012). Physiological studies indicate that the inducible HATS (iHATS) and the constitutive HATS (cHATS) are responsible for nitrate acquisition of plants at low external nitrate concentrations, typically below 25 μM, following a saturable pattern, with Km/Vmax values ranging between 6~20 μM/0.3~0.82 μmol g DW h^{-1} and 20~100 μM/3~8 μmol g DW h^{-1} (in Arabidopsis roots), respectively (Crawford and Glass, 1998). The only difference between iHATS and cHATS is that the former system requires prior exposure to external nitrate (hours or days) for induction, while the cHATS is constitutively active. The LATS functions at nitrate concentrations above 0.25 mM (up to 50 mM) and follows a linear nonsaturable transport pattern (Crawford and Glass, 1998). Unlike HATSs, LATS can either be constitutive or inducible, depending on the species of plant and the external provision of nitrate (Siddiqi et al., 1990; Tsay et al., 1993). The concentration boundary between the HATS and LATS systems can be variable,

which indicates that the nitrate uptake across a wide concentration range most likely involves multiple systems and or dual-affinity systems that operate at both low and high concentrations.

1.2.2 LATS nitrate uptake and AtNPF6.3, AtNPF4.6

The first plant nitrate transporter identified is AtNPF6.3 (also known as AtNRT1.1 or CHL1) (Tsay et al., 1993). AtNPF6.3 belongs to the NPF family, along with another 52 NPF members in Arabidopsis (Léran et al., 2014). It was firstly identified through a screen of Arabidopsis T-DNA mutants for plants displaying resistance (growth) to chlorate, a herbicide and a nitrate analog (Tsay et al., 1993). Using the *Xenopus laevis* oocyte expression system, AtNPF6.3 was characterized as a pH-dependent (proton-coupled) nitrate transporter, which is a common characteristic shared by most of the NPF members (Tsay et al., 1993; Crawford and Glass, 1998). A follow up study demonstrated that *AtNPF6.3* is expressed in the epidermis of the root tip, cortical and endodermal cells of mature roots and loss of AtNPF6.3 activity impaired the LATS nitrate uptake by ~50% (Huang et al., 1996). While most nitrate transporters from the NPF family are low-affinity nitrate transporters, AtNPF6.3 is an exception as it behaves as a dual-affinity nitrate transporter with a *K*m of ~50 μM in the high-affinity region and a second *K*m of ~4 mM in low-affinity region (Liu et al., 1999). However, this does not necessarily mean that AtNPF6.3 is also a main contributor in HATS nitrate uptake (reviewed by Glass and Kotur, 2013). It is believed that the affinity switch of AtNPF6.3 is regulated by the phosphorylation of the amino acid residue threonine 101 (Liu, 2003; Ho et al., 2009). Under low nitrate concentrations, a CBL-interacting protein kinase, CIPK23, phosphorylates the Thr101 of AtNPF6.3 allowing the transporter to function as a high-affinity nitrate transporter. Under high nitrate concentrations, AtNPF6.3 serves as a low-affinity nitrate transporter without T101 phosphorylation.

Recently, two structural biology studies further examined this functionality of this affinity switch residue (Parker and Newstead, 2014; Sun et al., 2014). Sun et al. suggested that the phosphorylation-controlled dimerization is the key of the affinity switch of AtNPF6.3, while Parker et al. suggested that the different nitrate transport rate is because of the changing structural flexibility of the transporter caused by the phosphorylation of Thr101 (Parker and Newstead, 2014; Sun et al., 2014). Besides being a nitrate transporter, AtNPF6.3 is also a nitrate sensor, regulating gene expression in the primary nitrate response that initiates lateral root elongation towards nitrate-rich patches (Remans et al., 2006; Ho et al., 2009). It has been reported that the root morphology regulation mediated by AtNPF6.3 could be attributed to its auxin transport activity (Krouk et al., 2010). *AtNPF6.3* expression has also been found in leaf guard cells and nascent organs, controlling the stomatal opening and proper nascent organ development (Guo et al., 2001; Guo et al., 2003).

The second nitrate transporter that participates in LATS nitrate uptake in Arabidopsis is AtNPF4.6 (also known as AtNRT1.2 or AtAIT1). In an Arabidopsis *AtNPF4.6* knockdown mutant, there was ~ 40% reduction in LATS nitrate uptake (Huang et al., 1999). Given the constitutive expression pattern in root epidermal and root hair cells, AtNPF4.6 is considered to be the constitutive component of LATS nitrate uptake (Huang et al., 1999). However, a recent study reported a much broader expression pattern of *AtNPF4.6*, including imbibed seeds, vascular tissues of cotyledons, true leaves, hypocotyls, roots, inflorescence stems (Kanno et al., 2012). In Kanno et al study, AtNPF4.6 was suggested to be an abscisic acid (ABA) transporter, rather than a nitrate transporter, as it displays ~10^4 times higher affinity to ABA than to nitrate. A putative function of AtNPF4.6 may be controlling stomatal opening, since lower inflorescence stem surface temperature was observed in an *AtNRT1.2*-mutant plant, possibly due to the excess water loss from poorly regulated open stomata.

1.2.3 HATS nitrate uptake and AtNRT2.1, AtNRT2.2, AtNRT2.3, AtNRT3.1

In Arabidopsis, there are three NRT2 family members (total 7 members) responsible for the HATS nitrate uptake, AtNRT2.1, AtNRT2.2 and AtNRT2.4 (Tsay et al., 2007; Glass, 2009). Physiological studies on *atnrt2.1* mutant plant revealed that AtNRT2.1 contributes up to 72% of the iHATS nitrate uptake in Arabidopsis (Filleur et al., 2001; Li et al., 2007). Promoter GUS/GFP analysis indicates AtNRT2.1 is localized to the plasma membrane and expressed in epidermal, cortical and endodermal cells of mature roots (Nazoa et al., 2003; Wirth et al., 2007). It has been suggested that *AtNRT2.1* expression can be induced by low concentrations of nitrate (200 μM) and down regulated by high nitrate concentrations (10 mM) (Nazoa et al., 2003). However, by measuring protein abundance using an ELISA-based assay, Wirth et al. (2007) reported that the NRT2.1 protein is relatively stable and abundant, regardless of nitrate treatment. This result suggested that the expression of *AtNRT2.1* might also be regulated post-translationally. In addition, AtNRT2.1 has also been suggested to be a nitrate sensor in its own right, repressing lateral root initiation under low nitrate conditions (Little et al., 2005).

AtNRT2.2 is another nitrate transporter that mediates nitrate uptake in the HATS region. Unlike AtNRT2.1, AtNRT2.2 appears to play a supporting role, contributing only 19% of the iHATS component (Li et al., 2007). However, when *AtNRT2.1* is absent, *AtNRT2.2* is up regulated ~3-fold to partially compensate the HATS nitrate uptake loss (Li et al., 2007).

While both AtNRT2.1 and AtNRT2.2 are nitrate inducible transporters, the third HATS contributor, AtNRT2.4, is down regulated by nitrate and up regulated by nitrate starvation (Kiba et al., 2012). The localization of AtNRT2.4 protein is also very unique, as its located in the external (abaxial) membrane of the epidermal cells facing the nutrient solution in lateral root (Kiba et al., 2012). The physiological function of AtNRT2.4 was suggested to be nitrate acquisition under

low nitrate conditions, and this function can only be revealed when AtNRT2.1 and AtNRT2.2 are absent (Kiba et al., 2012). Furthermore, *AtNRT2.4* was also found expressed in the phloem of Arabidopsis leaves and the shoot phloem nitrate content of the nitrate starved *atnrt2.4* mutant plant was lower than the wild type, suggesting that AtNRT2.4 may also involved in leaf nitrate remobilization during nitrate starvation (Kiba et al., 2012).

The functional activity of NRT2 transporters requires a group of membrane ancillary proteins, NRT3s (also known as NAR2). This NRT2/NRT3 high-affinity nitrate transport system is firstly suggested by (Quesada et al., 1994) where nitrate non-utilizing phenotype could only be rescued when two genes (*nar-2/nar-3* or *nar-2/nar-4*) were co-expressed in a mutant *Chlamydomonas reinhardtii* strain. Then it has been suggested that NRT3 proteins can form a dimer with NRT2 transporters and help target the transporter dimer to the plasma membrane (Wirth et al., 2007; Kotur et al., 2012). In Arabidopsis, there are two NRT3 proteins, AtNRT3.1 and AtNRT3.2 (Tsay et al., 2007). The former is believed to play the major role in the HATS nitrate uptake, since its transcript accounts for 99% of *NRT3* mRNA found in roots and loss of AtNRT3.1 reduces cHATS by 89% and iHATS 96%, respectively (Okamoto et al., 2006). Beside Arabidopsis, this two-component high-affinity nitrate uptake system is conserved across different kingdoms and differences species, such as *Chlamydononas reinhardtii*, barley and rice (Quesada et al., 1994; Zhou et al., 2000). However, not all the NRT2 transporters require the assistance of NRT3s since AtNRT2.4, AtNRT2.7 and CRNA (a NRT2 homolog from *Emericella nidulans*) can transport nitrate without the expression of NRT3 proteins in *Xenopus laevis* oocytes (Zhou et al., 2000; Chopin et al., 2007; Kiba et al., 2012; Kotur et al., 2012).

1.2.4 Nitrate root exclusion and AtNPF2.7

The net nitrate acquisition of plants consists of two components: exogenous nitrate uptake and endogenous nitrate efflux. In Arabidopsis, endogenous nitrate

efflux is facilitated by a low-affinity NPF nitrate transporter, AtNPF2.7 (also known as NAXT1), in a proton-coupled manner. This is supported by physiological evidence using an *AtNPF2.7* knockout, which eliminated endogenous proton (acid load treatment using 10 mM K-propionate solution) induced nitrate efflux (Segonzac et al., 2007). Interestingly, the increased nitrate efflux in wild type *Arabidopsis* is associated with an increase in AtNPF2.7 protein abundance, but not transcript abundance, which suggested that *AtNPF2.7* is regulated at the posttranscriptional level. Like other NPF transporters, AtNPF2.7 is also a plasma membrane protein but is solely expressed in the cortex of mature roots.

1.3 Nitrate Translocation

1.3.1 Long-distance nitrate xylem transport and AtNPF7.2, AtNPF7.3

Nitrate in root cells can be temporarily stored in the vacuole or alternatively be transferred to the shoot via the xylem for further assimilation or storage. The transfer of nitrate to the shoot is influenced by the casparian strip, which blocks the apoplastic pathway from delivering nitrate to the xylem. Instead, nitrate is exported using the symplastic pathway, where nitrate is loaded into xylem vessels through an efflux mechanism across the plasma membrane of pericycle cells within the stele. In Arabidopsis, nitrate xylem loading is facilitated by the low-affinity nitrate transporter AtNPF7.3 (also known as AtNRT1.5) (Lin et al., 2008). AtNPF7.3 is localized to the plasma membrane of root pericycle cells next to xylem vessels. The expression of *AtNPF7.3* shows a delayed response to nitrate induction increasing only after an 8 h nitrate treatment (Lin et al., 2008). Using an *arnpf7.3* knockout mutant, the root-to-shoot nitrate transport was found to be impaired, resulting in reduced shoot nitrate content and increased root nitrate accumulation compared to the wild type controls (Lin et al., 2008). An interesting feature of AtNPF7.3 is that it is the first identified bi-directional nitrate transporter, which can mediate both nitrate influx and efflux in cRNA-injected oocytes (Lin et al., 2008).

Unloading of nitrate from the xylem is suggested to involve a member of the same sub-family of AtNPF7.3, AtNPF7.2 (also know as AtNRT1.8) (Li et al., 2010). AtNPF7.2 is localized in the plasma membrane of xylem parenchyma cells and the expression of *AtNPF7.2* is regulated by nitrate. Removal of AtNPF7.2 activity, disrupts nitrate unloading from the xylem, resulting in high nitrate concentrations in the xylem sap.

In addition to their roles in long-distance nitrate transport, AtNPF7.2 and AtNPF7.3 also respond to abiotic stress treatments, including drought, salt and cadmium (Li et al., 2010; Chen et al., 2012). Cadmium alters the expression of *AtNPF7.2* and *AtNPF7.3* in two opposite ways. The expression of *AtNPF7.2* in roots are significantly up regulated (~191-fold) by cadmium treatment, while the transcript abundance of *AtNPF7.3* decreases. This response also occurs with sodium application and under drought conditions (Li et al., 2010; Chen et al., 2012). The phenotypes of the knockout mutants of these two transporters are different. Loss of AtNPF7.2, plants become hypersensitive to cadmium stress, while loss of AtNPF7.2 increased the tolerance against cadmium, salt and drought stress (Li et al., 2010; Chen et al., 2012). This data suggests that for AtNPF7.3 and AtNPF7.2, xylem nitrate loading and unloading may only be one of their many activities in plants.

1.3.2 Phloem nitrate transport and AtNPF2.9

AtNPF2.9 has been shown to be involved in the loading of nitrate into the phloem for basipetal nitrate transport to the root tip (Wang and Tsay, 2011). AtNPF2.9 is located on the plasma membrane of root companion cells. Its expression is not rapidly induced by nitrate, but does increase after long-term nitrate exposure. In the *atnpf2.9* knockout mutant, nitrate content of root phloem exudates was lower and shoot to root nitrate transport decreased. In contrast, root-to-shoot nitrate translocation was increased, resulting in higher shoot nitrate contents.

1.4 Nitrate Assimilation and Storage

1.4.1 Nitrate leaf storage and AtNPF6.2

In the shoot, nitrate is distributed to leaves for nitrate assimilation. The leaf petiole is considered to be a temporary storage site before assimilation in the leaf lamina. In *Arabidopsis*, leaf petiole nitrate homeostasis is controlled by a low-affinity nitrate transporter, AtNPF6.2 (also known as AtNRT1.4) (Chiu et al., 2004). The expression of *AtNPF6.2* is detected predominantly in the leaf petiole but this expression is not regulated by endogenous nitrate treatment. The *atnpf6.2* mutant shows reduced petiole nitrate content (by ~50%) and increased leaf lamina nitrate content (by ~113%) compared with wild type Arabidopsis. Additionally, the leaves of the mutant *atnpf6.2* were developmentally disrupted. This suggests leaf development is altered when AtNPF6.2 mediated leaf nitrate homeostasis is disrupted.

1.4.2 Vacuole nitrate storage and AtCLCa

Vacuole nitrate storage is a universal process that occurs across most plant tissues. It is important for maintaining nitrate homeostasis, generating turgor pressure and maintaining the steady state of cytosolic nitrate concentrations in individual cells (Miller and Smith, 2008). Before nitrate assimilation (and nitrate remobilization), 99% of the free nitrate is temporarily stored in the leaf vacuole (Martinoia et al., 1981). This process has been suggested to be facilitated by a nitrate transporter from the CLC family, AtCLCa (De Angeli et al., 2006). Different to the NPF nitrate transporters, AtCLCa is a two nitrate/one proton antiporter localized on the tonoplast membrane. The transporter activity of AtCLCa is supported by electrophysiological evidence that, by knocking out AtCLCa, the nitrate induced current across the tonoplast is eliminated (De Angeli et al., 2006). Other phenotypes of the *atclca* mutant, include low endogenous nitrate content, high nitrite content, reduced nitrate influx and down regulated expression of NRT

genes, suggesting nitrate vacuole storage and cell nitrate homeostasis is impaired without AtCLCa.

1.5 Nitrate Remobilization

1.5.1 Nitrate remobilization in senescent leaves and AtNPF1.1, AtNPF1.2, AtNPF2.13

During both vegetative and reproductive growth, stored nitrate can be remobilized from older tissues to younger developing leaves and seeds (Simpson and Lambers, 1983; Rossato et al., 2001; Schiltz et al., 2005). The molecular basis of leaf nitrate remobilization in Arabidopsis has been suggested to involve AtNPF1.1, AtNPF1.2 and AtNPF2.13 (also known as AtNRT1.11, AtNRT1.12 and AtNRT1.7, respectively) (Fan et al., 2009; Hsu and Tsay, 2013). AtNPF2.13 has been identified as a low-affinity nitrate transporter expressed in the phloem of the minor veins of leaves. Its expression level is higher in older leaves than in younger leaves. Furthermore, in each leaf, the distal part of the leaf possesses higher *AtNPF2.13* expression levels than the proximal leaf and the petiole. In an *atnpf2.13* mutant, there were reduced nitrate content in phloem exudates of old leaves and impaired nitrate remobilization from old to young leaves.

Unlike AtNPF2.13, AtNPF1.1 and AtNPF1.2 are expressed in the companion cells of the major veins of old leaves where they are predicted to function as nitrate redistributor and remobilizers, respectively (Hsu and Tsay, 2013). AtNPF1.1 and AtNPF1.2 can both redirect root-derived nitrate to young leaves by transferring nitrate from the xylem to the phloem in older leaves. In the *atnpf1.1 atnpf1.2* double mutants, nitrate redistribution is impaired resulting in more nitrate being accumulated in older leaves rather than in nitrate demanding young leaves. During nitrate remobilization, it has been proposed there is crosstalk between AtNPF1.1/1.2 and AtNPF2.13 which allows AtNPF2.13 retrieved nitrate to be transferred from the minor veins to the major veins in young leaves (Hsu and Tsay, 2013).

1.5.2 Seed nitrate and AtNPF2.12, AtNPF5.5, AtNRT2.7

After being retrieved from old leaves, nitrate can also be transferred to developing seeds, where it is considered to be important for seed dormancy and early embryo development (Alboresi et al., 2005). Two NPF nitrate transporters have been suggested to be involved in nitrate seed accumulation, AtNPF2.12 (also known as AtNRT1.6) and AtNPF5.5 (Almagro et al., 2008; Léran et al., 2015). AtNPF1.6 is a low-affinity nitrate transporter exclusively expressed in the vascular tissue of the silique and funiculus and its expression increases immediately after the pollination. Loss AtNPF2.12 results in reduced seed nitrate content, higher seed abortion rate and abnormal embryo development compared with the wild type plant. AtNPF5.5 is also a low-affinity nitrate transporter and it is the first NPF transporters found expressed in the embryo (Xiang et al., 2011). Without AtNPF5.5, the embryos nitrogen content in knockout mutants is reduced by ~8% compared with wild type Arabidopsis (Léran et al., 2015).

One NRT2 member, AtNRT2.7, is also involved in nitrate seed accumulation (Chopin et al., 2007). Distinctive from the other plasma membrane nitrate transporters, the high-affinity nitrate transporter AtNRT2.7 is localized in the tonoplast and the expression of *AtNRT2.7* can only be detected in reproductive organs, especially in dried seeds. The *atnrt2.7* mutant plants show a lower seed nitrate content and delayed seed germination, up to 7 days compared with the wild type plants. Recently, another study has suggested that AtNRT2.7 is also involved in seeds proanthocyanidins accumulation and oxidation (David et al., 2014).

1.6 Identified Nitrate Transporter in Maize

Currently, two *AtNRT2.1* homologous genes, *ZmNRT2,1* and *ZmNRT2.2*, have been identified in maize (Quaggiotti et al., 2003; Trevisan et al., 2008). *ZmNRT2.1* is expressed in the root epidermis and cortex. Based on its expression level,

ZmNRT2.1 has been suggested to have a role in iHATS nitrate uptake. *ZmNRT2.2* is expressed in the endodermis near the xylem and the central cylinder. *ZmNRT2.2* expression shows a similar pattern with *AtNPF7.3* where expression is delayed after the induction by nitrate. This suggested that ZmNRT2.2 may be involved in xylem loading for root-to-shoot nitrate translocation. However, no evidence is available to directly support the transporter activity of ZmNRT2.1 or ZmNRT2.2. Functional characterization studies using heterologous expression system, such as *Xenopus* Oocyte or yeast, is still required.

1.7 Defining the Nitrate transport network in Maize

As discussed above, significant advances have been made in defining the molecular control of nitrate transport in the model plant *Arabidopsis thaliana* (Table 1.1). However, there are still major gaps in understanding how these transport systems work to support growth and their response to nitrogen supply or deficiency. For example, there is little data describing the functional properties (apart from transcriptional analysis and localization) of the majority of NRT2 transporters in Arabidopsis and for that matter any plant system including Maize. There is also little information about their coordination between plant organs and during developmental growth stages. It will be important to effectively transfer as much information to Maize from research obtained using Arabidopsis, although differences in plant structure and development as well as C and N metabolism will make this process challenging and complex. A recent phylogenetic study comparing dicot and monocot species demonstrated that maize genome contains a family of genes closely related to the NPF gene family in Arabidopsis (Plett et al., 2010). In contrast, there is a significant separation in the *NRT2* phylogenetic tree between maize and Arabidopsis. This result suggests that it may be possible to reliably predict the function of NPFs (NRT1s) but not NRT2s by sequence homology. Ultimately genetic analysis and functional evaluation of maize proteins will be required.

Central to this transition in technology will be to balance differences in how maize utilize nitrogen (a fast growing monocot) to that of Arabidopsis. For example, during reproductive growth, 50%~90% of maize leaf N, depending on the cultivar, will be remobilized for final grain production (Celine et al., 2001; Kichey et al., 2007), which means when applied with the same amount of N, a maize cultivar with high nitrogen utilization efficiency (NUtE) will accumulate more N in the grain and have higher yield than a low NUtE cultivar. Several Arabidopsis NPF nitrate transporters involved in leaf nitrate accumulation have been identified and characterized, such as AtNPF1.1, AtNPF1.2 and AtNPF2.13, who exhibit higher expression level exclusively in old leaves than in young leaves (Fan et al., 2009; Hsu and Tsay, 2013). In maize, NPF family members with similar expression patterns have been revealed by transcriptomic studies. Located to the bundle sheath cells in the leaf tip, three maize NPF genes, *ZmNPF6.8*, *ZmNPF8.13* and *ZmNPF8.14*, exhibit undetectable or low expressions until the end of the vegetative growth period but peaked during the grain filling stage (Provart et al., 2010; Sekhon et al., 2011). Therefore, a thorough understanding of these maize NPF genes will help to unravel the maize leaf nitrate accumulation / remobilization pathway, an important step to enhance maize NUE.

Some traits show similarity between maize and Arabidopsis. In maize, kernel number is highly responsive to N supply and yield (Moose and Below, 2009). Under N stress, some ovules on the ear cannot be pollinated while others, even though they are pollinated do not complete kernel development. Only ovules that are successfully fertilized with complete kernel development contribute to final kernel number. In Arabidopsis, the requirement of nitrate transporters for proper embryo development and seed nitrate accumulation has been well documented (Chopin et al., 2007; Almagro et al., 2008; Léran et al., 2015). These Arabidopsis studies provide a potential clue to what may occur in maize and the possible transporters that impact upon yield. Indeed, two maize NPF genes, ZmNPF4.10 and ZmNPF7.12, were found exclusively expressed in the embryo, the endosperm and

the germinating seeds in maize (Sekhon et al., 2011). It is possible that they function as nitrate accumulators during maize embryo development. In addition, ZmNPF4.10 is closely related to the nitrate/ABA (abscisic acid) transporter, AtNPF4.6, and it has been reported that embryonic ABA plays an important role in the induction and maintenance of seed dormancy (Kucera et al., 2005; Matilla et al., 2009). Therefore, ZmNPF4.10 may also regulate maize seed dormancy/germination while controlling the embryonic ABA content.

Maize is a C4 plant mainly growing in tropical or sub-tropical areas where often carbon from photosynthesis is not limited for nitrogen assimilation. In addition, the favorable carbon derived from C4 photosynthesis provides a great opportunity to increase nitrogen uptake without considering the feedback inhibition caused by excessive primary nitrogen assimilation products (Moose and Below, 2009). There is tremendous potential to improve maize NUE and final yield. However, there is a long way ahead for scientists to achieve this goal. Genes belonging to *NPF*, *NRT2* and *CLC* families require a thorough investigation to establish and fully understand the nitrate assimilation network that extends from root uptake to the shoot and eventually to the seeds. Although the nitrate transport network in the model plant Arabidopsis has been well established, considering the differences between dicot and monocot species and differences in C3 and C4 carbon metabolism and the inherent requirements for N, it is difficult to simply describe the function of any transporter based on orthologous sequence-based matches. Gene identification, characterization of expression, and functional activity of the encoded proteins are all required to properly define the nitrogen transport network in maize and other plant species.

Transporter	Other Names	AC Number	Affinity	Direction	Subcellular Localization	Expression Tissue	Expression pattern	Function	Reference
AtNPF1.1	AtNRT1.12	AT3G16180.1	Low -affinity, with Km of 7.2mM	Influx	Plasma membrane	Companion cells of the major vein	Increase expression as leaf aging	Redistributing nitrate to developing tissues	Hsu & Tsay 2013
AtNPF1.2	AtNRT1.11	AT1G52190.1	Low -affinity, with Km of 9.2mM	Influx	Plasma membrane	Companion cells of the major vein	Increase expression as leaf aging	Redistributing nitrate to developing tissues	Hsu & Tsay 2013
AtNPF2.12	AtNRT1.6	AT1G18880.1	Low -affinity, with Km of 6mM	Influx	Plasma membrane	vascular tissue of the silique and funiculus	Express after pollination	Delivering nitrate from maternal tissue to the developing embryo	Almagro, Lin & Tsay 2008
AtNPF2.13	AtNRT1.7	AT1G69870.1	Low -affinity, with Km of 2.8mM	Influx	Plasma membrane	phloem of the leaf minor vein	Increase expression as leaf aging	Remobilizing nitrate from older leaves	Fan et al. 2009
AtNPF2.7	AtNAXT1	AT1G52190.1		Efflux	Plasma membrane	Root cortex	Constitutive, but regulate at posttranscriptional level by medium acidification	Excrete nitrate from plant	Segonzac et al. 2007
AtNPF2.9	AtNRT1.9	AT1G18880.1	Low -affinity, with Km of 7mM	Influx	Plasma membrane	Root phloem companion cells	Induce by long term nitrate exposure	Loading nitrate into root phloem and enhance downward nitrate transport in root	Wang & Tsay 2011
AtNPF4.6	AtNRT1.2/ AIT1	AT1G69850.1	Low -affinity, with Km of 5.9mM	Influx	Plasma membrane	Root epidermis, imbibed seeds, cotyledons, leaves, hypocotyls and inflorescence stems	Constitutive	Nitrate uptake in root, transport ABA with a Km 5uM to ABA	Huang, NC et al. 1999; Kanno et al. 2012
AtNPF5.5		AT2G38100.1		Influx		Embryo		Involving in embryo N accumulation	Leran et al. 2015
AtNPF5.10		AT1G22540.1		Influx					Leran et al. 2015
AtNPF6.2	AtNRT1.4	AT1G69850.1	Low -affinity, with Km of 2.4mM	Influx		Petiole and midrib	Constitutive	Petiole and midrib nitrate storage	Chiu et al. 2004
AtNPF6.3	AtNRT1.1/ CHL1	AT1G69850.1	Dual-affinity, high affinity Km 50μM and low affinity Km 4mM	Influx/Efflux	Plasma membrane	Epidermis of root tip, cortex or endodermis of mature root, leaf stomatal guard cells	Induce by nitrate and switch affinity by T101 phosphorylation	Nitrate uptake in root, trigger root grow to N-rich patches, regulate primary nitrate response, regulate stomatal opening	Tsay et al. 1993; Huang, N et al. 1996; Liu, KH, Huang & Tsay 1999; Guo, Young & Crawford 2003;Ho et al. 2009; Krouk et al. 2010
AtNPF7.2	AtNRT1.8	AT1G69850.1	Low -affinity, with Km of 12mM	Influx	Plasma membrane	xylem parenchyma cells in stele	Induce by Cd2+ stress	Unload nitrate from xylem	Li, J-Y et al. 2010
AtNPF7.3	AtNRT1.5	AT1G69850.1	Low -affinity, with Km of 6mM	Influx/Efflux	Plasma membrane	Root pericycle cells	Induce by long term nitrate exposure	Nitrate xylem loading	Lin et al. 2008; Chen et al. 2012
AtNRT2.1		AT1G08090.1		Influx	Plasma membrane	Epidermal, cortical and endodermal cells of mature root	Induce by low nitrate and repress by high nitrate	Nitrate uptake by HATS and induce lateral root initiation in response to nutritional cues	Filleur et al. 2001; Nazoa et al. 2003; Little et al. 2005; Li, W et al. 2007; Wirth et al. 2007
AtNRT2.2		AT1G08100.1		Influx				Nitrate uptake by HATS and compensate AtNRT2.1 when it was knocked out	Li, W et al. 2007
AtNRT2.4		AT5G60770.1		Influx	Plasma membrane (outer face of root epidermis)	Lateral root epidermis, shoot phloem	Induce by nitrate starvation	Nitrate uptake in high-affinity range and deliver nitrate into phloem for remobilization during nitrate starvation	Kiba et al. 2012
AtNRT2.7		AT5G14570.1		Influx	Tonoplast	Reproductive organ and dry seeds		Accumulate nitrate in the seed and prevent seed dormancy, PA accumulation/oxidation	Chopin et al. 2007; David et al. 2014
AtCLCa		AT5G40890.1		Influx	Tonoplast			Accumulate nitrate in plant vacuoles	De Angeli et al. 2006; Monachello et al. 2009

Table 1.1 Characterized Arabidopsis Nitrate Transporters

Chapter 2: Identification and Cloning of NPF Nitrate Transporters in Maize

2.1 Introduction

NPF (NRT1) nitrate transporters are mainly considered low-affinity nitrate transporters with exception of the dual-affinity transporters AtNPF6.3 and MtNPF6.8. Common characteristics shared by all NPF nitrate transporters are a pH-dependent (proton-coupled) nitrate transport activity, nitrate affinity in the mM range and a plasma membrane localization (Tsay et al., 2007; Dechorgnat et al., 2011; Xu et al., 2012). NPF nitrate transporters also share structural homologies with 12 transmembrane domains (TM) and a long central hydrophilic loop between the 6th and the 7th TM spanning domains. These structural similarities are used as a basis in defining members of the NPF family (NRT1 & PTR FAMILY). In doing so, NPF has replaced the names of the following families: NRT1, POT (proton-coupled oligopeptide transporter), PTR (peptide transporter) and SLC15 (solute carrier 15) from bacteria, fungi and animals (Léran et al., 2014). Since the discovery of the first plant NPF nitrate transporter in 1993, 17 NPF nitrate transporters have been identified and characterized in Arabidopsis, rice and *Medicago*. In maize, there are 81 NPF proteins (Léran et al., 2014). Although extensively studied in model plants, little is known about the functional properties of the nitrate NPF transporters from maize.

With the full sequencing and annotation of the B73 maize genome, ten putative maize NPF nitrate transporters were originally identified using eight characterized Arabidopsis NPF transporters as phylogenetic templates (Plett et al., 2010). Recently, another five Arabidopsis NPF nitrate transporters as well as five nitrate transporters from other plant species have been cloned and studied for their

nitrate transport properties (Morère-Le Paven et al., 2011; Wang and Tsay, 2011; Hsu and Tsay, 2013; Léran et al., 2015). As these large protein families are dissected through combined bioinformatic, transcriptome and *in vitro* assays (Provart et al., 2010; Sekhon et al., 2011; Xiang et al., 2011; Downs et al., 2013; Eveland et al., 2014; Wang et al., 2014), it is clear that more maize NPF nitrate transporters will be identified in the future and will need to be defined for their role in nitrate transport in plants. In this chapter, I highlight the identification and cloning of selected maize NPF transporters.

2.2 Results

2.2.1 Identification of NPF nitrate transporters

To select candidate maize nitrate transporters for functional characterization, BLAST searches were conducted using NPF nitrate transporters from Arabidopsis, Rice, Medicago, *Brassica campestris* and *Brassica napus* as query sequences against maize B73 genome. By setting the sequence identity threshold at 40% and sequence length threshold at 500, the number of putative NPF nitrate transporters was narrowed down from total 81 to 36. Another 7 NPFs were eliminated due to undetectable or extremely low expression of their coding sequences (Winter et al., 2007; Sekhon et al., 2011). Details of the 29 putative maize NPF nitrate transporters are listed in Table 2.1.

Phylogenetic relationships of 17 characterized NPF nitrate transporters and putative maize NPF nitrate transporters were analyzed based on amino acid differences (Figure 2.1). As expected, NPFs from the same sub-families are divided into the same clusters as shown in Léran et al's (2014) phylogenetic study, except AtNPF5.5 and ZmNPF7.4. The former forms a distinct branch far away from other NPF5s and the latter joins in the NPF8 cluster.

2.2.2 Molecular cloning of selected NPF nitrate transporters

In the beginning of the candidature, I was interested in two aspects of the maize nitrate assimilation pathway: 1) nitrate root uptake and 2) root-to-shoot nitrate translocation. As reviewed in Chapter 1, AtNPF6.3 plays a pivotal role in nitrate root acquisition/signaling and AtNPF7.2/7.3 regulates long distance nitrate translocation through xylem nitrate loading/unloading (Tsay et al., 1993; Lin et al., 2008; Ho et al., 2009; Li et al., 2010). Therefore three maize *AtNPF6.3* homologous, *ZmNPF6.4/6.5/6.6*, and one maize *AtNPF7.2/7.3* homolog, *ZmNPF7.10*, were chosen as four candidate genes to begin my research.

ZmNPF6.4 (GRMZM2G086496_T01), *ZmNPF6.5* (GRMZM2G161483_T01) and *ZmNPF6.6* (GRMZM2G161459_T02) full-length cDNA were cloned using high fidelity RT-PCR based on the sequence information from the MaizeSequence.org database (PCR primers are listed in Table 2.2). Genomic regions of both *ZmNPF6.4* and *ZmNPF6.6* are predicted to contain four exons and three introns, encoding proteins with 608 and 595 amino acids, respectively. The genomic DNA region encoding ZmNPF6.5 contains three exons and two introns encoding a putative protein of 600 amino acids. Although *ZmNPF6.6* can be alternatively spliced into five exons and four introns, with the last exon locating in the 3' UTR, the identified coding sequence is similar between the two. The deduced protein of ZmNPF6.4 and ZmNPF6.6 share 61.5% amino acid identity with AtNPF6.3 while ZmNPF6.5 shares a lower amino acid identity, 58%, with AtNPF6.3 (Figure 2.2). Interestingly, most of the key residues are conserved between ZmNPF6.4, ZmNPF6.5, ZmNPF6.6 and AtNPF6.3, including an equivalent of the affinity phosphorylation switch residue Thr101, the proton-coupling motif ExxER and the salt bridge residues Lys164 and Glu476, which are important for the functional structure of AtNPF6.3 (Liu, 2003; Winter et al., 2007; Parker and Newstead, 2014; Sun et al., 2014). Similar to other characterized members of the NPF family, ZmNPF6.4, ZmNPF6.5 and ZmNPF6.6 are all predicted to contain 12 transmembrane domains and a long hydrophilic loop between transmembrane domains 6 and 7.

ZmNPF7.10 (GRMZM2G044851_T01) was cloned using high fidelity RT-PCR and gene specific primers listed in Table 2.2. ZmNPF7.10 is closely related to two Arabidopsis NPF7 members (AtNPF7.2 and AtNPF7.3). According to the MaizeSequence.org database, *ZmNPF7.10* is annotated in two ways: the first includes five exons, four introns and the second includes six exons and five introns. Using primers to amplify either cDNA, only the first annotation resulted in an amplified transcript. The amplified cDNA encoded a protein of 613 amino acids. The sequence analysis revealed that ZmNPF7.10 shares 54% and 53% amino acid identity with AtNPF7.2 and AtNPF7.3, respectively (Figure 2.3). ZmNPF7.10 is predicted to contain only 11 transmembrane domains, with transmembrane domain 7 missing compared to AtNPF7.2 and AtNPF7.3.

2.2.3 Sub-cellular localization of ZmNPF6.4/6.5/6.6 and ZmNPF7.10

As each NPF has 12 predicted transmembrane domains (expect ZmNPF7.10), it is more than likely that the putative maize NPFs are membrane localized proteins (Tsay et al., 2007; Léran et al., 2014). To investigate their subcellular localization yellow fluorescent protein (YFP) was fused to the C-terminal of ZmNPF6.4, ZmNPF6.5, ZmNPF6.6 and ZmNPF7.10. Each was transiently expressed in onion epidermal cells under the control of the cauliflower mosaic virus 35S RNA promoter. ECFP-Rop11 construct was co-expressed with the YFP fused ZmNPFs to act as a plasma membrane marker (Molendijk et al., 2008). Images of transformed onion cells revealed that all the ZmNPF6 proteins were localized to the cell periphery and overlapped with the ECFP marker, suggesting a plasma membrane localization of ZmNPF6s (Figure 2.4A). This result was further confirmed in plasmolyzed onion cells where YFP stained Hechtian strands (stretched plasma membrane attached to cell wall) can be identified (Figure 2.4B). Unfortunately, the sub-cellular localization ZmNPF7.10 could not be determined as YFP signal was not detected in the onion epidermal peels.

2.2.4 Expression of *ZmNPF6.4* and *ZmNPF6.6* responds to nitrate

According to Sekhon et al. (2011), the expression of *ZmNPF6.4* and *ZmNPF6.6* is similar to that of *AtNPF6.3*. Both genes are expressed in multiple regions of the plant, including roots and leaves (Table 2.1). This result has been further confirmed by a preliminary mRNA expression analysis of maize tissues (Figure 2.5, Dechorgnat, unpublished data).

AtNPF6.3 is linked to nitrate acquisition in Arabidopsis roots, where its expression is regulated by nitrate (Tsay et al., 1993; Huang et al., 1996). I examined if nitrate also influenced the expression of *ZmNPF6.4* and *ZmNPF6.6* using quantitative RT-PCR (primers are listed in Table 2.3). Maize seedlings were grown in basal nutrient solution supplied with 2.5 mM NH_4NO_3 for 7 days and then shifted to a nutrient solution with no nitrogen (-N) for 4 days. Plants were then shifted to nutrient solutions containing 5 mM NO_3^-, 5 mM NH_4^+ or 5 mM Cl^-. After 4 hours, plants were harvested. As shown in Figure 2.6A, *ZmNPF6.6* was mainly expressed in roots but downregulated by the 4-day nitrogen starvation period. After 4-hour re-supply of nitrate, ZmNPF6.6 was strongly up regulated (Figure 2.6B). Neither re-supply of ammonium or chloride influenced the expression of *ZmNPF6.6* (Figure 2.6B). In shoots, the expression of *ZmNPF6.6* was very low and did not respond to any of the treatments (Figure 2.6B). In contrast, *ZmNPF6.4* expression was very low in both root and shoots. Unlike *ZmNPF6.4*, *ZmNPF6.4* was unresponsive to the treatments (Figure 2.6C).

In Arabidopsis roots, the expression of *AtNPF6.3* is induced by nitrate within 2 hours of supply (Tsay et al., 1993). I profiled the induction pattern of *ZmNPF6.6* in response to nitrate re-supply after a 4-day nitrogen starvation period. Similar to *AtNPF6.3*, the expression of *ZmNPF6.6* is also induced within 30 min of nitrate supply, where its peak in expression occurs 2 hours after treatment and then continues to remain high (Figure 2.7).

ZmNPF6.5 and *ZmNPF7.10* were not included in this expression analysis as their expression in maize seedlings were not detected in either the published transcriptomic study of Sekhon et al. (2011) nor in internal expression data from our lab (Figure 2.5, Dechorgnat, unpublished data).

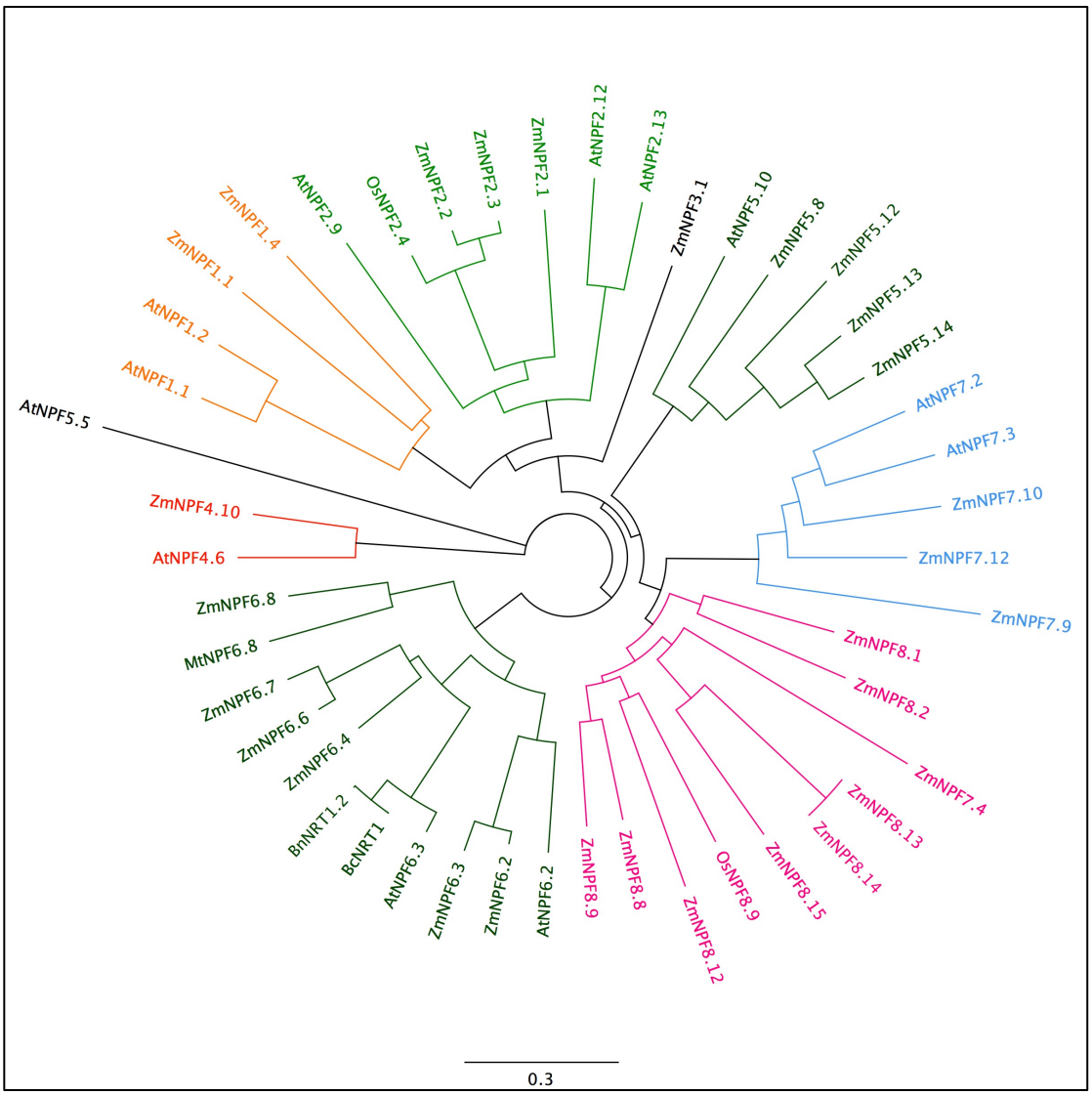

Figure 2.1 Phylogenetic Tree of NPF Nitrate Transporters

Unrooted neighbor-joining tree of characterized NPF nitrate transporters from *Arabidopsis thaliana*, *Oyrza sativa*, *Medicago truncatula*, *Brassica campestris, Brassica napus* and putative *Zea mays* NPF nitrate transporters was generated using the Geneious Tree Builder (Biomatters) in the Jukes-Cantor model with gap open penalty of 12 and gap extension penalty of 3. The scale bar represents a 0.1 estimated amino acid substitution per residue.

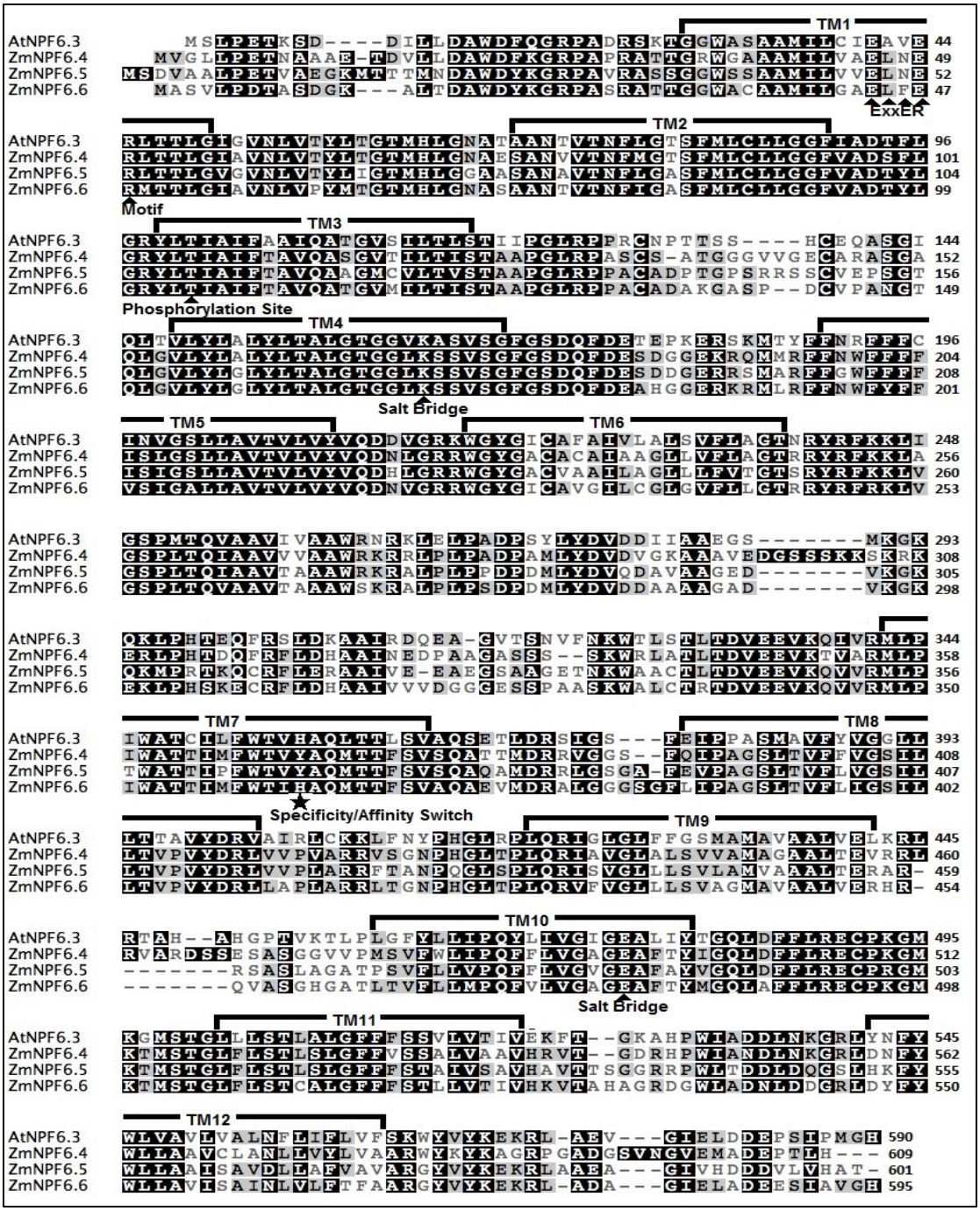

Figure 2.2. Amino Acid Sequence Alignment of AtNPF6.3, ZmNPF6.4, ZmNPF6.5 and ZmNPF6.6.

Sequence alignment was performed using the Geneious alignment tool (Biomatters) with open-gap penalty of 12, gap extension penalty of 3 and refinement iteration of 2. Conservative residues are colored in black shade. Key residues are indicated by black triangles. The putative transmembrane domains (TM) are underlined and numbered.

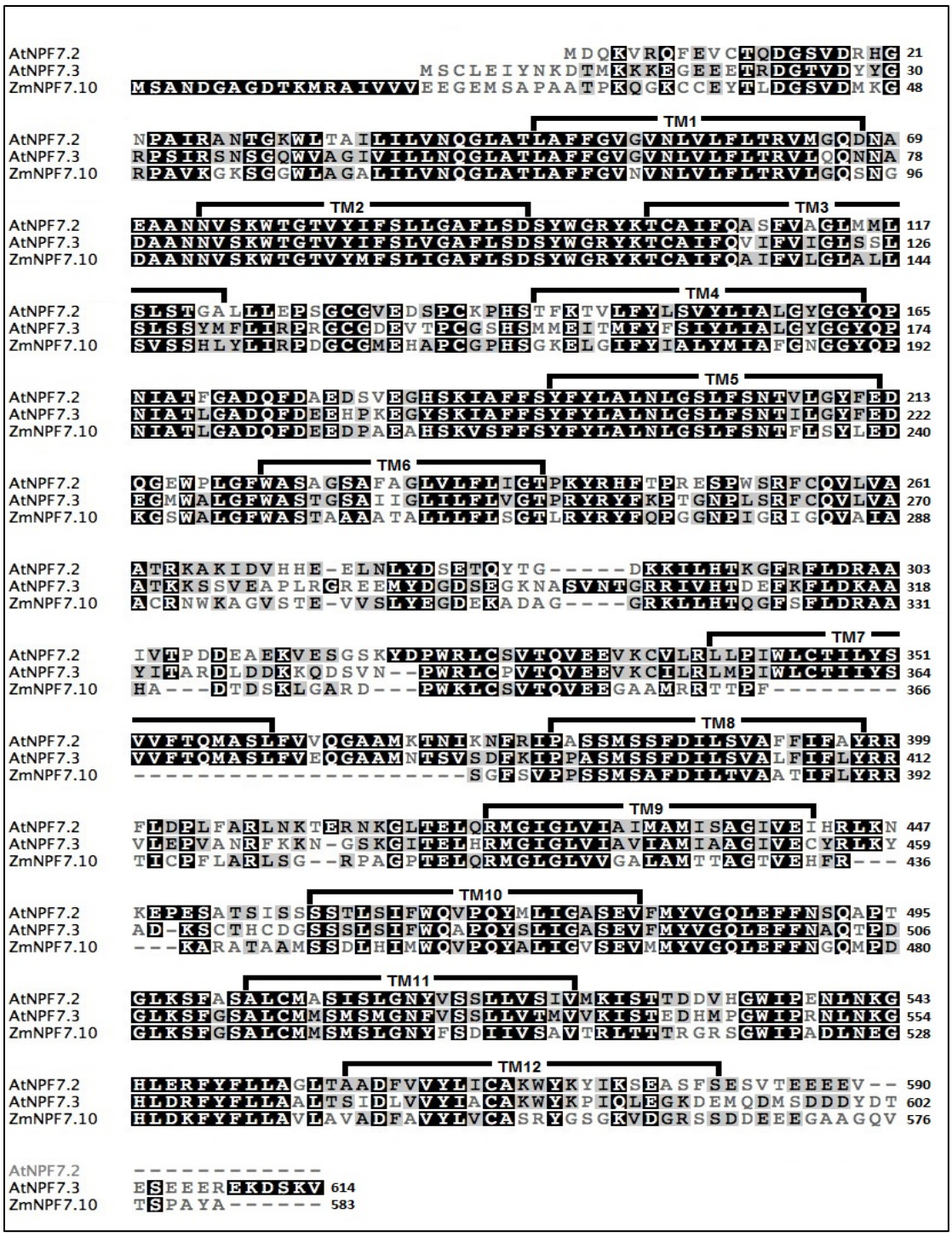

Figure 2.3. Amino Acid Sequnece Alignment of AtNPF7.2, AtNPF7.3 and ZmNPF7.10

Sequence alignment was performed using the Geneious alignment tool (Biomatters) with gap open penalty of 12, gap extension penalty of 3 and refinement iteration of 2. Conservative residues are colored in black shade. The putative transmembrane domains (TM) are underlined and numbered.

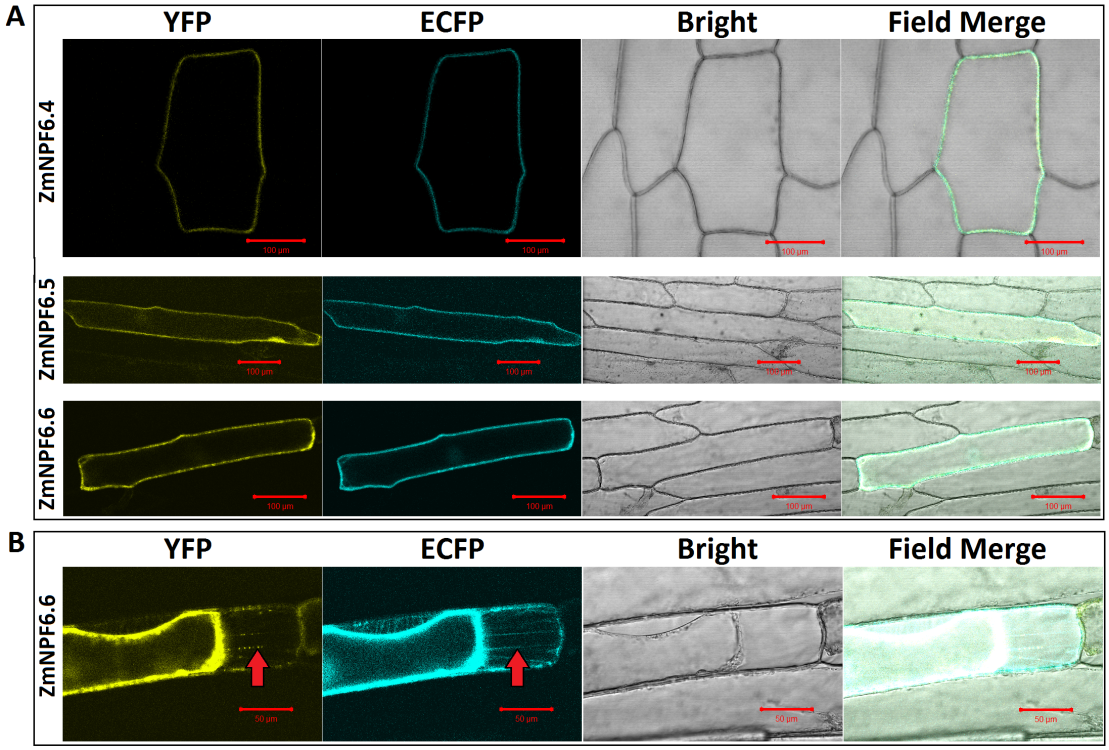

Figure 2.4. Sub-cellular localization of ZmNPF6.4, ZmNPF6.5 and ZmNPF6.6

A. ZmNPF6.4, ZmNPF6.5 and ZmNPF6.6 are localized on the plasma membrane of onion epidermal cells (bars = 100 µm). **B**. Plasma membrane localization is further supported by the visualization of YFP stained Hechtian strands (red arrow) in plasmolyzed onion epidermal cell (bars = 50 µm). Onion epidermal cells were transformed with *ZmNPF6-YFP* and *ECFP-Rop11* constructs using a biolistic PSD-1000/He particle delivery system. Images were taken using a LSM 5 PASCAL laser-scanning microscope (Zeiss) 12 hours after bombardment.

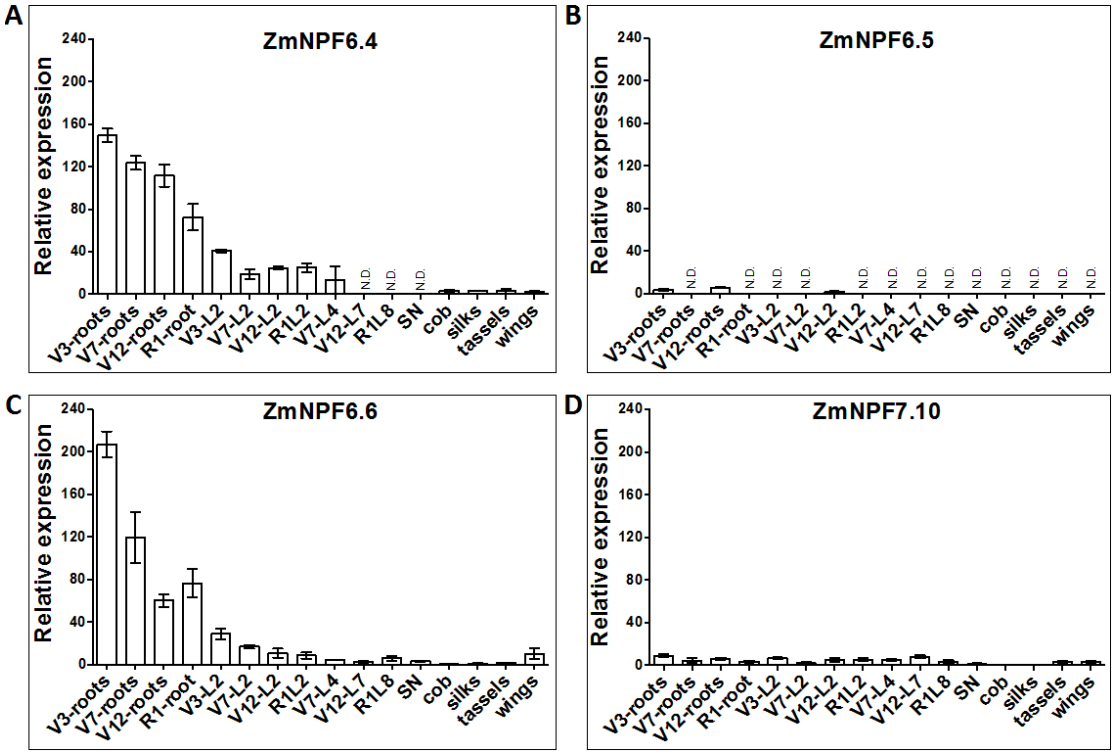

Figure 2.5 The Expression of *ZmNPF6.4* (A), *ZmNPF6.5* (B), *ZmNPF6.6* (C) and *ZmNPF7.10* (D) during Maize Development

B73 seedlings were grown in a growth basal solution supplied with 2.5 mM NH_4NO_3. Plant tissues were harvested at different development stages (V3/7/12: development stage of 3/7/12 extended leaves; R1: reproductive stage but before pollination; L2/4/7/8: the second/fourth/seventh/eighth leaf; SN: the senescent leaf). Quantitative RT-PCR was performed using cDNA derived from root and shoot tissues. Relative expression was normalized based on the maize *GaPDh*, *EF1A* and *Actin* genes. Data points in each experiment represent means of 3 (n = 3) samples. Error bars indicate mean ± SEM. This unpublished data set is from Dr. Julie Dechorgnat.

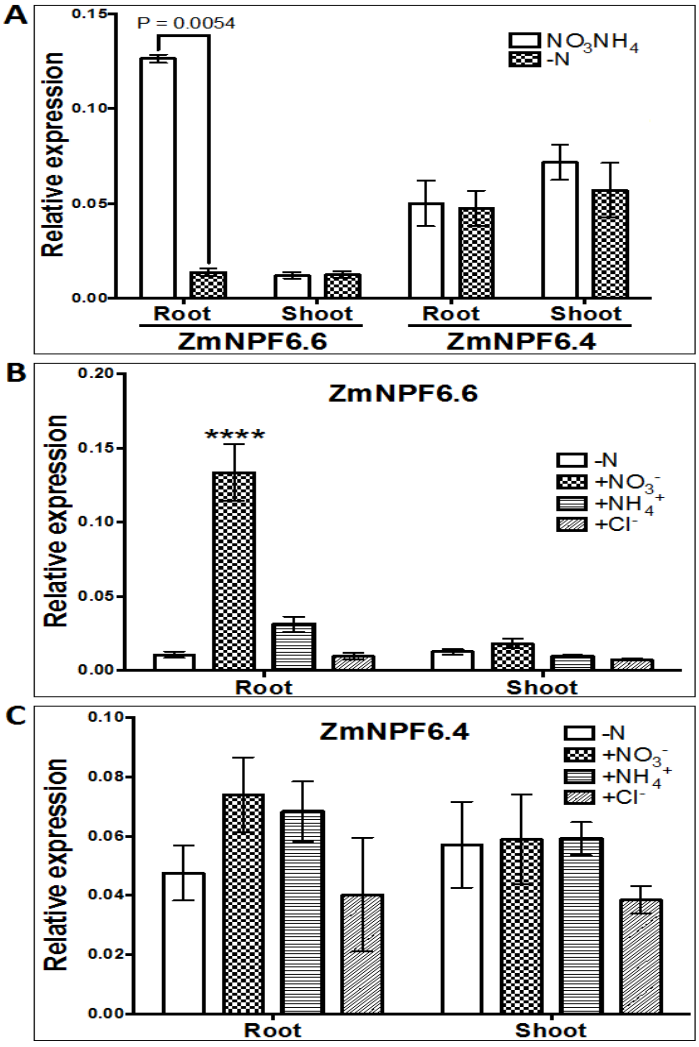

Figure 2.6. Expression of *ZmNPF6.4* and *ZmNPF6.6* in Response to Nitrate, Ammonium and Chloride Supply.

B73 seedlings were grown in a growth basal solution supplied with 2.5 mM NH_4NO_3 for 7 days after germination. At 7 days, the solution was changed to a growth basal solution with no nitrogen supplementation and grown further for 4 days. After starvation treatment, maize seedlings were treated with either 5 mM nitrate, 5 mM ammonium or 5 mM chloride for 4 hours before harvest. Quantitative RT-PCR was performed using cDNA derived from root and shoot tissues. **A.** The expression of *ZmNPF6.6* is depressed by nitrogen starvation. **B**. The expression of *ZmNPF6.6* is regulated by nitrate re-supply in roots. **C**. The expression of *ZmNPF6.4* is low in both root and shoot and is not regulated by nitrate, ammonium or chloride supply. Relative expression was normalized based on the maize *GaPDh*, *EF1A* and *Actin* genes. Similar results were obtained from three independent biological replications. Data points in each experiment represent means of 3 (n = 3) samples. Error bars indicate mean ± SEM, and asterisks denote significance (****P<0.00005) using the One-way ANOVA statistical analysis.

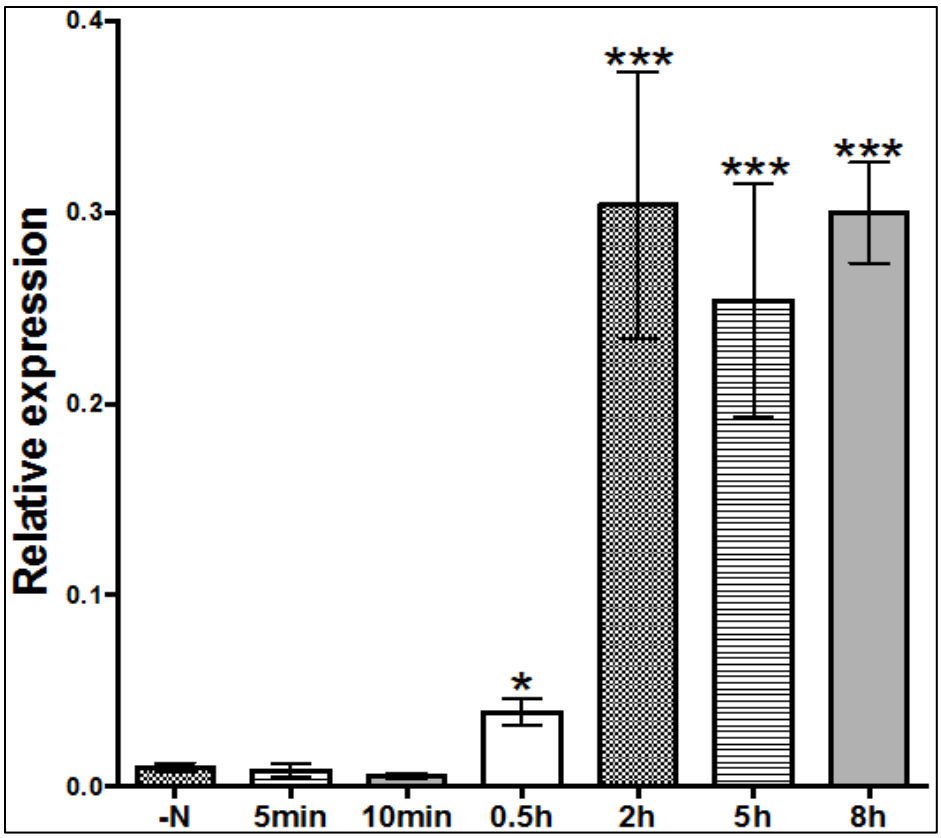

Figure 2.7. Time-course of *ZmNPF6.6* Expression with Nitrate re-supply.

The induction of *ZmNPF6.6* starts 30 min after nitrate re-supply and peaks 2 hours later. Maize seedlings were grown in a basal nutrient solution supplied with 2.5 mM NH_4NO_3 for 7 days after germination. For selected plants (-N and +N resupply), the solution was changed to a basal solution without nitrogen supplementation for 4 days. After starvation, B73 seedlings were supplied with 5 mM nitrate for 5 min, 10 min, 0.5 h, 2 h, 5 h and 8 h before harvest. Relative expression was normalized based on the maize GaPDh, EF1A and Actin genes. Quantitative RT-PCR was performed using cDNA derived from these maize seedlings. Similar results were obtained from three independent biological experiments. Data points in each experiment represent means of 3 independent (n = 3) samples. Error bars indicate ± SEM, and asterisks denote significance (*P<0.05, ***P<0.005) using the One-way ANOVA statistical analysis.

Maize NPFs	MaizeSequence ID	Length	Expression Tissue
ZmNPF1.1	GRMZM2G158807_P01	577	Meiotic tassel and seeds
ZmNPF1.4	GRMZM2G035790_P02	593	Meiotic tassel and anthers
ZmNPF2.1	GRMZM2G085411_P01	596	High expression in anthers
ZmNPF2.2	GRMZM2G104542_P01	479	No Expression in Embryo
ZmNPF2.3	GRMZM2G122251_P01	591	All tissues except embryo
ZmNPF3.1	GRMZM2G361652_P01	594	All Tissue
ZmNPF4.10	GRMZM2G137421_P01	609	Germinating seed, endosperm and mature kernel
ZmNPF5.8	GRMZM2G077498_P01	538	High expression in anthers
ZmNPF5.12	GRMZM2G085210_P01	547	High expression in anthers
ZmNPF5.13	GRMZM2G316889_P01	564	All Tissue
ZmNPF5.14	GRMZM2G378604_P02	567	High expression in anthers
ZmNPF6.2	GRMZM2G064091_P01	591	Leaves
ZmNPF6.3	GRMZM2G476069_P01	587	Anthers, tassel and leaves
ZmNPF6.4	GRMZM2G086496_P01	608	All tissues except endosperm
ZmNPF6.6	GRMZM2G161459_P01	595	Leaves and root
ZmNPF6.7	GRMZM2G112154_P01	588	Leaves, Internode and Root
ZmNPF6.8	GRMZM2G176253_P01	596	Leaves
ZmNPF7.4	GRMZM2G076313_P01	573	Silks and primary root
ZmNPF7.9	GRMZM2G156794_P01	640	Immature seeds
ZmNPF7.10	GRMZM2G044851_P01	582	Leaves and Root
ZmNPF7.12	GRMZM2G061303_P01	582	Embryo and germinating seed
ZmNPF8.1	GRMZM2G020484_P09	580	All Tissue
ZmNPF8.2	GRMZM2G419328_P02	556	Leaves
ZmNPF8.8	GRMZM5G867390_P01	587	All Tissue
ZmNPF8.9	GRMZM2G079889_P02	592	All Tissue
ZmNPF8.12	GRMZM2G101576_P01	663	Leaves and Mature Embryo
ZmNPF8.13	GRMZM2G041631_P01	562	Leaves
ZmNPF8.14	GRMZM2G141491_P01	562	Leaves
ZmNPF8.15	GRMZM2G015767_P01	574	All tissues except endosperm

Table 2.1. Putative NPF Nitrate Transporters in Maize

Putative maize NPF nitrate transporters were identified based on BLAST searches using characterized NPF nitrate transporters against the maize genome. The expression information of maize NPFs were from the Sekhon et al. (2011).

ZmNPF6.4 Clone Forward Primer	CCGCCGGCACACAGATATAG
ZmNPF6.4 Clone Reverse Primer	TCATTCTGAGTTTGCTCAGTGTCCC
ZmNPF6.4 C-terminal Reverse Primer	GTGGAGCGTGGGCTCGTC
ZmNPF6.5 Clone Forward Primer	TGCTGCTGCCTGCTACTTCATC
ZmNPF6.5 Clone Reverse Primer	TCAGGTGGCATGGACGAGTACG
ZmNPF6.5 C-terminal Reverse Primer	GGTGGCATGGACGAGTACG
ZmNPF6.6 Clone Forward Primer	TCCCCAACCCCTCATCCATC
ZmNPF6.6 Clone Reverse Primer	AATACATCACGCATGGCCCC
ZmNPF6.6 C-terminal Reverse Primer	GTGGCCGACGGCAATAGAC
ZmNPF7.10 Clone Forward Primer	ATCCCGTGGTCGAGAAGAGG
ZmNPF7.10 Clone Reverse Primer	ACGCAAAGAACAGTCGTGGT
ZmNPF7.10 C-terminal Reverse Primer	TGCGTAAGCCGGGGATGTC

Table 2.2. Primers used in Molecular Cloning of *ZmNPF6.4/6.5/6.6* and *ZmNPF7.10*

ZmNPF6.4 qPCR Forward	CCTCGACAACTTCTACTGGC
ZmNPF6.4 qPCR Reverse	AATTTAGGGTCGTCCGTCGC
ZmNPF6.6 qPCR Forward	GTCATCAGCGCCATCAACCT
ZmNPF6.6 qPCR Reverse	GGGTCACACCGTGTGCCAAA
ZmActin qPCR Forward	CCAATTCCTGAAGATGAGTCT
ZmActin qPCR Reverse	TGGTAGCCAACCAAAAACAGT
ZmGaPDh qPCR Forward	GACAGCAGGTCGAGCATCTTC
ZmGaPDh qPCR Reverse	GTCGACGACGCGGTTGCTGTA
ZmElF1 qPCR Forward	GCCGCCAAGAAGAAATGATGC
ZmElF1 qPCR Reverse	CGCCAAAAGGAGAAATACAAG

Table 2.3. Primers used in Expression Analysis of *ZmNPF6.4* and *ZmNPF6.6*

2.3 Materials and Methods

2.3.1 Sequence alignment and phylogenetic analysis

NPF protein amino acid sequences were obtained from the Arabidopsis Information Resource, Maizesequence.org and National Center for Biotechnology Information databases. All sequence alignments were conducted using the Geneious R7 software alignment tool (Biomatters) with gap-open penalty of 12, gap-extension penalty of 3 and refinement iteration of 2. The phylogenetic tree was generated using the Geneious tree builder software (Biomatters) using the Jukes-Cantor genetic distance model and neighbor-joining tree build method.

2.3.2 Seed germination and seedling growth conditions

All maize seedlings were grown in a hydroponic system. Briefly, the system consisted of two parts, a solution tank and planting tub. The solution tank (29 ×39 ×13 cm) was covered by a removable plastic rack (30 × 40 x 0.5 cm) with 24 square holes (5 × 5 cm). The planting unit was a plastic frame where 6 cm squares were cut and glued to a piece of nylon mesh. Single seedlings were grown per mesh square which sat 1 cm above the solution tank surface. Plants were moved between solution tanks for each of the growth treatments.

Maize (*Zea mays*) B73 seeds were imbibed in aerated water for 4 hours. Seeds were planted in wet diatomite rock and covered with aluminum foil and allowed to germinate (20 °C for 4 days). Germinated seeds were transferred to the hydroponic system filled with growth basal solution (0.5 mM $MgSO_4$, 0.5 mM KH_2PO_4, 25 µM H_3BO_3, 2 µM $MnSO_4$, 2 µM $ZnSO_4$, 0.5 µM $CuSO_4$, 0.5 µM Na_2MoO_4, 1.05 mM KCl, 0.1 mM Fe-EDTA, 0.1 mM FeEDDHA, 1.25 mM K_2SO_4, 0.25 mM $CaCl_2$, 1.75 mM $CaSO_4$, pH5.9) supplemented with 2.5 mM NH_4NO_3 and grown for 7 days in a temperature controlled growth chamber with a 16 h/8 h light/dark regime at 20 °C.

2.3.3 RNA extraction and reverse transcription

Maize root and shoot tissues were separated at the coleoptyl/mesocotyl interface, ground in liquid nitrogen and stored at −80 °C. Total RNA was extracted from 100 mg of ground tissue powder using TRIzol reagent (Ambion) following the manufacturer's instructions. RNAs were quantified and qualified using a ND-1000 spectrophotometer (Nanodrop). 1 μg of total RNA from each sample was used for cDNA synthesis, using SuperScript III reverse transcriptase (Invitrogen) and the oligo dT primer, following the manufacturer's instructions.

2.3.4 Molecular cloning

ZmNPF6.4, *ZmNPF6.5*, *ZmNPF6.6* and *ZmNPF7.10* full-length coding sequences were amplified from maize B73 cDNA using Platinum *Taq* DNA polymerase (Invitrogen). PCR products were subsequently inserted into pCR8/GW/TOPO vector (Invitrogen) and transformed into *E.coli* One Shot TOP10 strain (Invitrogen) for propagation. For *ZmNPF6.4*, the construct was transformed into XL1-Blue strain (Stratagene) as propagation by TOP10 constantly introduced mutations in the *ZmNPF6.4* coding sequence. Details of the PCR primer used are listed in Table 2.2.

2.3.5 Sub-cellular localization

ZmNPF6.4, *ZmNPF6.5*, *ZmNPF6.6* and *ZmNPF7.10* C-terminal coding sequences were fused with yellow fluorescent protein by sub-cloning from *pCR8/GW/TOPO* vector into the transient expression vector, *pBS-35S-attR-YFP*, using LR Clonase II (Invitrogen) (Subramanian et al., 2006). The plasma membrane marker, *ECFP::Rop11* vector, was also used in the experiments (Molendijk et al., 2008). High concentrations of quality plasmid is essential for onion bombardment experiments. This was achieved using a modified version of the plasmid maxi-prep protocol (Li et al., 2010). Briefly, 100 ml LB medium with appropriate antibiotic

was inoculated by *E.coli* containing the plasmid and grown overnight at 37 °C. Bacteria were harvested by centrifugation and re-suspended in 2 ml of solution I (50 mM Tris-HCl pH7.5 and 10 mM EDTA) supplied with 8 mg/ml lysozyme and 100 µg/ml RNaseA, incubating at room temperature for 10 min. The bacteria were lysed by 2 ml of solution II (0.2 M NaOH and 1% (w/v) SDS) and 10 min incubation on ice, following with a neutralization step by adding 2 ml solution III (1.32 M KOAc, pH4.8 adjusted with HCl). After 10 min centrifugation at 20,000 g, the supernatant was poured through a layer of miracloth to filter out any floating cell debris. Plasmid DNA was precipitated by adding 4 ml of 100% isopropanol and centrifuged at 16,000 x *g* for 10 min. The pellet was then washed with 2.5 ml of 70% (v/v) ethanol and centrifuged again at 16,000 x *g* for 10 min. The pellet was re-suspended in 250 µl of solution I containing 10 µg of RNaseA and incubated at 37 °C for 20 min to remove RNA from the plasmid DNA. 750 µl of 6 M NaI and 100 µl 250 mg/ml SiO_2 suspension were added and mixed thoroughly by vortex for 5 min and centrifuged at 16,000 x *g* for 15 sec. The pellet was washed twice with solution E (50% (v/v) ethanol, 10 mM Tris-HCl pH7.5, 100 mM NaCl and 1 mM EDTA) and dried for 5 min at 50 °C. The pellet was then re-suspended in 100 µl of sterile water. The last elution step was often repeated up to three times with one additional NH_4OAc precipitation step after elution to improve the quality of the plasmid DNA. The final concentration of plasmid DNA was adjusted to 0.5 µg/µl.

0.25 µg of *ECFP::Rop11* plasmid and 0.25 µl of *pBS-35S-ZmNPFs-YFP* plasmid were coated onto 1.5 mg of gold microcarriers (Bio-Rad, 0.6 µm diameter, pre-washed by 70% (v/v) ethanol and suspended in 50 µl of 50% (v/v) glycerol). Before bombardment, the onion epidermal cells were incubated on osmotic stress medium for 4 hours (1 pack of Murashige and Skoog basal medium with vitamins (*Phyto*Technology Laboratories), 500 mg/L tryptone, 120 g/L sucrose and 4 g/L gelrite, pH adjusted to 5.85). The DNA coated gold microcarriers were bombarded into onion epidermal cells using a biolistic PSD-1000/He particle delivery system with an 1100 psi rupture disc (Bio-Rad). The transformed onion epidermal peels

were transferred to a recovery medium, containing 1 pack of Murashige and Skoog basal medium with vitamins (*Phyto*Technology Laboratories), 500 mg/L tryptone, 30 g/L sucrose and 4 g/L gelrite, pH adjusted to 5.85, for 12-24 hours in the dark before visualization. Images were obtained using a LSM 5 PASCAL laser scanning microscope (Zeiss) with two excitation wavelength, 458 nm and 514, using an argon laser combined with two bandpass filters, 470-500 nm and 570-590 nm, for ECFP and YFP respectively. For further confirmation of the plasma membrane localization, transformed onion epidermal peels were treated with 0.75 M mannitol for 15 mins to induce plasmolysis as described by Campos-Soriano et al. (2011).

2.3.6 *ZmNPF6.4* and *ZmNPF6.6* gene expression

B73 seedlings were grown as described in 2.3.2. 7-day-old seedlings were removed from the NH_4NO_3 solution and rinsed with RO water before transferring to the basal solution for a 4-day nitrogen starvation treatment. The seedlings were then transferred to re-supply solutions (basal solution supplemented with either 5 mM NO_3^-, NH_4^+ or Cl^-) for 4 hours before harvest. Harvested samples were immediately frozen in liquid nitrogen and stored at -80 °C. RNA extraction and reverse transcription were conducted as described in 2.3.3.

1 µl synthesized cDNA and 4 µM forward and reverse primers was added in each reaction with SYBR Green real-time PCR master mixes (LifeTechnology) as manufacturer's instruction. Reactions were performed in a QuantStudio 12K flex real-time PCR system (LifeTechnology) with an initial denaturation of 95 °C for 20 s, followed by 40 cycles of (95 °C for 1 s and 55 °C for 20 s). One additional melting curve step was added at the end of qPCR reaction to ensure the quality of reaction. qPCR primers of *ZmNPF6.4*, *ZmNPF6.6* and 3 endogenous reference genes, *ZmActin*, *ZmElF1* and *ZmGaPDh* were designed using Primer 3 software and primer efficiency were tested with threshold of 90% (Table 2.2). Relative expression level

of each gene was calculated using equation by $2^{-\Delta Ct}$, which ΔCt is the sample Ct subtracted by the geometric mean of the Ct of 3 reference genes.

2.4 Discussion

NPF family members are membrane proteins consisting of 12 transmembrane domains (TM) and a long hydrophilic loop between transmembrane domains 6 and 7. Functionally characterized NPFs have been shown to transport different substrates, such as nitrate, peptides and hormones (Léran et al., 2014). In maize, a recent phylogenetic study identified 86 NPF genes within the sequenced genome (Léran et al., 2014). Of these it is uncertain how many genes encode nitrate transport proteins. For example, some putative annotated NPFs look to be partial genes encoding proteins between 200 and 300 amino acids in length (e.g. ZmNPF1.3, ZmNPF4.8 and ZmNPF4.9). When characterized against known plant NPF nitrate transporters (using gene and amino acid sequence comparisons), the number of defined maize NPF transporters is approximately 29 (Sekhon et al., 2011) (Table 2.1).

In this chapter, four putative maize NPF nitrate transporter genes were cloned, including three *AtNPF6.3* maize homologous, *ZmNPF6.4*, *ZmNPF6.5*, *ZmNPF6.6,* and an *AtNPF7.2/7.3* homologue, *ZmNPF7.10*. Sequence analysis revealed that all three ZmNPF6s contain the typical NPF structure of 12 TMs and show high amino acid sequence similarity with AtNPF6.3. With their putative plasma membrane location, supported by the transient expression experiments in onion epidermal cells, it is possible that ZmNPF6s probably have similar nitrate transporter activities to the well-characterized homolog, AtNPF6.3. This is also supported by the fact that they share structural similarities and key amino acid residues with AtNPF6.3, including the phosphorylating residue T101 and in most cases the putative nitrate binding site His356. His356 has recently been identified as a key residue located on the TM7 of AtNPF6.3. Based on structural studies, it has been suggested to be the putative substrate binding site for nitrate and possibly a dual-affinity

determination site for the low-affinity transporter dominated NPF family (Sun et al., 2014). Among ZmNPF6.4, ZmNPF6.5 and ZmNPF6.6, only ZmNPF6.6 harbors a histidine in the equivalent site of AtNPF6.3, suggesting ZmNPF6.6 may function as a dual-affinity nitrate transporter while the other two function as low-affinity transport proteins. ZmNPF7.10 shared ~50% sequence similarity to its Arabidopsis homologs (AtNPF7.2 and AtNPF7.3). However it did not contain the 7th TM, which contains the putative nitrate-binding site. As a result it is unlikely that ZmNPF7.10 is a nitrate transporter. Failure to see targeting of ZmNPF7.10 expressed in onion epidermal cells may relate to the absence of the 7th TM and possible mis-targeting of the YFP fused ZmNPF7.10.

It has been reported that AtNPF6.3 is responsible for nitrate uptake in Arabidopsis roots, where the expression of *AtNPF6.3* is nitrate inducible (Tsay et al., 1993; Huang et al., 1996). *ZmNPF6.6* expression is also induced by nitrate (within 30 min). This result suggests a possible participation of ZmNPF6.6 in LATS and/or HATS nitrate uptake in maize roots. In contrast, *ZmNPF6.4* did not exhibit a nitrate inducible pattern, but rather a constitutive one, regardless of nitrate, ammonium or chloride treatment. This constitutive expression pattern is similar to the Arabidopsis nitrate transporter *AtNPF4.6*, which is the constitutive component of the Arabidopsis nitrate LATS (Huang et al., 1999). It is possible that ZmNPF6.4 may also be a LATS component of B73 root nitrate uptake. Furthermore, its broad expression across multiple tissues (this study and the results of Sekhon et al. (2011)) suggests that ZmNPF6.4 may have a much wider role in maize nitrate transport than just uptake into the root.

A more detailed expression analysis of two other candidate genes, *ZmNPF6.5* and *ZmNPF7.10*, was not pursued in this study due to a lack of expression in the transcriptomic study of Sekhon et al. (2011) or from in-house B73 expression data (J. Dechorgnat, unpublished results). Whether the lack of expression is a result of the growing conditions used, the age of the plant or the type of tissue harvested remains to be determined. In Arabidopsis, some nitrate transporter genes are not

induced by nitrate (*AtNRT2.4*) (Kiba et al., 2012), while both AtNPF1.2 and AtNPF2.13 show nitrate insensitivity (Fan et al., 2009; Hsu and Tsay, 2013). It was pre-mature to conclude that *ZmNPF6.5* and *ZmNPF7.10* are simply nonfunctional pseudogenes. For these reasons, both genes were included in the functional characterization study described in the next chapter.

3 Functional Characterization of Maize NPF Nitrate Transporters

3.1 Introduction

Unfertilized oocytes of the African clawed frog, *Xenopus laevis,* have been an important heterologous expression system to study animal and plant transport proteins and membrane receptors (Schroeder, 1994; Frommer, 1995). The advantages of the *Xenopus* oocyte system includes their relatively large size (2-3 mm) and their high resilience and resistance to voltages, which allows them to be electrically clamped as low as −180 mV without membrane dielectric breakdown. Furthermore, the lack of a vacuole in oocytes forces tonoplast localized plant proteins to be re-targeted to the plasma membrane. This helps to simplify localization and increases the success rate of experiments requiring transport measurements. These features make *Xenopus* oocytes an ideal system for chemical flux measurements (using isotopes) and electrophysiology experiments. Currently, 31 plant nitrate transporters (17 NPFs, 1 CLC and 13 NRT2s) have been studied and nearly all have been functionally characterized using the *Xenopus laevis* oocyte system. In this chapter, selected maize NPF nitrate transporters (ZmNPF6.4, ZmNPF6.5, ZmNPF6.6 and ZmNPF7.10) were functionally characterized in *Xenopus* oocytes for their nitrate transport properties.

3.2 Results

3.2.1 Nitrate transport activity of maize NPFs

The nitrate transport activities of ZmNPF6.4, ZmNPF6.5, ZmNPF6.6 and ZmNPF7.10 were tested using the *Xenopus laevis* oocyte expression system. A

preliminary screen of nitrate uptake (^{15}N influx) capacity was tested with each of the four genes. Two days after cRNA injection, oocytes were incubated in nitrate containing buffer, pH 5.5 (for buffer contents see Section 3.3.3). Since most of the nitrate transporters from the NPF family are predicted to be low-affinity transport systems, 10 mM ^{15}N-nitrate solution was used for the initial screen. In the first instance, ZmNPF6.4 was used to define the optimal incubation time for nitrate influx. As shown in Figure 3.1A, nitrate uptake by *ZmNPF6.4*-injected oocytes was found to be linear against the incubation period, with no apparent saturation of uptake capacity of oocytes. All subsequent nitrate uptake experiments thereafter used a one-hour incubation period. As shown in Figure 3.1B, *ZmNPF6.4*- and *ZmNPF6.6*-injected oocytes accumulated nitrate from the external solution, while there was no nitrate transport activity in either *ZmNPF6.5* or *ZmNPF7.10*-injected oocytes. The latter result was surprising, as it was expected that both of these transporters would have a nitrate flux activity (HATS or LATS). The lack of activity could be due to many factors. Unfortunately time didn't permit a detailed investigation. No further experiments were conducted with either ZmNPF6.5 or ZmNPF7.10.

3.2.2 Nitrate transport activity of ZmNPF6.4 and ZmNPF6.6

The nitrate transport activity of ZmNPF6.4 and ZmNPF6.6 was characterized using both electrophysiology and chemical flux analysis. The electrophysiological study involved the use of the two-electrode voltage clamp technique (Preuss et al., 2011). As expected, a larger voltage dependent inward current was elicited by external nitrate supply at pH 5.5 for both *ZmNPF6.4* and *ZmNPF6.6* cRNA-injected oocytes compared with the water-injected control oocytes (Figure 3.2A). Combined with the preliminary nitrate influx result (Fig 3.1B), the results suggest that ZmNPF6.4 and ZmNPF6.6 are potentially low-affinity nitrate transporters.

Given that only inward currents (net cation influx) were elicited by external nitrate anions (Figure 3.2B), the result suggests that nitrate influx was probably coupled

with cations, where the cation/nitrate ratio would need to be greater than 1. Most NPF nitrate transporters have been previously categorized as proton symporters (Miller and Smith, 1996; Tsay et al., 2007). So I tested the pH dependent nitrate transport properties of *ZmNPF6.4*- and *ZmNPF6.6*-injected oocytes using nitrate solutions buffered at pH 5.5 or pH 7.5. As expected, high pH nitrate solutions, compared with the low pH solutions, reduced nitrate uptake of *ZmNPF6.4*- and *ZmNPF6.6*-injected oocytes by ~45% and ~75%, respectively, (Figure 3.3). Similar results were observed using electrophysiological approaches (Figure 3.4).

Two closely related proteins of ZmNPF6.4 and ZmNPF6.6 (AtNPF6.3 and MtNPF6.8) have previously been shown to transport nitrate in *Xenopus* oocytes across both low (high-affinity range) and high (low-affinity range) nitrate concentrations – hence behaving in a dual-affinity manner. This property was tested in both ZmNPF6.4 and ZmNPF6.6 with AtNPF6.3 acting as a positive control. *ZmNPF6.4*- and *ZmNPF6.6*-injected oocytes were incubated in a ^{15}N-nitrate-containning solution (250 μM, pH 5.5) for one hour. Similar to AtNPF6.3, ZmNPF6.6-injected oocytes accumulated nitrate at low (250 μM, high-affinity range) nitrate concentrations (Figure 3.5A). To the contrary, *ZmNPF6.4*-injected oocytes did not absorb nitrate in the high-affinity range (Figure 3.5A). As shown previously in low-affinity range, ZmNPF6.6 in the high-affinity range is also pH dependent as high pH conditions blocked nitrate uptake (Figure 3.5B).

The dual-affinity nitrate transport activity of ZmNPF6.6 was further analyzed with a more detailed kinetic study using a broad range of nitrate concentrations, from 25 μM to 30 mM (Figure 3.6). Across the high-affinity range (25 μM to 250 μM), nitrate uptake of *ZmNPF6.6*-injected oocytes could be fitted with the Michaelis-Menten equation which provided a calculated *K*m of ~80 μM. This is similar to *AtNPF6.3*-injected oocytes (Liu et al., 1999). In the low-affinity range (250 μM to 30mM), nitrate uptake occurred for both *ZmNPF6.4* and *ZmNPF6.6* and could be fitted with a linear model. Collectively, these functional studies suggested that ZmNPF6.4 is a proton-coupled low-affinity nitrate transporter and ZmNPF6.6 is

also a proton-coupled nitrate transporter but with a dual-affinity nitrate transport activity.

3.2.3 Chloride transport properties of ZmNPF6.4 and ZmNPF6.6

During the electrophysiological analysis of ZmNPF6.4 and ZmNPF6.6, it was noticed that the original basal solution, which contained 1 mM KCl, could induce a positive directed shift in reversal potential (Figure 3.7). This suggested that net cation influx, in both *ZmNPF6.4* and *ZmNPF6.6*-injected oocytes (compared with water-injected oocytes), occurred without the presence of nitrate and potentially was caused by chloride (Figure 3.7A and 3.7B). This raised the question about the potential chloride transport activities of the ZmNPFs. To answer this question, a new electrophysiological experiment was conducted in which chloride, instead of nitrate, was used as a potential substrate. With chloride in the bath solution (pH 5.5), oocytes displayed a larger voltage dependent current in both *ZmNPF6.4* and *ZmNPF6.6*-injected oocytes compared to the water-injected controls (Figure 3.8). This result indicates that chloride, as well as nitrate, is a potential substrate for the two transporters.

To further confirm the transport activity of ZmNPF6.4 and ZmNPF6.6, a set of chemical flux experiments were performed. As shown in Figure 3.9A, both *ZmNPF6.4*- and *ZmNPF6.6*-injected oocytes were able to accumulate ^{36}Cl compared with the water-injected oocytes. This uptake, like nitrate, was linear against increasing chloride concentrations. This non-saturable LATS chloride transport activity of ZmNPF6.4 and ZmNPF6.6 is similar to that of nitrate. Furthermore, the chloride transport activity was also pH dependent where high pH reduced chloride uptake in both *ZmNPF6.4*- and *ZmNPF6.6*-injected oocytes by ~47% and ~96%, respectively, compared with low pH chloride solution (Figure 3.9B).

3.2.4 Substrate specificity study of ZmNPF6.4 and ZmNPF6.6

Given that ZmNPF6.4 and ZmNPF6.6 both transport nitrate and chloride in a similar proton-coupled manner, nitrate and chloride may share the same transport mechanism in ZmNPF6.4 and ZmNPF6.6. This raises another question about the substrate preference of the two ZmNPFs. To help elucidate this, a substrate competition flux experiment was conducted where nitrate and chloride uptake was tested against equimolar amounts of chloride and nitrate, respectively. In ZmNPF6.4, there was a ~50% reduction in net 10 mM nitrate uptake in the presence of 10 mM NaCl (Figure 3.10A). Even though there was a strong reduction in nitrate flux, the flux levels were still significantly above that of the water injected controls. Interestingly, nitrate uptake in *ZmNPF6.6*-injected oocytes was not affected by equimolar concentrations of chloride. As the chloride ion was supplemented in a sodium salt form, it was necessary to exclude the possibility that the nitrate uptake reduction was caused by extra sodium in the solution. So a control experiment was conducted where *ZmNPF*-injected oocytes were incubated in solution containing 10 mM $^{15}NaNO_3$ and 10 mM Na_2SO_4. As shown in Figure 3.10B, nitrate uptake of both *ZmNPF6.4* and *ZmNPF6.6*-injected oocytes were not affected by sodium (also SO_4^{2-}) supplementation. These results suggested that both ZmNPF6.4 and ZmNPF6.6 can transport nitrate in the presence of chloride. However nitrate transport by ZmNPF6.4 was more susceptible to chloride competition than ZmNPF6.6.

These experiments were tested in reverse using ^{36}Cl as the tracer and nitrate as the competitor. Net chloride uptake in *ZmNPF6.6*-injected oocytes was reduced by ~84% in the presence of nitrate (Figure 3.11A), values which were indistinguishable from the water-injected controls. In contrast, chloride uptake by *ZmNPF6.4*-injected oocytes was not significantly decreased by nitrate. A similar control experiment with equal concentrations of Na_2SO_4 in a ^{36}Cl chloride flux solution were also performed to rule out the possibility of a sodium effect on chloride uptake (Figure 3.11B). Together these results suggest that ZmNPF6.4 can transport chloride in the

presence of nitrate, while nitrate strongly competes with ^{36}Cl uptake in ZmNPF6.6. In summary, it would appear ZmNPF6.4 is a non-selective nitrate and chloride transporter while ZmNPF6.6 is a nitrate specific transporter, which can transport chloride in the absence of a nitrate competitor.

3.2.5 Auxin transport activity of ZmNPF6.4 and ZmNPF6.6

Some NPF nitrate transporters (notably AtNPF6.3) have been shown to also transport auxin (Krouk et al., 2010). A test for auxin transport activity in ZmNPF6.4 and ZmNPF6.6-injected oocytes was conducted by incubating oocytes for 1 hour in a modified Ringers solution supplemented with 1 μM ^{3}H-IAA (10%, PerkinElmer). There was no measureable ^{3}H-IAA transport for either NPF (Figure 3.12). This preliminary result suggests that ZmNPF6.4 and ZmNPF6.6 may not transport IAA, which is a contrast to the phenotype displayed by the Arabidopsis homolog, AtNPF6.3 (Krouk et al., 2010; Bouguyon et al., 2015).

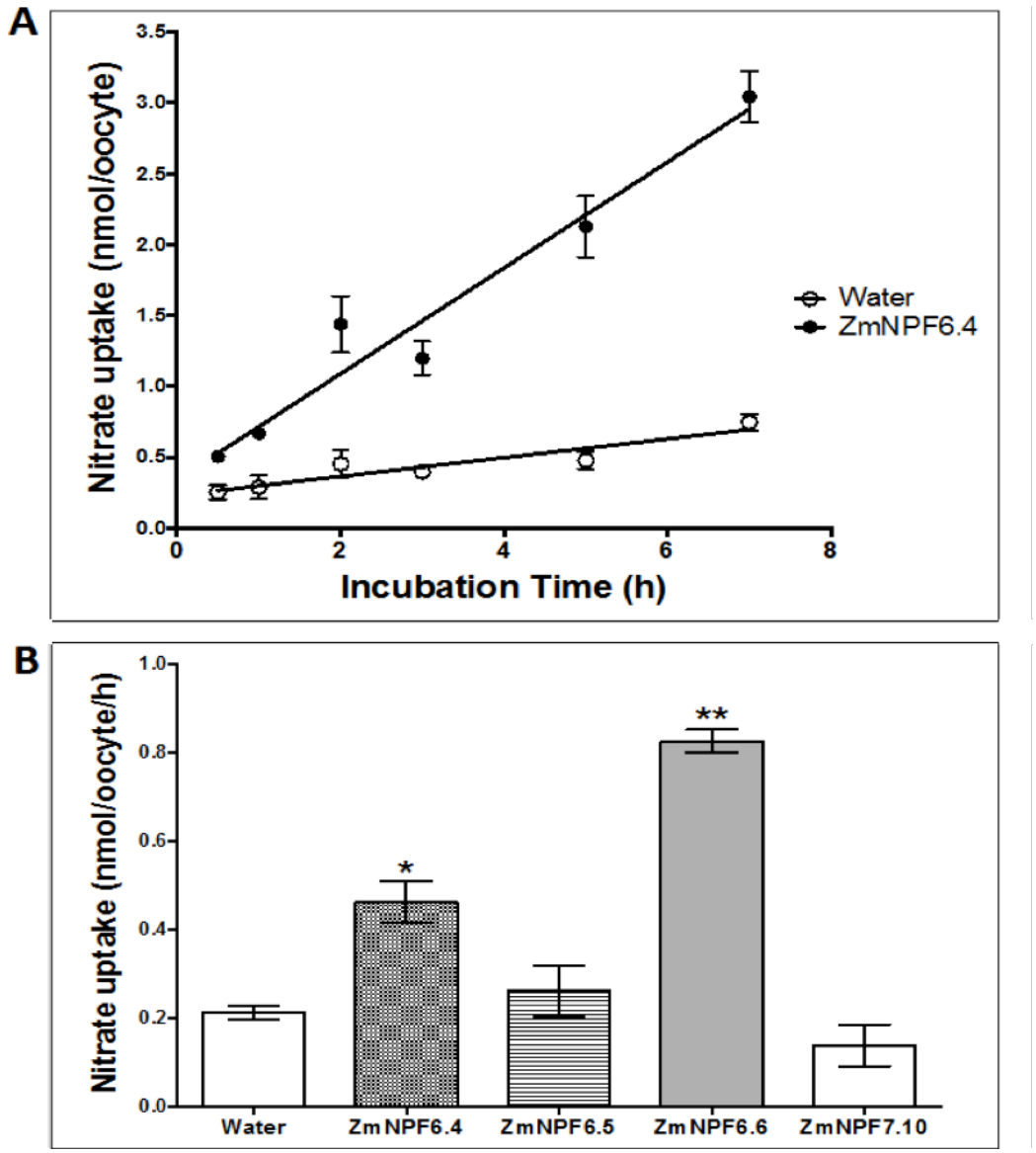

Figure 3.1. Oocyte Nitrate Uptake Capacity Test and Preliminary Activity Screen

A. Oocyte nitrate uptake over time. *ZmNPF6.4*-injected oocytes and water-injected oocytes were incubated in ^{15}N labeled nitrate solution (10 mM, pH 5.5) from 0.5, 1, 2, 3, 5 and 7 h. Accumulated nitrate per oocyte was quantified by an IRMS. Data points in each experiment represent means of 12 replicate oocytes (n=12). **B**. ZmNPF6.4 and ZmNPF6.6 transport nitrate at 10 mM external concentrations. *ZmNPF6.4*, *ZmNPF6.5*, *ZmNPF6.6* and *ZmNPF7.10*-injected oocytes and water-injected oocytes were incubated in ^{15}N labeled nitrate solution (10 mM, pH 5.5) for 1 hour and accumulated nitrate was quantified by an IRMS. Average values and standard errors of the mean were calculated from 9 replicate oocytes and equivalent results were obtained from three repeat experiments with oocytes derived from different frogs. Error bars indicate ± SEM, and asterisks denote significance (*P<0.05, **P<0.005) using the One-way ANOVA statistical analysis.

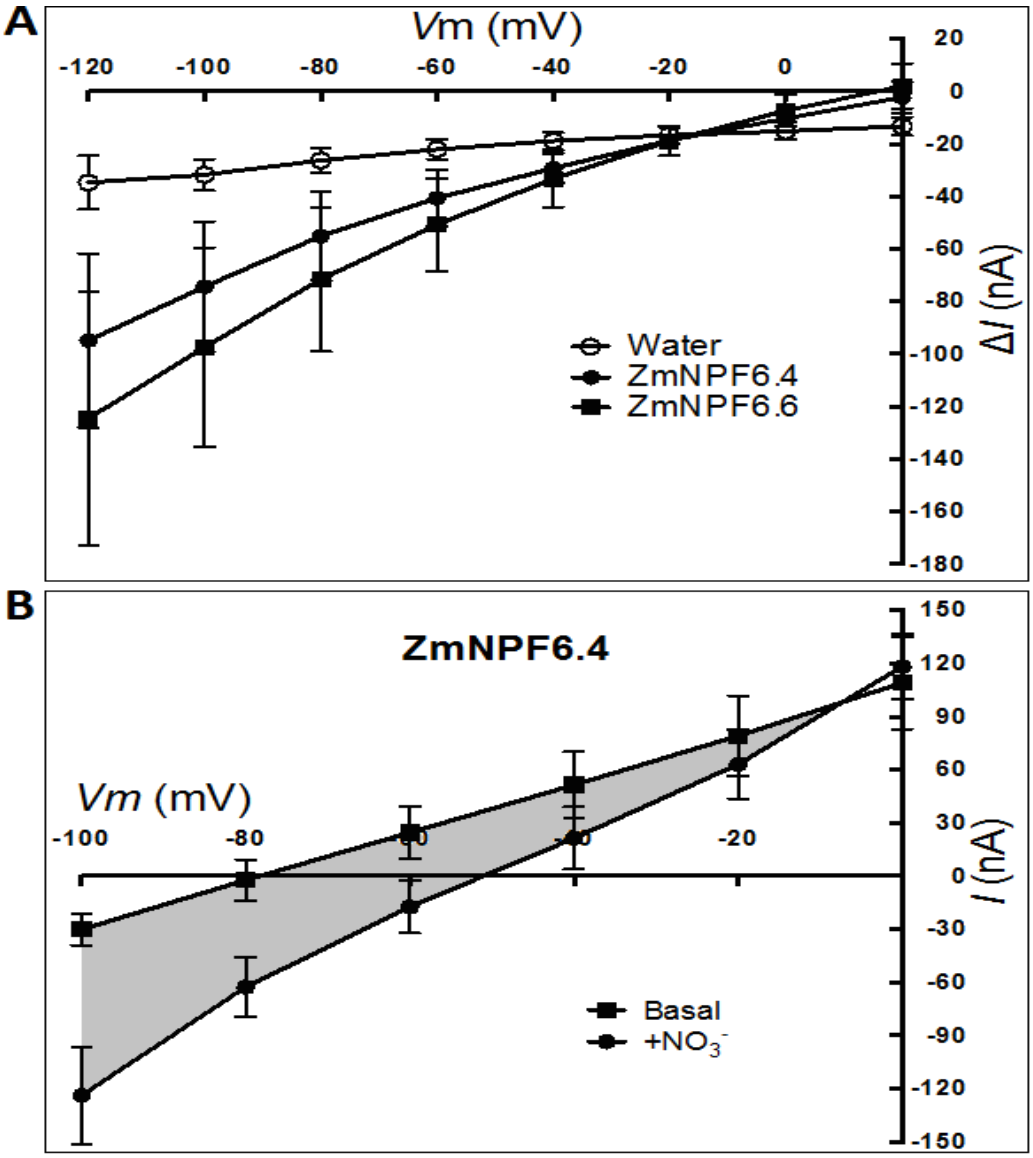

Figure 3.2. Current-to-Voltage Relationship in *ZmNPF6.4* and *ZmNPF6.6*-Injected Oocytes

A. Nitrate elicited currents in *ZmNPF6.4* and *ZmNPF6.6*-injected oocytes. **B**. Nitrate induced inward current and reversal potential shift in *ZmNPF6.4*-injected oocytes. *ZmNPF6.4* and *ZmNPF6.6*-injected oocytes and water injected oocytes were voltage clamped from −120mV to +20mV with 20mV increments while perfusing in a nitrate solution (10 mM nitrate, pH 5.5). Currents (Δ*I*) presented in panel A are the substrate-elicited current representing the current change before and after the solution switch from the basal solution to the nitrate solution. Currents (*I*) presented in panel B are the recorded raw data. Average values and standard errors of the mean were calculated from six replicated oocytes and equivalent results were obtained from three repeat experiments with oocytes derived from different frogs. Error bars indicate ± SEM.

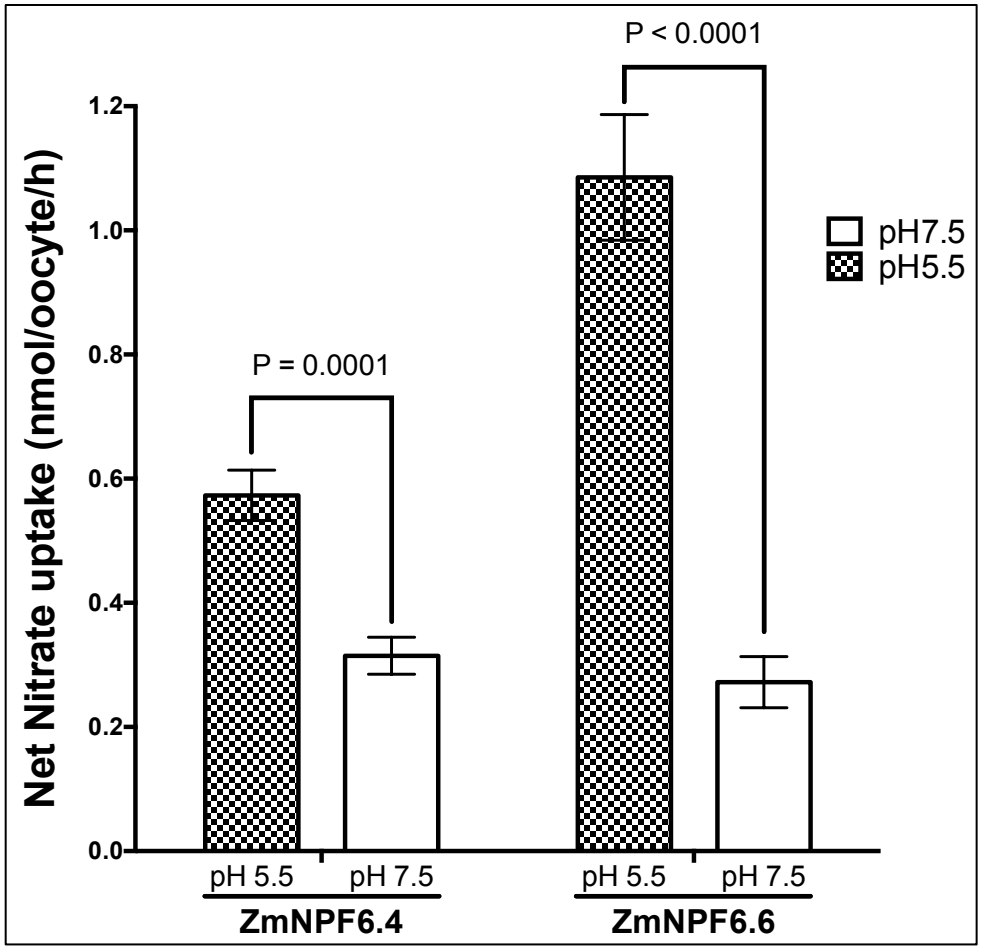

Figure 3.3. pH Dependent Nitrate Transport Activity of ZmNPF6.4 and ZmNPF6.6

ZmNPF6.4, *ZmNPF6.6*-injected oocytes and water-injected oocytes were incubated in a nitrate solution (10 mM, pH 5.5 or 7.5) for 1 hour. Accumulated ^{15}N-nitrate was quantified by an IRMS. Net nitrate uptake values were normalized by subtracting the mean of water control value from the value of NRT injected groups. Average values and standard errors of the mean were calculated from 9 replicate oocytes and equivalent results were obtained from three repeat experiments with oocytes derived from different frogs. Error bars indicate ± SEM and significance was determined using an unpaired t-test.

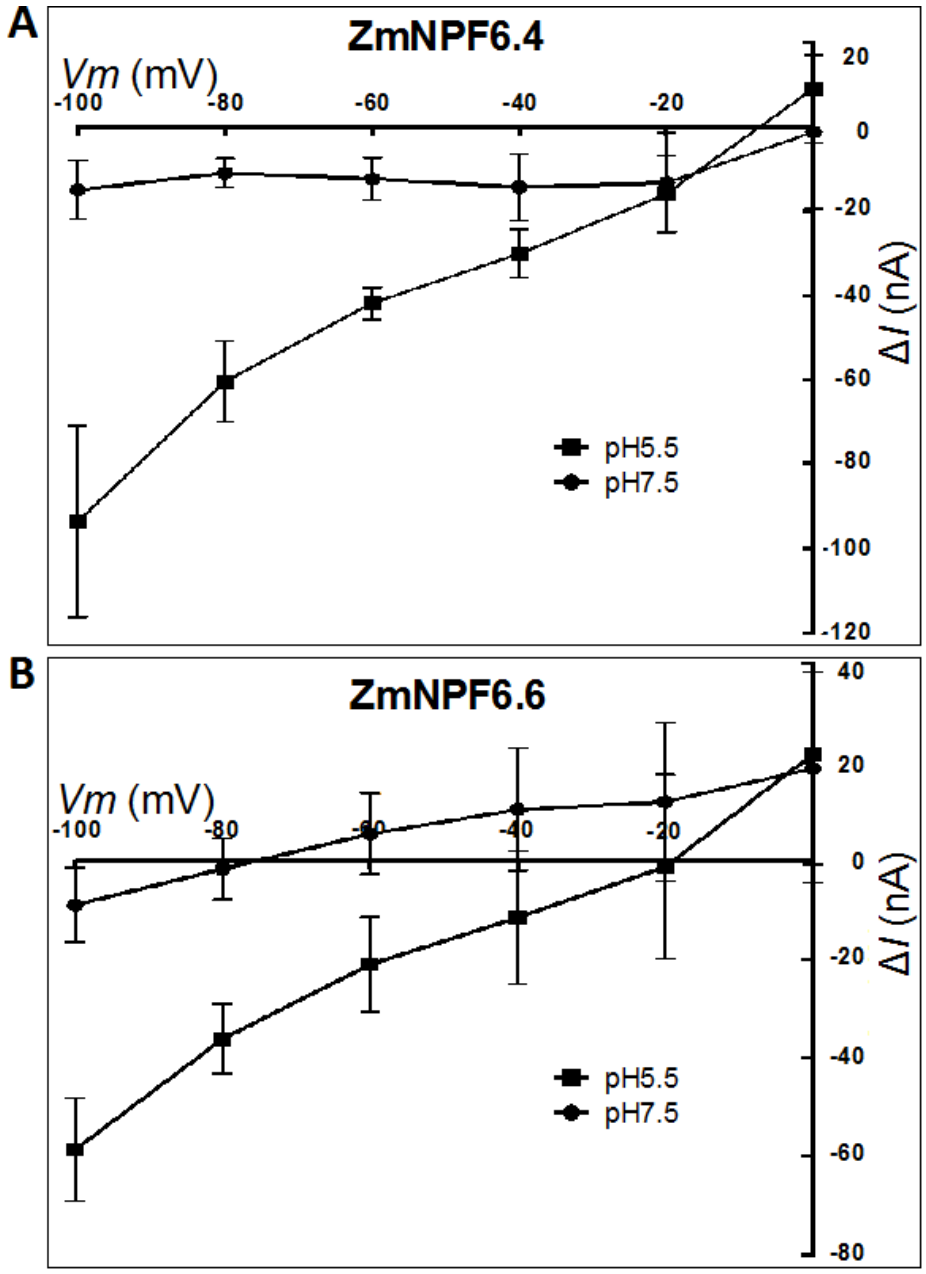

Figure 3.4. pH Dependent Nitrate Elicited Current in *ZmNPF6.4* (A) and *ZmNPF6.6* (B) Injected Oocytes

ZmNPF6.4 and *ZmNPF6.6*-injected oocytes and water injected oocytes were voltage clamped from −100mV to 0mV with 20mV increments while perfusing in a nitrate solution (10 mM nitrate, pH 5.5 or pH7.5). Currents (ΔI) presented are the substrate-elicited current representing the current change before and after the solution switch from the basal solution to the nitrate solution. Average values and standard errors of the mean were calculated from six replicated oocytes and equivalent results were obtained from three repeat experiments with oocytes derived from different frogs. Error bars indicate ± SEM.

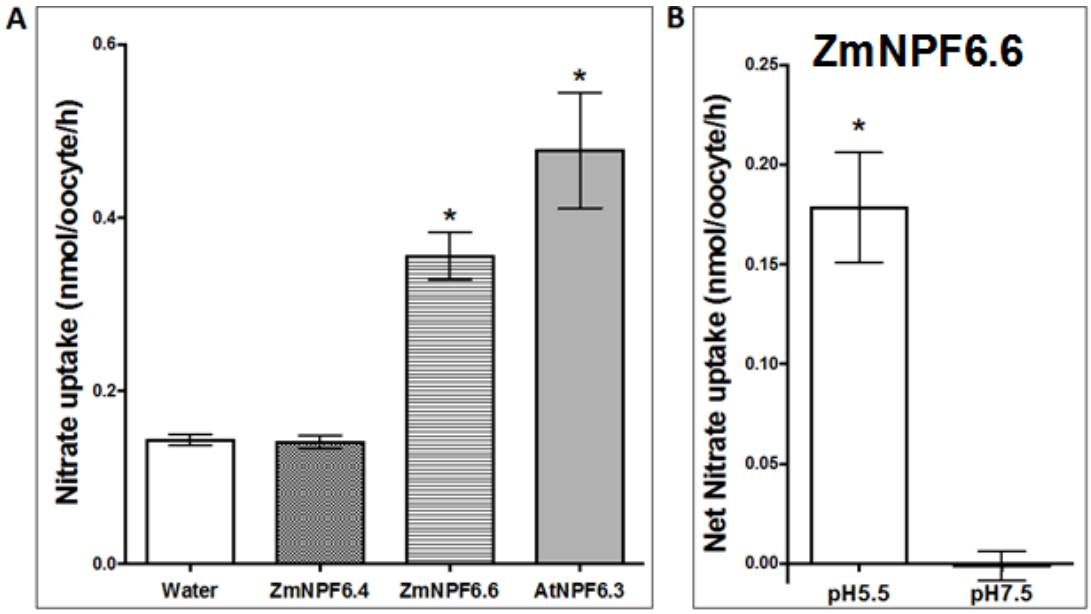

Figure 3.5. High-Affinity Nitrate Transport Activity of ZmNPF6.6

A. *ZmNPF6.6*-injected oocytes accumulate nitrate in the high-affinity range (250 µM). Water-injected, *ZmNPF6.4*, *ZmNPF6.6* and *AtNPF6.3*-injected oocytes were incubated in nitrate solution (250 µM, pH 5.5) for 1 hour and accumulated nitrate was quantified by an IRMS. **B**. The high-affinity nitrate transport activity of ZmNPF6.6 is pH dependent. *ZmNPF6.6* and water-injected oocytes were incubated in nitrate solution (250 µM, pH 5.5 or pH7.5) for 1 hour. In panel B, net nitrate uptake values were normalized by subtracting the mean of water control value from the value of *ZmNPF6.6*-injected oocytes. Average values and standard errors of the mean were calculated from 9 replicate oocytes and equivalent results were obtained from three repeat experiments with oocytes derived from different frogs. Error bars indicate ± SEM, and asterisks denote significance (*P<0.05) using the One-way ANOVA statistical analysis.

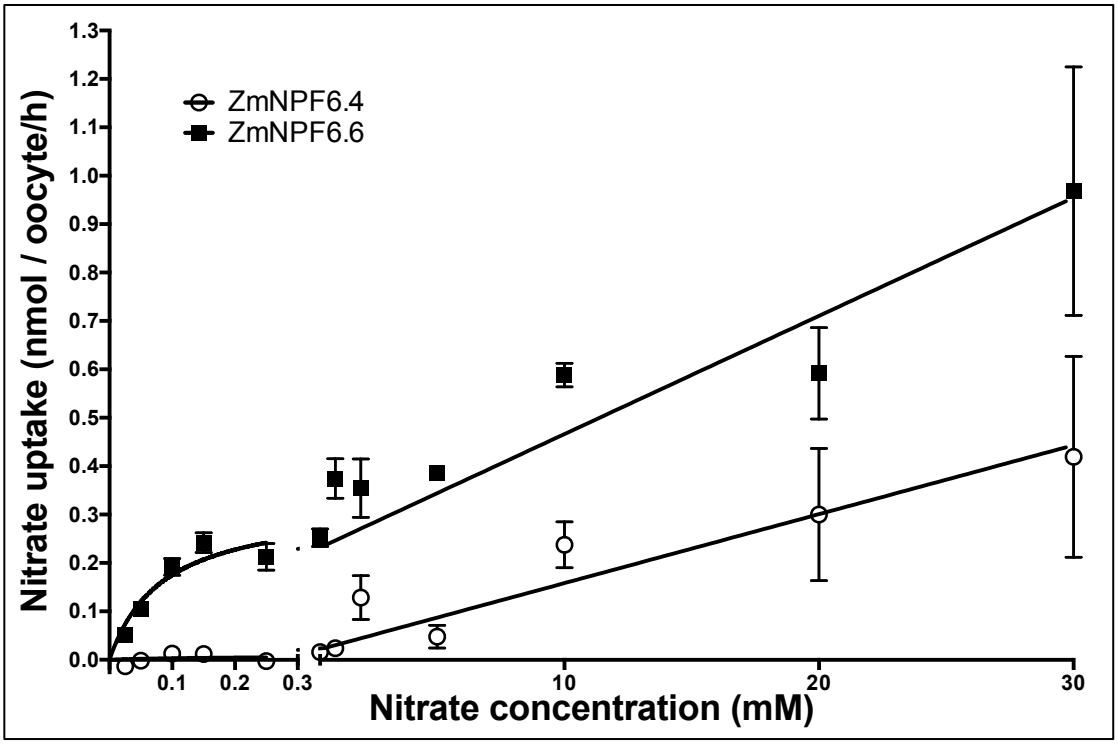

Figure 3.6. Kinetic Analysis of ZmNPF6.4 and ZmNPF6.6

ZmNPF6.4 and *ZmNPF6.6* and water-injected oocytes were incubated in solution containing nitrate concentrations ranging from 25 μM to 30 mM (pH5.5) for 1 hour. Accumulated nitrate was quantified using an IRMS. Net nitrate uptake values were normalized by subtracting the mean of water control value from the value of NPF injected groups. The nitrate uptake values from 25 μM to 250 μM are fitted using the Michaelis-Menten equation while values from 0.4 mM to 30 mM are fitted onto a linear model using software Prism 6 (Graphpad Software). Average values and standard errors of the mean were calculated from 9 replicate oocytes and equivalent results were obtained from three repeat experiments with oocytes derived from different frogs. Error bars indicate ± SEM.

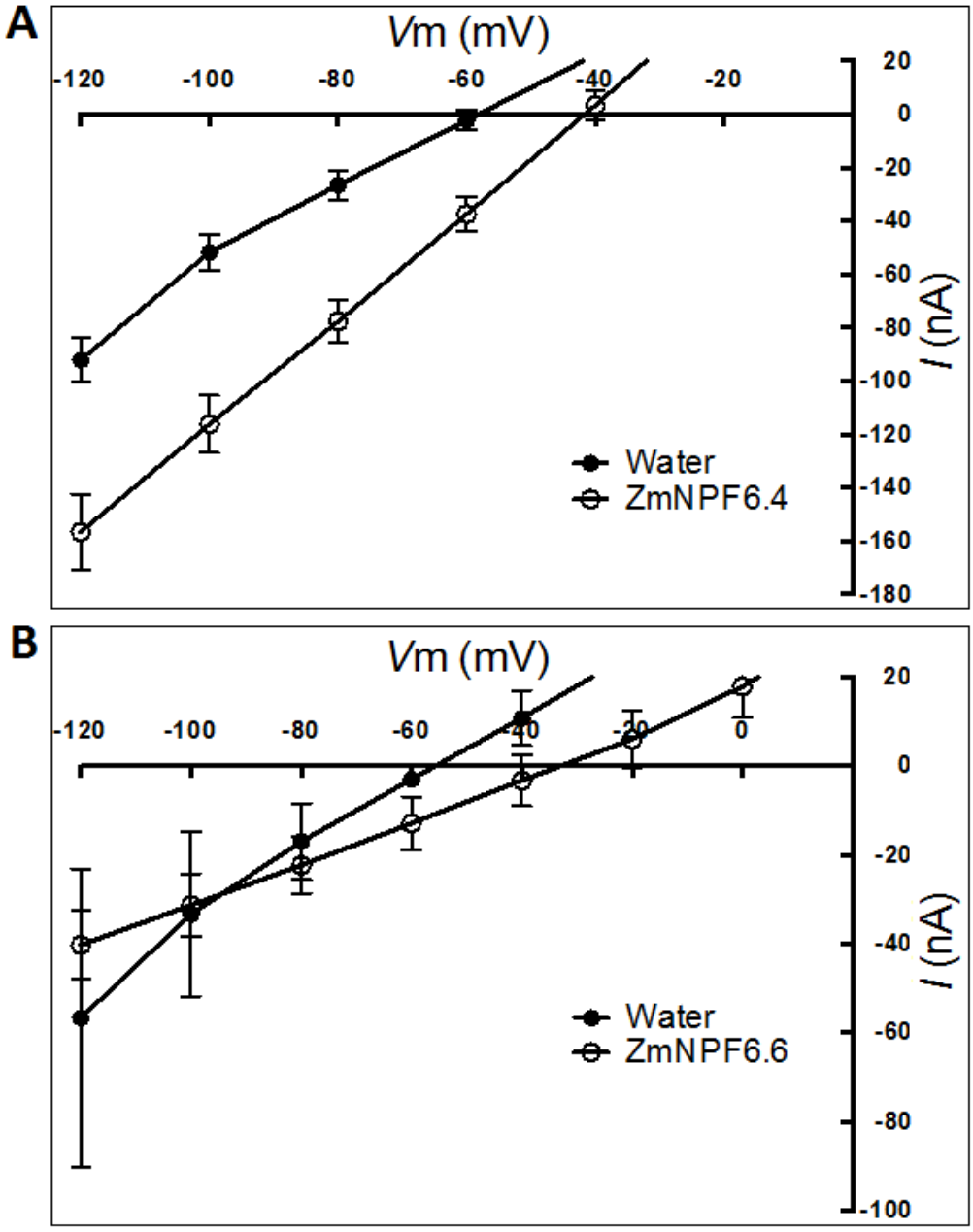

Figure 3.7. Chloride Induced Reversal Potential Shift

A & B. Reversal potential of *ZmNPF6.4* and *ZmNPF6.6*-injected oocytes shift positively from ~−57 mV to ~−41 mV and ~−33 mV, respectively, in chloride basal solution. *ZmNPF6.4* and *ZmNPF6.6*-injected oocytes and water-injected oocytes were voltage clamped from −120 mV to +20 mV with 20 mV increments while perfusing in original base solution containing 0.15 mM Ca^{2+}, 1 mM KCl and 3 mM MES, pH 5.5 adjusted with BIS-TRIS propane, osmolality 230 mmol/kg adjusted with mannitol. Average values and standard errors of the mean were calculated from six replicated oocytes and equivalent results were obtained from three repeat experiments with oocytes derived from different frogs. Error bars indicate ± SEM.

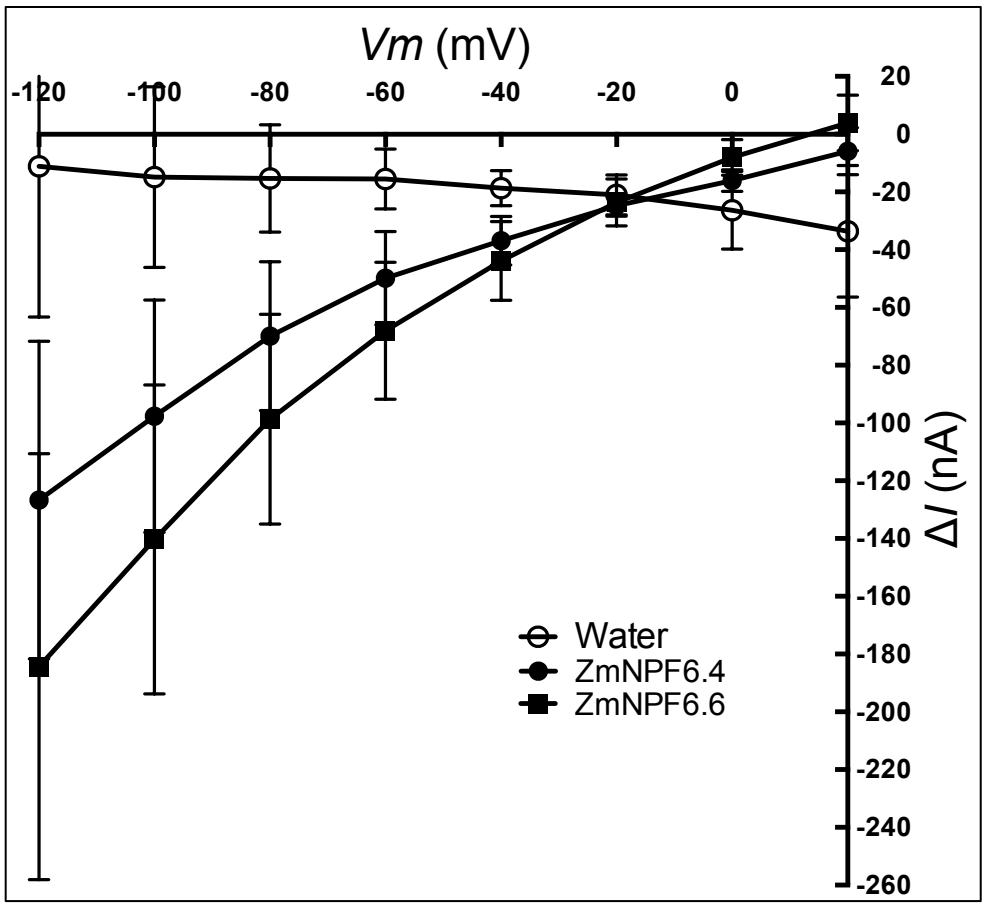

Figure 3.8. Chloride Elicited Current in *ZmNPF6.4* and *ZmNPF6.6*-injected Oocytes

*ZmNPF6.*4 and *ZmNPF6.6*-injected oocytes and water-injected oocytes were voltage clamped from −120mV to +20mV with 20mV increments while perfusing in chloride solution (5 mM chloride, pH 5.5). Currents (Δ*I*) presented here are the substrate-elicited current representing the current change before and after the solution switch from the basal solution to the chloride solution. Average values and standard errors of the mean were calculated from six replicated oocytes and equivalent results were obtained from three repeat experiments with oocytes derived from different frogs. Error bars indicate ± SEM.

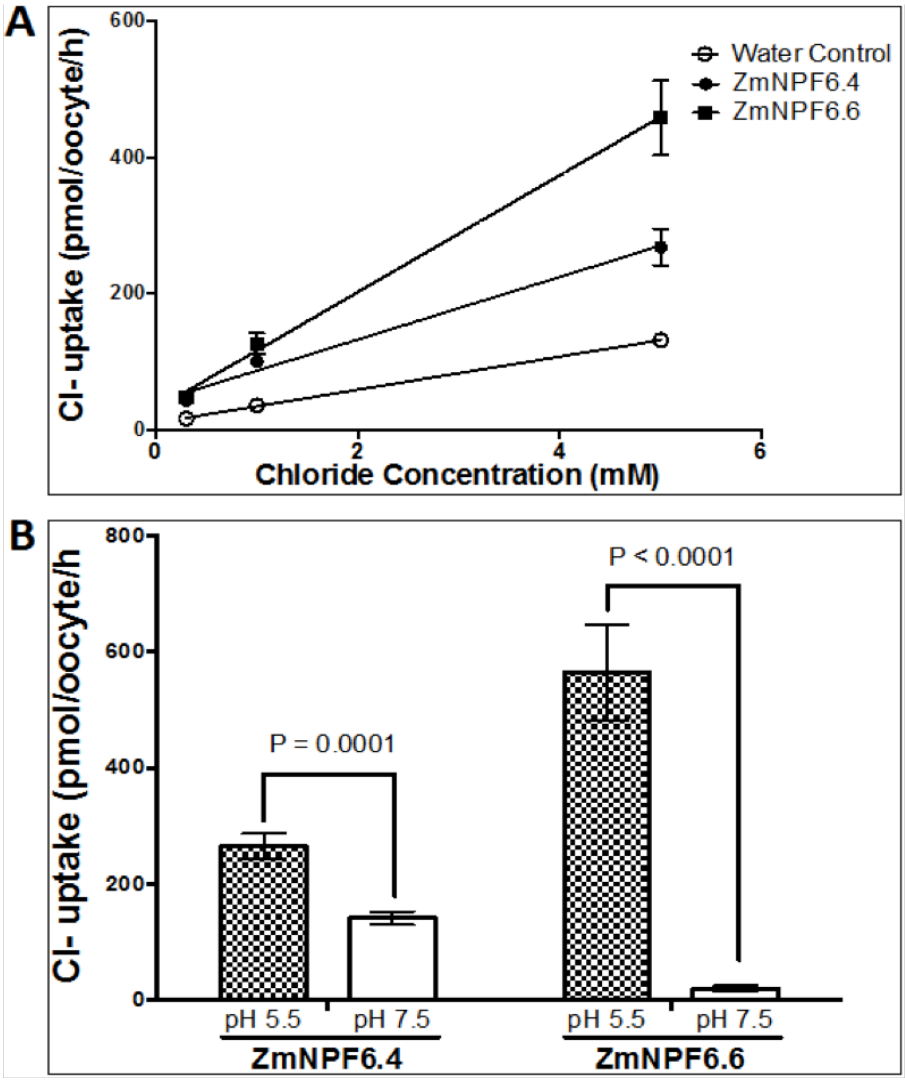

Figure 3.9 Chloride Flux Experiments

A. *ZmNPF6.*4 and *ZmNPF6.6*-injected oocytes accumulate chloride in an un-saturable manner. *ZmNPF6.4* and *ZmNPF6.6*-injected oocytes (and water-injected control oocytes) were incubated in ^{36}Cl labeled chloride solution (0.3 mM, 1 mM or 5 mM, pH 5.5) for 1 hour. **B**. The chloride transport activity of ZmNPF6.4 and ZmNPF6.6 is also pH dependent. *ZmNPF6.4* and *ZmNPF6.6*-injected oocytes (and water-injected control oocytes) were incubated in ^{36}Cl labeled chloride solution (1 mM, pH 5.5 or 7.5) for 1 hour. Accumulated ^{36}Cl was quantified using a liquid scintillation analyzer. In panel B, net chloride uptake values were normalized by subtracting the mean of water control value from the value of *ZmNPFs*-injected groups. Average values and standard errors of the mean were calculated from 8 replicate oocytes and equivalent results were obtained from three repeat experiments with oocytes derived from different frogs. Error bars indicate ± SEM, and asterisks denote significance (*P<0.05) using the unpaired t-test statistical analysis.

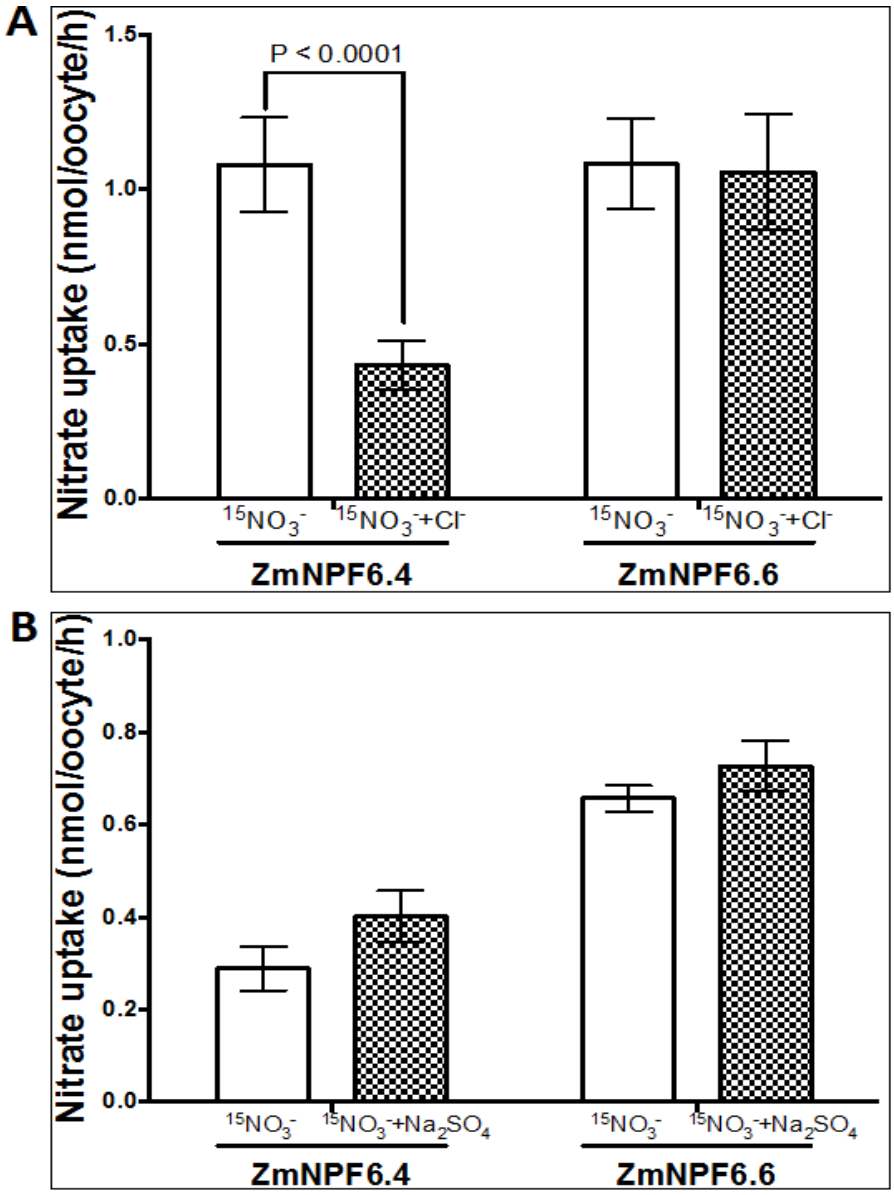

Figure 3.10. ^{15}Nitrate/Chloride Competition Flux Experiments

A. Nitrate uptake of *ZmNPF6.4*-injected oocytes reduced in the presence of chloride. **B**. Sodium (and SO_4^{2-}) does not affect chloride uptake of *ZmNPFs*-injected oocytes. *ZmNPF6.4* and *ZmNPF6.6*-injected oocytes (and water-injected control oocytes) were incubated in ^{15}N labeled nitrate solution (10 mM) supplemented with equal molar concentrations of NaCl (A) or Na_2SO_4 (B), respectively, at pH 5.5 for 1 hour. Accumulated nitrate was quantified using an IRMS. Net nitrate uptake values were normalized by subtracting the mean of the water control value from the value of *ZmNPF*-injected groups. Average values and standard errors of the mean were calculated from 9 replicate oocytes and equivalent results were obtained from three repeat experiments with oocytes derived from different frogs ($P<0.0001$ in unpaired t-test). Error bars indicate ± SEM.

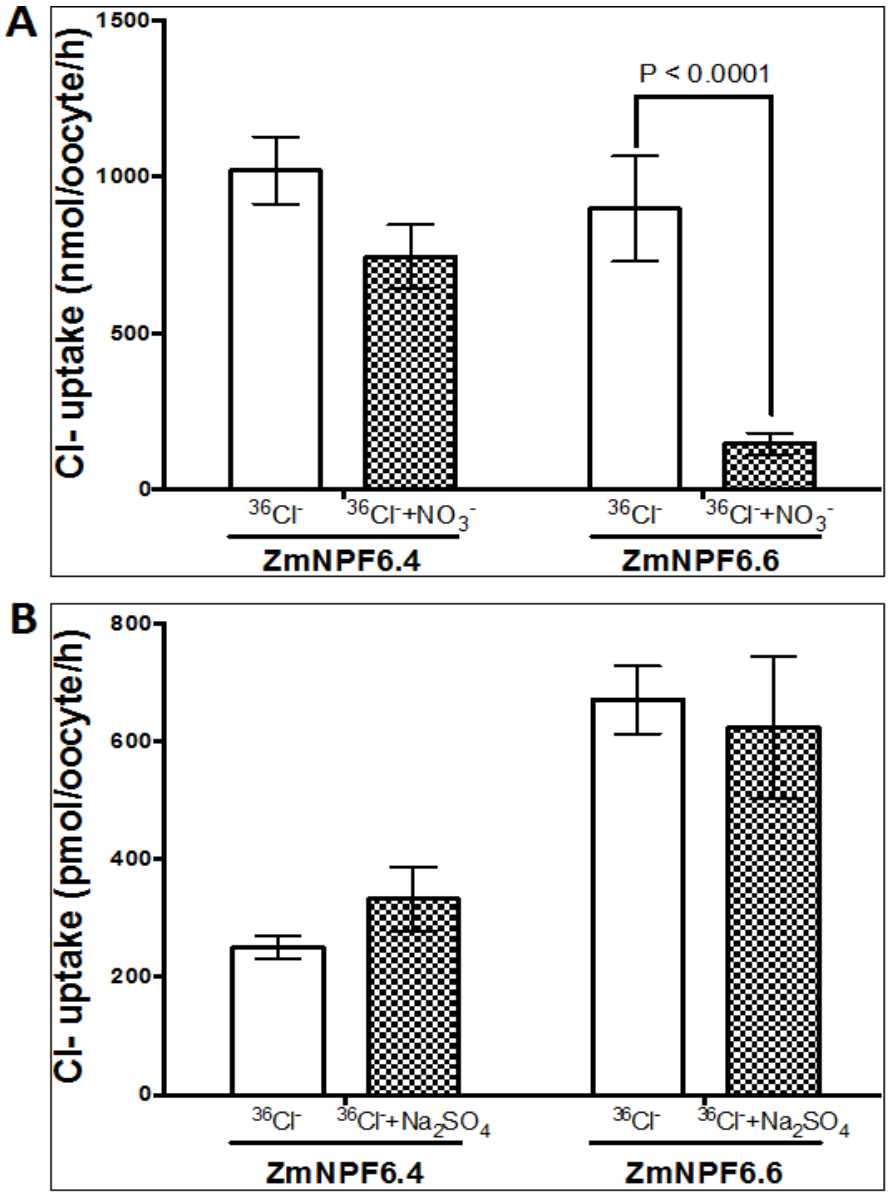

Figure 3.11. ^{36}Chloride/Nitrate Competition Flux Experiments

A. Chloride uptake of *ZmNPF6.6*-injected oocytes was reduced in the presence of nitrate. **B**. Sodium (and SO_4^{2-}) does not influence chloride uptake of *ZmNPFs*-injected oocytes. *ZmNPF6.4* and *ZmNPF6.6*-injected oocytes (and water-injected oocytes) were incubated in ^{36}Cl labeled chloride solution (1 mM) mixed with equal molar concentrations of $NaNO_3$ (A) or Na_2SO_4 (B), at pH 5.5 for 1 hour. Accumulated chloride was quantified by a liquid scintillation analyzer. Net chloride uptake values were normalized by subtracting the mean of water control value from the value of *ZmNPFs*-injected groups. Average values and standard errors of the mean were calculated from 8 replicate oocytes and equivalent results were obtained from three repeat experiments with oocytes derived from different frogs (*P < 0.0001 in unpaired t-test). Error bars indicate ± SEM.

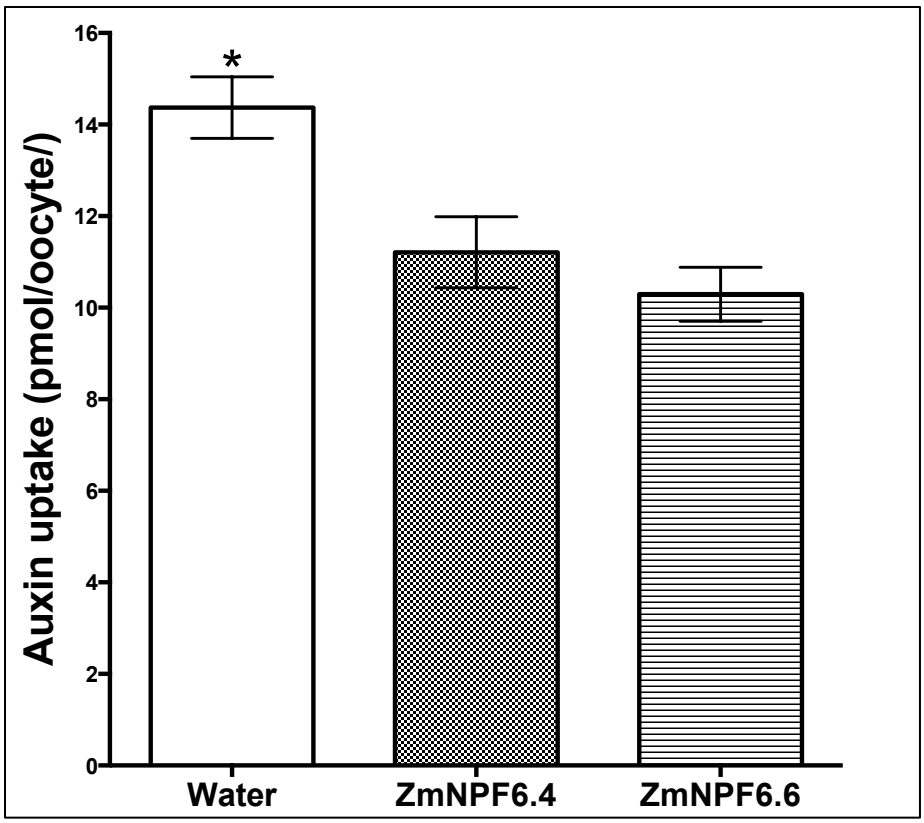

Figure 3.12. ZmNPF6.4 and ZmNPF6.6 Do Not Transport Auxin

ZmNPF6.4, *ZmNPF6.6* and water-injected oocytes were incubated in ^{3}H-labeled IAA solution (10 μM, pH 5.5) for 1 hour and accumulated IAA was quantified using a liquid scintillation analyzer. Average values and standard errors of the mean were calculated from 10 replicate oocytes (*P < 0.005 in ordinary one-way ANOVA test). Error bars indicate ± SEM.

3.3 Materials and Methods

3.3.1 Molecular cloning and cRNA transcription

ZmNPF6.4, *ZmNPF6.5*, *ZmNPF6.6* and *ZmNPF7.10* coding sequences (Section 2.3.4) were sub-cloned into a *Xenopus laevis* oocyte expression vector, *pGEMHE* (Liman et al., 1992), using the LR clonase II (Invitrogen) following the manufacturer's instructions. To linearize cDNA template, *pGEMHE-ZmNPF6.6* was digested with restriction enzyme *Sbf*I and *Sph*I was used to digest the other three constructs. Linearized constructs were then used as templates for *in vitro* cRNA synthesis using the mMESSAGE mMACHINE T7 kit (Ambion). Purified cRNA (using the lithium chloride precipitation method) were quantified and qualified by spectrophotometry (ND-1000 spectrophotometer, Nanodrop) and RNA electrophoresis, respectively.

3.3.2 Oocytes preparation and injection

Oocytes were isolated and prepared by research assistant, Wendy Sullivan, in the lab of Prof. Steve Tyerman. Briefly, a mature female *Xenopus* frog was anesthetized using 0.1% solution of Tricaine (about 5 mins). Two small incisions (~1 cm) were made in the lower abdominal quadrant of the frog using a sterile surgery blade to expose the ovary. The ovary lobes were teased out and immediately transferred to a modified ND96 solution containing 96 mM NaCl, 2 mM KCl, 1 mM $MgCl_2$, 5 mM HEPES, pH7.6. After suturing The incisions of the frog were sutured and then placed in recovery. The isolated ovary lobes were defolliculated with modified ND96 solution supplemented with 1 g/L collagenase type Ia (Sigma) for 30 min to 1 hour. The oocytes were then transferred to a modified Ringers solution containing 96 mM NaCl, 2 mM KCl, 5 mM $MgCl_2$, 5 mM HEPES, 0.6 mM $CaCl_2$, 5% horse serum (Sigma), 1% penicillin-streptomycin (Sigma) and 50 mg/L tetracycline, pH 7.6. At this stage the eggs were ready for selection and injection.

Micropipettes were prepared using a micropipette puller (PP-83, NARISHIGE, Inc.) and a microgrinder (EG-400, NARISHIGE, Inc.). The micropipette was filled with silicon oil and assembled onto the plunger of a Nanoinject II microinjector (3-000-204, Drummond Scientific). After discharging silicon oil, the tip of the micropipette was inserted into the cRNA droplet (~4 μl) placed on a clean Petri dish. The cRNA was slowly loaded into the micropipette to prevent bubble formation inside the micropipette. Oocytes were injected with 46 nl (23 ng) of cRNA or 46 nl water using a Nanoinject II microinjector (Drummond Scientific) setting at the slow mode (23 nl/s) and incubated for 2 days in modified Ringers solution before experiments.

3.3.3 Chemical flux experiment

For nitrate flux experiments, oocytes were washed three times with basal solution (pH 7.5) and transferred to the ^{15}N labeled (10%) nitrate solution (basal solution supplemented with 0.25 mM or 10 mM $Na^{15}NO_3$ (10%, Sigma), pH 5.5 or 7.5). After one hour, oocytes were washed three times with ice-cold basal solution (pH 7.5) and dried individually in tin capsules at 60 °C for 3 days. The capsules were sealed and analyzed for the %N and the $^{14}N/^{15}N$ ratios using an isotope ratio mass spectrometer (Sercon 20-20) coupled to a front-end elemental analyzer (Sercon). In the kinetic study, oocytes were incubated in nitrate solutions with 12 different concentrations (25 μM, 50 μM, 100 μM, 150 μM, 250 μM 400 μM, 1 mM, 2 mM, 5 mM, 10 mM, 20 mM and 30 mM, pH5.5) for one hour.

For chloride flux experiments, similar protocols were used as described in the nitrate flux experiments. Instead of using 10 mM nitrate, only 1mM NaCl was added into the uptake solution to achieve high radioactive specific activity (~3810 Bq/ml). Before each experiment, radioactive $Na^{36}Cl$ (Amersham Biosciences) was added into the uptake solution to a concentration of 0.1% (v/v). After one hour incubation, each oocyte was washed three times with ice-cold basal solution (pH 7.5) and dissolved in 100 ml of 10% SDS in a 5 ml scintillation vial. Incorporated

radioactivity of each oocyte was quantified using a liquid scintillation analyzer (TRI-CARB 2100TR).

For substrate competition flux experiments, equal concentration of unlabeled chloride (or nitrate) was added into ^{15}N nitrate solution (or ^{36}Cl chloride solution). The rest of the method are similar for both nitrate or chloride flux experiments.

To measure auxin influx, the method from Yang et al. (2006) was modified and adopted. Briefly, cRNA injected (or water injected) oocytes were incubated in modified Ringers solution supplemented with 1 μM ^{3}H-IAA (10%, PerkinElmer) for one hour. Each oocyte was then washed three times with ice-cold basal solution (pH 7.5) and dissolved in 100 ml of 10% SDS in a 5 ml scintillation vial. Incorporated radioactivity of each oocyte was quantified using a liquid scintillation analyzer (TRI-CARB 2100TR).

3.3.4 Electrophysiology experiment

For electrophysiological studies, the method by Huang et al. (1999) was adopted but modified. Briefly, oocytes were impaled by two microelectrodes and the membrane potential of each oocyte were measured when perfused in the basal solution (0.15 mM Ca^{2+} and 3 mM MES, pH 7.5 adjusted with BIS-TRIS propane, osmolality 230 mmol/kg adjusted with mannitol). Healthy oocytes, with a membrane potential < −30 mV, were perfused in a similar basal solution at pH 5.5 for approximately 5∼10 min until the membrane potential became stable. Currents were recorded before and after changing the solution from basal solution to either nitrate or chloride solutions (basal solution supplemented with 10mM HNO_3 or 5mM HCl, pH 5.5 or 7.5, osmolality 230 mmol/kg adjusted with mannitol). Oocytes were clamped with 600 ms pulses from −120 mV to +20 mV with 20mV increments. Between each pulse, oocytes were clamped to −40 mV for 180 ms. Nitrate or chloride elicited currents were calculated by subtracting the current recorded in basal solution from the current recorded in nitrate or chloride solution

(as shown in Figure 3.2B shade area), representing the actual current change caused by nitrate or chloride in the single oocyte. Currents were recorded just after first contact with nitrate or chloride solutions to minimize extended incubations which limits substrate elicited currents. Clamping and measurements were achieved using an OC-725 Oocyte Clamp (Warner Instrument) and Digidata 1440A digitizer (Axon) with pCLAMP program, respectively.

3.4 Discussion

From the four putative maize NPF nitrate transporters cloned in Section 2.2.2, ZmNPF6.4 and ZmNPF6.6 were functionally characterized as pH-dependent nitrate transporters. However they differed by their substrate affinities and substrate preferences. *ZmNPF6.4* encodes a low-affinity non-selective nitrate and chloride transporter, while ZmNPF6.6 is a dual-affinity nitrate specific transporter, which can also transport chloride in the absence of nitrate. The expression of *ZmNPF6.5* or *ZmNPF7.10* did not mediate nitrate accumulation in oocytes, suggesting they are not functional nitrate transporters.

The transport activity of ZmNPF6.4 suggests two possible activities in maize. In the first instance, ZmNPF6.4 behaves like a constitutive component of the low-affinity nitrate uptake system (cLATS). In Arabidopsis, AtNPF4.6 is regarded as a member of nitrate cLATS. It mediates low-affinity nitrate transport and is constitutively expressed and not regulated by external supply of nitrate (Huang et al., 1999). ZmNPF6.4 displayed a similar nitrate transport activity, and ZmNPF6.4 was also not regulated by nitrate provision in maize roots (Figure 2.6). Together this data suggests ZmNPF6.4 may have a similar role to AtNPF4.6. Its second function could be related to the transport of chloride into guard cells, In plant leaves, stomatal opening is associated with proton coupled chloride influx across the plasma membrane of guard cells (Cosgrove and Hedrich, 1991; Assmann and Wang, 2001). However, the chloride transporter (a proton/chloride symporter) responsible for this chloride influx has yet to be genetically identified. Given the pH-dependent

chloride transport activity of ZmNPF6.4 and its expression in maize leaves (Figure 2.5A and Sekhon et al. (2011)), the data highlights a possibility it may fulfill this role. Future work needs to define its intercellular localization in leaves and through knockout studies to determine its influence on stomatal opening and closing.

Similar to AtNPF6.3, ZmNPF6.6 is also a dual-affinity nitrate transporter that is predominantly expressed in the root and induced by exogenous nitrate supply (Huang et al., 1996; Liu et al., 1999). ZmNPF6.6 could share a similar role with AtNPF6.3 in mediating both iHATS and iLATS nitrate uptake in maize roots. AtNPF6.3 has also been characterized as a nitrate sensor that regulates gene expression linked to lateral root growth during the primary nitrate response and according to nitrate availability (Remans et al., 2006; Ho et al., 2009). This sensor-like function of AtNPF6.3 was considered to be associated with its auxin transport activity and/or the nitrate inhibition on auxin transport (Krouk et al., 2010). However, a very recent study demonstrated that the membrane mistargeting mutant AtNPF6.3 P492L can still induce the expression of *AtNRT2.1* in the primary nitrate response without transporting auxin or nitrate (Bouguyon et al., 2015). This means that AtNPF6.3's role in modulating either lateral root elongation or gene regulation during the primary nitrate response, are two independent nitrate sensing/transduction mechanisms that coexist in AtNPF6.3 (Bouguyon et al., 2015). There was no auxin transport detected with ZmNPF6.6. This may limit its role in lateral root development in response to nitrate supply. Whether ZmNPF6.6 acts as a nitrate sensor through regulation of gene expression during the primary nitrate response remains unknown and still need to be tested. Both maize and Arabidopsis share a similar primary nitrate response where *ZmNRT2.1* expression in maize lateral roots is induced by nitrate (Liu et al., 2008). Whether the induction of *ZmNRT2.1* is mediated by ZmNPF6.6 still requires further study.

The identification of a dual-affinity activity in ZmNPF6.6 supports the hypothesis of Sun et al. (2014) in that His356 is a key residue in determining dual-affinity

nitrate transport of AtNPF6.3. In contrast, with tyrosine in the equivalent site in ZmNPF6.4 (Tyr370) and in most NPF nitrate transporters, the lack of histidine would suggest that only low-affinity nitrate transport is possible. However, MtNPF6.8, which is another dual-affinity nitrate transporter, which possesses a tyrosine in the equivalent site (Morère-Le Paven et al., 2011). This would suggest dual-affinity, at least, in MtNPF6.8 is different to AtNPF6.3 and ZmNPF6.6. Further research on the crystal structures of ZmNPF6.6 and MtNPF6.8 could help elucidate this discrepancy.

NPF nitrate transporters can transport multiple substrates. For example, the first identified plant nitrate transporter, AtNPF6.3, was later suggested to also transport auxin (Krouk et al., 2010). Other examples of different roles include the nitrate/ABA (abscisic acid) transporter, AtNPF4.6 (also known as AtNRT1.2) and MtNPF6.8, and a nitrate/histidine transporter, BnNRT1.2 (Zhou et al., 1998; Kanno et al., 2012; Pellizzaro et al., 2014). It has been previously suggested that AtNPF6.3 may act as a chloride transporter Schroeder (1994). The results presented here is the first direct evidence of a chloride transport activity in an NPF. Interestingly, it would appear the lack of a histidine residue for tyrosine in the substrate binding/recognition site of ZmNPF6.4, promotes equal affinity to nitrate and chloride. In contrast, ZmNPF6.6 displays high nitrate selectivity over that of chloride. This suggests, that the histidine residue could be responsible for the nitrate selectivity of the NPF nitrate transporter.

No nitrate transport activity was detected from ZmNPF6.5 and ZmNPF7.10 using a ^{15}N-nitrate flux assay. The lack of activity in ZmNPF7.10 could be related to its absence of a predicted 7th TM. This may have influenced activity and or membrane targeting while expressing in *Xenopus* oocytes. The 7th TM in ZmNPF7.10 is also the location of the predicted substrate binding/recognition site discussed previously. Lack of this region would most likely have significant impact on activity.

4 Mutagenesis to Unravel Functional Properties of ZmNPF6.4 and ZmNPF6.6

4.1 Introduction

In the dual-affinity nitrate transporter AtNPF6.3, the switch between the high- and low-affinity activity is believed to involve the phosphorylation of its Thr101 residue (Liu et al., 1999; Liu, 2003). When Thr101 is phosphorylated (or mutated to aspartic acid to partially mimic a phosphorylation response), AtNPF6.3 functions as a high-affinity nitrate transporter, while un-phosphorylated AtNPF6.3 (and phosphorylation-defective T101A mutants) functions as a low-affinity transporter. Recently, two crystal structures of AtNPF6.3 have been produced (Parker and Newstead, 2014; Sun et al., 2014). These studies examined this post-translational modification switch but proposed two alternative mechanisms. Sun et al. (2014) suggested the phosphorylation-controlled dimerization as an important component of the AtNPF6.3 affinity switch. It was proposed that a dimer of two phosphorylated AtNPF6.3 molecules is required for high-affinity nitrate transport. On the other hand, Parker and Newstead (2014) suggest the high-affinity transporter activity of AtNPF6.3 is obtained from an increased flexibility of the transporter caused by Thr101 phosphorylation. In addition, another key residue, His356 was nominated in both studies, as a putative nitrate binding site and quite possibly a participating residue in dual-affinity transport activity determination. The potential functions of this His356 were discussed in the previous chapter and partly supported by evidence derived from the activity differences between ZmNPF6.4 and ZmNPF6.6, including substrate selectivity and substrate affinity. In this chapter, a mutagenic study was conducted on the equivalent Thr101 and His356 residues in ZmNPF6.4 (Thr106 and His370) and

ZmNPF6.6 (Thr104 and His362) to explore their functional role in nitrate transport.

4.2 Results

4.2.1 Thr101/106/104 and the nitrate uptake affinity of AtNPF6.3, ZmNPF6.4 and ZmNPF6.6

To explore the predicted 'affinity switch residue' in the maize dual-affinity nitrate transporter ZmNPF6.6, a mutagenesis experiment was conducted as described by Liu (2003). The equivalent residue of the AtNPF6.3 Thr101 was identified in ZmNPF6.6 as Thr104 (Figure 2.2). It was mutated into either alanine or aspartic acid by generating *pCR8-ZmNPF6.6:T104A* and *pCR8-ZmNPF6.6:T104D* constructs using site-directed mutagenesis (mutagenic PCR primers are listed in Table 4.1). Sequence verified cDNA was sub-cloned into *pGEMHE* vector for cRNA synthesis. Nitrate flux experiments were preformed using *Xenopus* oocytes injected with wild type cRNA or water as a control. Since the affinity switch residue Thr101 is also conserved in the low-affinity transporter ZmNPF6.4 (Figure 2.2), the equivalent Thr106 in ZmNPF6.4 was also converted to T106A and T106D and included in the experiments.

Unexpectedly, neither the T104A nor T104D mutations changed the affinity of ZmNPF6.6 as previously observed with T101A or T101D in AtNPF6.3. The high-affinity nitrate transport activity of ZmNPF6.6 was reduced but not abolished in the dephosphorylation mimic T104A (Figure 4.1A). There was no change to high-affinity transport activity in the phosphorylation mimic mutant T104D (Figure 4.1A). At elevated nitrate concentrations (10 mM, low-affinity range), nitrate transport in T1014A and T104D were both reduced (Figure 4.1B). However, when the high-affinity uptake values (0.25 mM) (Figure 4.1A) was subtracted from the low-affinity measurements (Figure 4.1B), the resulting net low-affinity flux of ZmNPF6.6:T104A is equivalent to the water injected controls (Figure 4.1C). Overall

this data suggests that both the high-affinity and low-affinity transport activities were being influenced in both mutants (T104A, T104D) and that low-affinity transport activity in particular is the most compromised.

With ZmNPF6.4, there is no recognizable high-affinity transport activity (see Chapter 3, Figure 3.5A). Neither T106A or T106D could create a high-affinity transport activity in ZmNPF6.4 (Figure 4.2A). Similar to ZmNPF6.6, the low-affinity transport activity was abolished in both T106A and T106D mutations (Figure 4.2B and 4.2C).

Given that no maize NPF mutant behaved in a similar manner to that of Liu et al., (2003), I re-tested the function of Thr101 in AtNPF6.3 by creating AtNPF6.3:T101A and AtNPF6.3:T101D mutants for expression in *Xenopus* oocytes. Surprisingly, both T101A and T101D reduced the high- and low-affinity nitrate transport rates of AtNPF6.3 (Figure 4.3). When the high-affinity uptake values is subtracted from the low-affinity transport values, the data indicates the net low-affinity transport activity was also abolished by the mutations, similar to ZmNPF6.4 and ZmNPF6.6. It's unclear why T101A and T101D mutant activities were different to those already published by Liu et al., (2003). Differences between oocytes and/or levels of endogenous phosphorylation levels may be involved.

4.2.2 His370/362 and the nitrate transport affinity of ZmNPF6.4 and ZmNPF6.6

The alignment of the amino acid sequences of ZmNPF6.4, ZmNPF6.6 and AtNPF6.3 showed that the putative nitrate substrate-binding site, His356, was not conserved in ZmNPF6.4 (Figure 2.2). Instead, ZmNPF6.4 harbored a tyrosine (Tyr370) instead of a histidine residue common with both ZmNPF6.6 and AtNPF6.3. However, ZmNPF6.4 and ZmNPF6.6 were capable of nitrate transport albeit with clearly different activities. The recent release of two crystal structures of AtNPF6.3 has allowed the structural model of ZmNPF6.4 and ZmNPF6.6 to be predicted by homology modeling. Using the SWISS-MODEL server, ZmNPF6.4 and ZmNPF6.6

were threaded against the apo structure of AtNPF6.3 (Protein Data Bank accession code 4cl4) (Arnold et al., 2006; Guex et al., 2009; Kiefer et al., 2009; Biasini et al., 2014; Parker and Newstead, 2014). The predicted models show that each protein contains 12 transmembrane helices and a large hydrophilic loop between the 6th and the 7th transmembrane helix (Figure 4.4 and 4.5). This structure supports the prediction based on the sequence alignment of NPF nitrate transporters described in Section 2.2.2. Similar to AtNPF6.3 His356, both Tyr370 and His362 are localized on the 7th transmembrane helix of ZmNPF6.4 and ZmNPF6.6, respectively. This position is located within the center of the substrate-binding pocket (Figure 4.6). This location suggests that the charged residue, ZmNPF6.6 His362, may share the same function of the His365 in AtNPF6.3 in stabilizing the substrate within the pocket through a predicted electrostatic interaction (Sun et al., 2014). However, with a hydrophobic side chain, Tyr370 is unlikely to allow binding of nitrate in ZmNPF6.4. Combined with the functional differences between these two transporters (low-affinity vs. dual-affinity and NO_3^-/ Cl^- non-selective vs. NO_3^- specific), one possible explanation is that histidine is a key residue for the dual-affinity nitrate transport activity and high nitrate selectivity of ZmNPF6.6.

To test this hypothesis, the Tyr370 residue in ZmNPF6.4 was mutated to histidine (mutagenic primers are listed in Table 4.1) with the expectation that the Y370H substitution would create a dual-affinity nitrate transport activity in ZmNPF6.4. The mutant construct *pCR8-ZmNPF6.4:Y370H* was generated as described in Section 4.2.1 and nitrate flux experiments (250 μM or 10 mM, pH 5.5) were performed with *ZmNPF6.4:Y370H*-injected oocytes. In addition, a second construct, *pCR8-ZmNPF6.4:Y370A*, was also generated and included in these experiments as a negative control. It was assumed the alanine substitution would help abolish the activity of the transporter as has been previously shown (Parker and Newstead, 2014; Sun et al., 2014). *ZmNPF6.4:Y370H*-injected oocytes were able to accumulate nitrate in both the high and low-affinity range, suggesting a dual-affinity nitrate transport activity created by the Y370H substitution. In the high-affinity range

(from 25 μM to 250 μM), the nitrate uptake values of *ZmNPF6.4:Y370H*-injected oocytes fitted into a saturable curve using the Michaelis-Menten equation. The calculated *K*m was ~100 μM. This is a similar *K*m to ZmNPF6.6 (and AtNPF6.3) (Figure 4.7C). These results suggest that the histidine residue is important for high-affinity transport activity in the ZmNPF proteins. Another mutagenesis study was conducted, in which the ZmNPF6.6 His362 residue was mutated into a tyrosine (primers are listed in Table 4.1). However, instead of converting the dual-affinity transporter into a low-affinity one, the H362Y substitution totally abolished the activity of ZmNPF6.6 (Figure 4.8).

4.2.3 Tyr370 and the substrate specificity of ZmNPF6.4

To determine if the histidine residue is also responsible for the substrate selectivity of NPF transporters, substrate competition flux experiments were performed with ZmNPF6.4:Y370H mutant. In a ^{15}nitrate/chloride competition experiment, chloride supplementation no longer decreased the nitrate transport capacity of ZmNPF6.4:Y370H (Figure 4.9A). In the ^{36}chloride/nitrate competition experiments, the Y370H substitution enabled *ZmNPF6.4:Y370H*-injected oocytes to reduce their chloride uptake through nitrate supplementation by ~77%. In these two substrate competition experiments, the Y370H mutated version ZmNPF6.4 behaved similar to the ZmNPF6.6 in Section 3.2.4, suggesting the Y370H substitution created an enhanced nitrate selectivity in the NO_3^-/Cl^- non-selective transporter ZmNPF6.4.

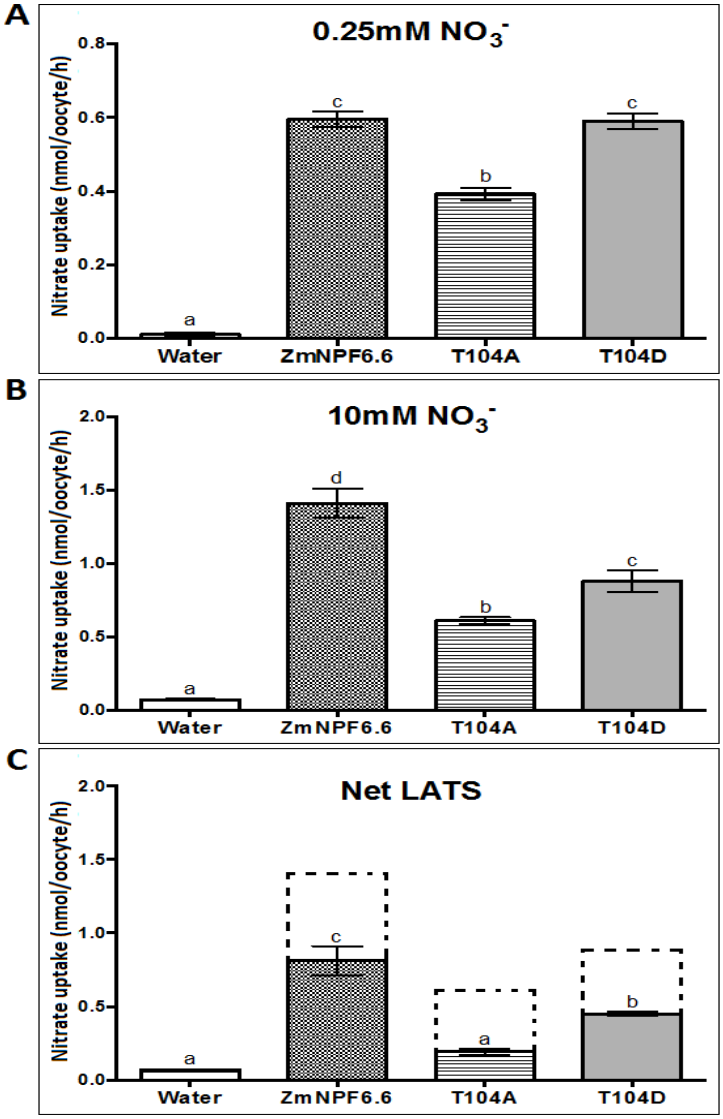

Figure 4.1. Nitrate Flux Experiments of ZmNPF6.6, ZmNPF6.6:T104A and ZmNPF6.6:T104D.

ZmNPF6.6, *ZmNPF6.6:T104A*, *ZmNPF6.6:T104D* and water-injected oocytes were incubated in ^{15}N labeled nitrate solutions (0.25 mM or 10 mM, pH 5.5) for 1 hour. Accumulated ^{15}N-nitrate was quantified by an IRMS. **A**. The dephosphorylation mimic mutation T104A partially disrupted the high-affinity transport activity of ZmNPF6.6. **B** and **C**. The ZmNPF6.6 low-affinity activity was abolished by T104A mutation and partially disrupted by the phosphorylation mutation T104D. Panel **C** represents the net low-affinity transport activities of ZmNPF6.6 and mutants by subtracting the high-affinity uptake values (blank area) from the low-affinity uptake values. Data represents mean ± SEM (n=10 oocytes). Equivalent results were obtained from three repeat experiments with oocytes derived from different frogs. Where indicated with different letters the averages are significantly different (one-way ANOVA test, $p<0.05$).

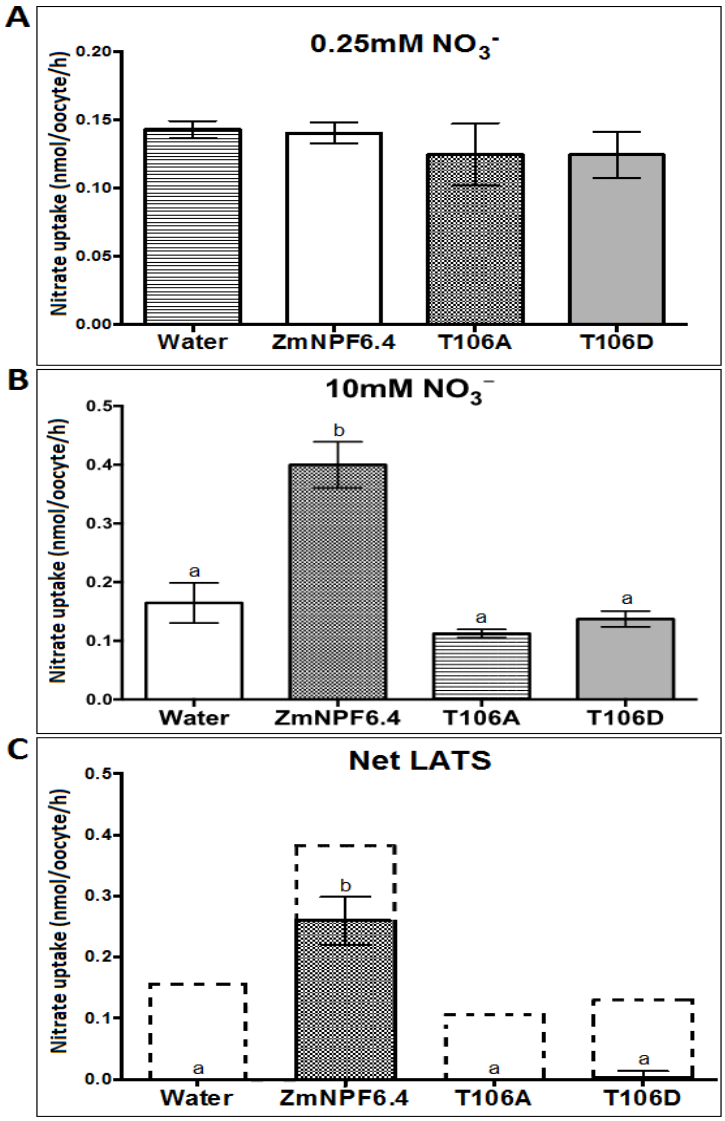

Figure 4.2. Nitrate Flux Experiments of ZmNPF6.4, ZmNPF6.4:T106A and ZmNPF6.4:T106D.

ZmNPF6.4, *ZmNPF6.4:T106A*, *ZmNPF6.4:T106D* and water-injected oocytes were incubated in ^{15}N labeled nitrate solutions (0.25 mM or 10 mM, pH 5.5) for 1 hour. Accumulated ^{15}N-nitrate was quantified by an IRMS. **A**. The phosphorylation mimic mutation T106D does not enhance high-affinity transport activity in ZmNPF6.4. **B** and **C**. The ZmNPF6.4 low-affinity activity was abolished by the dephosphorylation mutation T106A and phosphorylation mutation T106D. Panel **C** represents the net low-affinity activities of ZmNPF6.4 and mutants by subtracting the high-affinity uptake values (blank area) from the low-affinity uptake values. Data represents mean ± SEM (n=10 oocytes). Equivalent results were obtained from three repeat experiments with oocytes derived from different frogs. Where indicated with different letters the averages are significantly different (one-way ANOVA test, $p<0.05$).

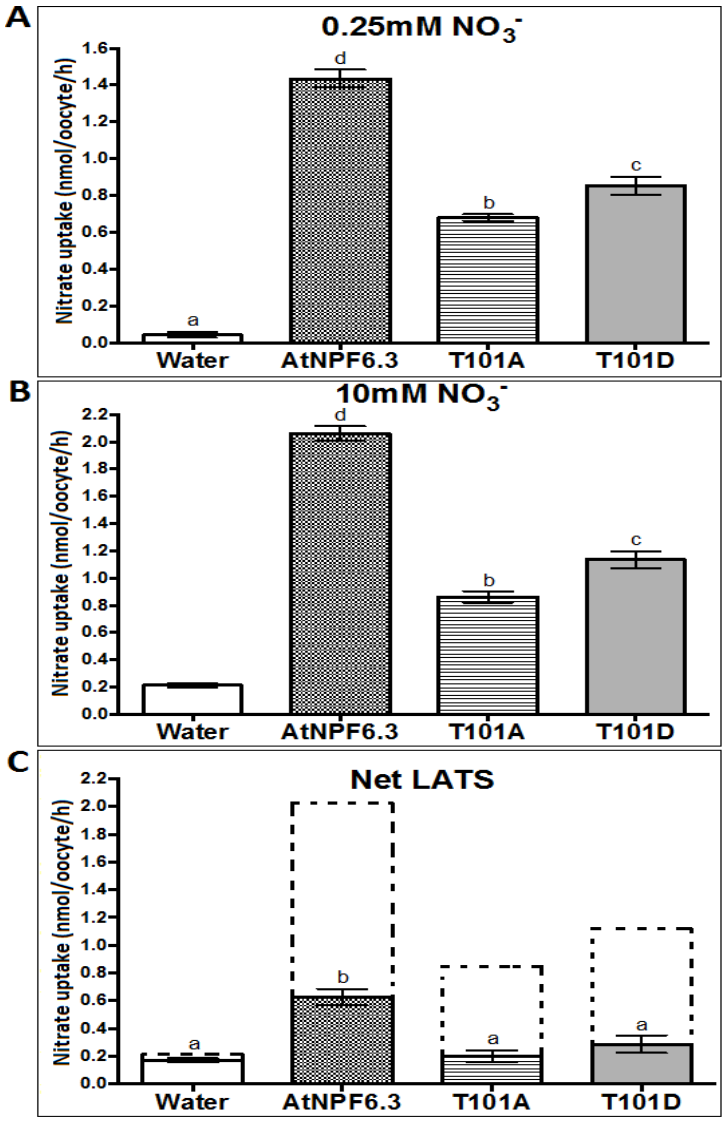

Figure 4.3. Nitrate Flux Experiments of AtNPF6.3, AtNPF6.3 T101A and AtNPF6.3 101D

AtNPF6.3, *AtNPF6.3:T101A*, *AtNPF6.3:T101D* and water-injected oocytes were incubated in ^{15}N labeled nitrate solutions (0.25 mM or 10 mM, pH 5.5) for 1 hour. Accumulated ^{15}N-nitrate was quantified by an IRMS. **A**. The dephosphorylation mimic mutation T101A and phosphorylation mutation T101D partially disrupted the high-affinity activity of AtNPF6.3. **B** and **C**. The AtNPF6.3 low-affinity activity was abolished by T104A and T104D mutations. Panel **C** represents the net low-affinity transport activities of AtNPF6.3 and mutants by subtracting the high-affinity uptake values (blank area) from the low-affinity uptake values. Data represents mean ± SEM (n=10 oocytes). Equivalent results were obtained from three repeat experiments with oocytes derived from different frogs. Where indicated with different letters the averages are significantly different (one-way ANOVA test, $p<0.05$).

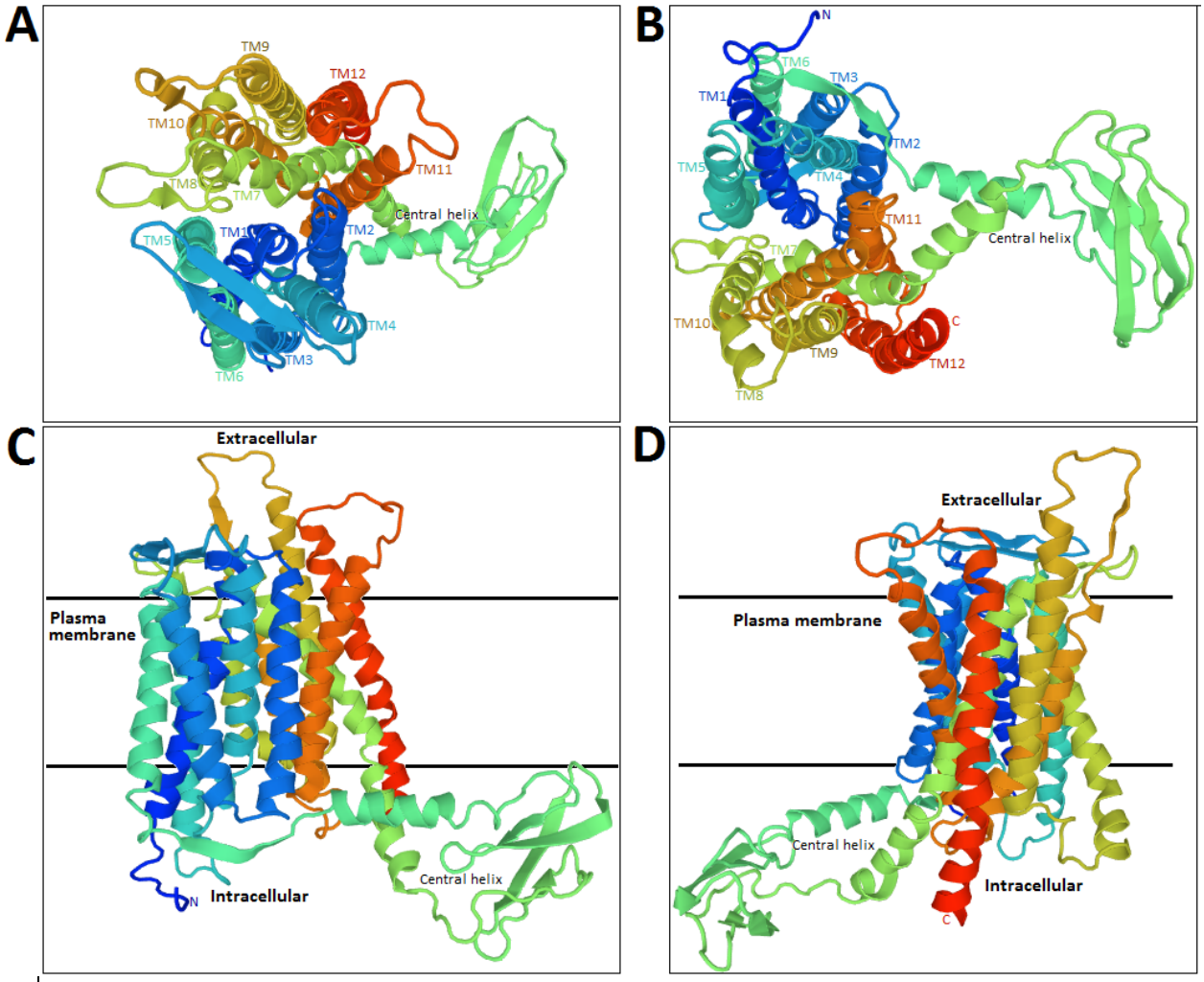

Figure 4.4. Cartoon Representation of the Crystal Structure of ZmNPF6.4

Vertical view (**A** and **B**) and side view (**C** and **D**)of a predicted structural model of ZmNPF6.4. Transmembrane domains (TM) 1-12 are colored blue at the amino terminus to red at the carboxy terminus. The structure was generated using SWISS-MODEL server against the template of the apo structure of AtNPF6.3 (Protein Data Bank accession code 4cl4). The structures were visualized using the PV JavaScript Protein Viewer.

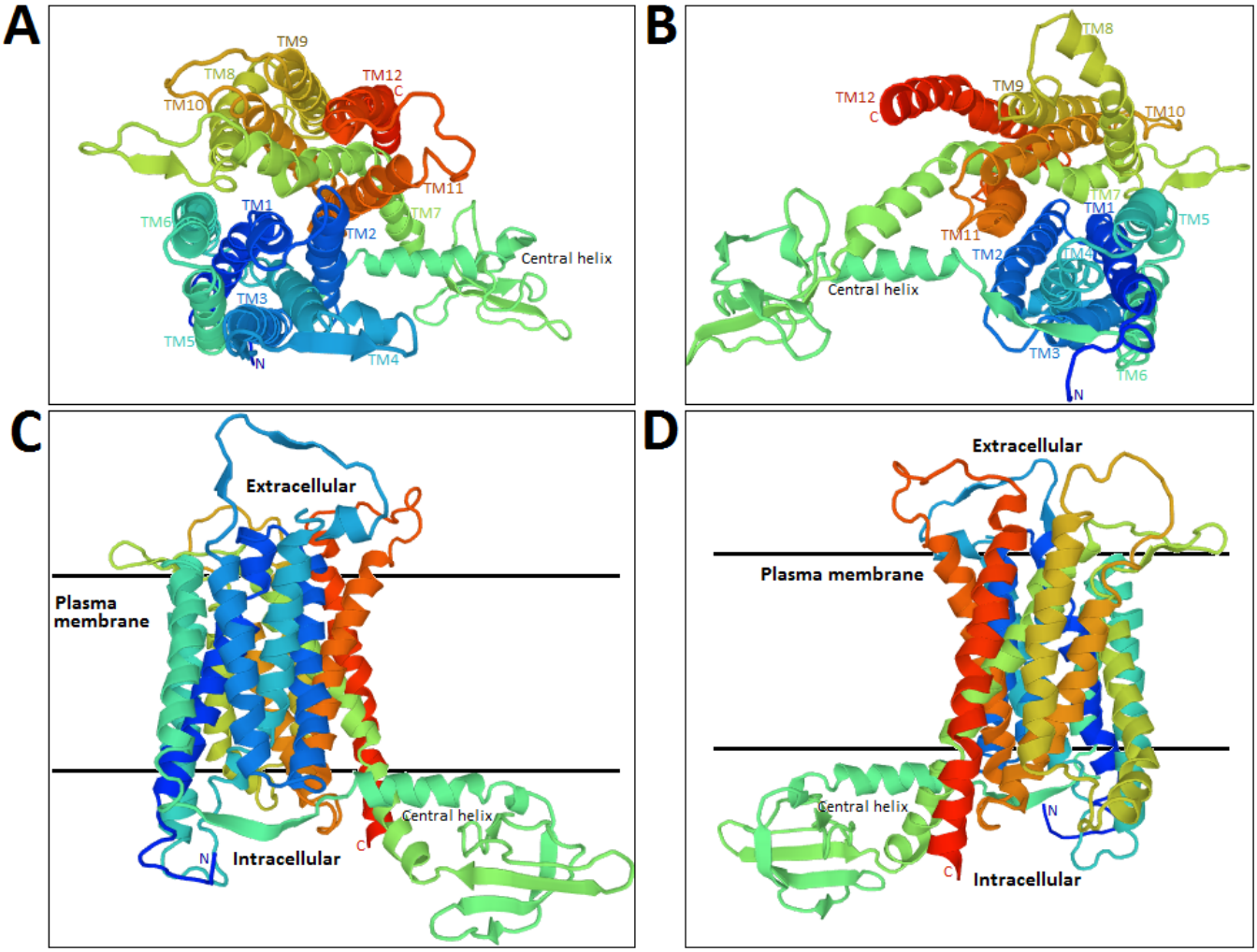

Figure 4.5. Cartoon Representation of the Crystal Structure of ZmNPF6.6

Vertical view (**A** and **B**) and side view (**C** and **D**) of a predicted structural model of ZmNPF6.6. Transmembrane domains (TM) 1-12 are colored blue at the amino terminus to red at the carboxy terminus. The structure was generated using SWISS-MODEL server against the template of the apo structure of AtNPF6.3 (Protein Data Bank accession code 4cl4). The structures were visualized using the PV JavaScript Protein Viewer.

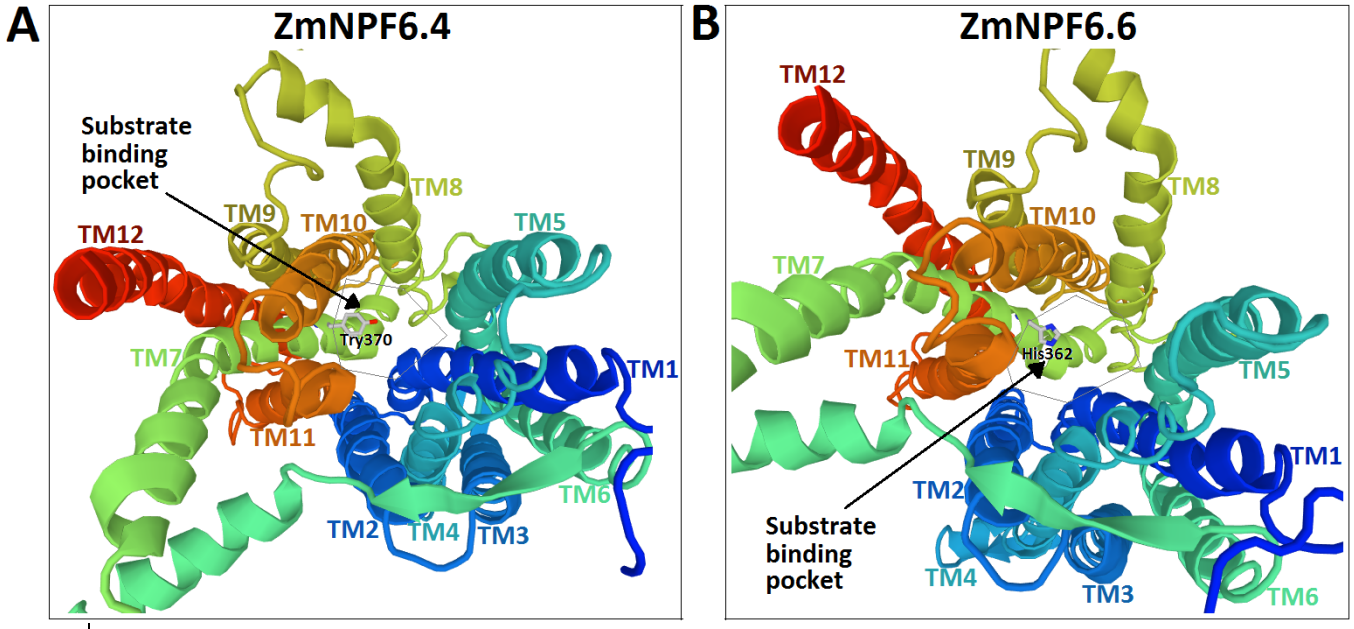

Figure 4.6. ZmNPF6.4 (Tyr370) and ZmNPF6.6 (His362) Localized to the 7th TM and Location relative to the Center of the Substrate-Binding Pocket

Vertical views of predicted structural models of ZmNPF6.4 (**A**) and ZmNPF6.6 (**B**) from the intracellular side. Arrow and grey circle indicate the substrate-binding pocket and the putative substrate-binding site, Tyr370 and His362 (in ZmNPF6.4 and ZmNPF6.6 respectively). Transmembrane domains (TM) 1-12 are colored blue at the amino terminus to red at the carboxy terminus. The structures were visualized using the PV JavaScript Protein Viewer.

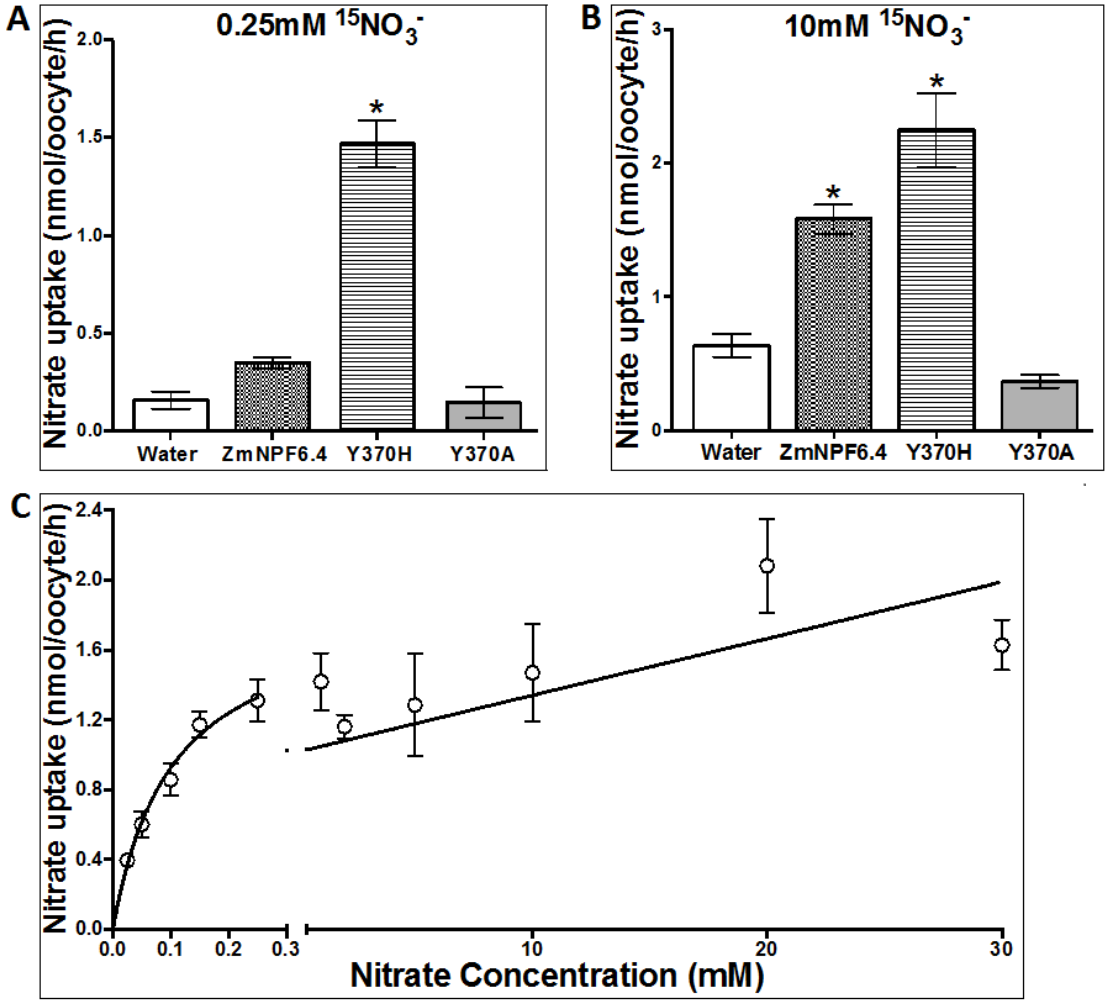

Figure 4.7. Nitrate uptake by the ZmNPF6.4:Y370H Mutant

A. The Y370H mutation conferred high-affinity nitrate transport activity in ZmNPF6.4. **B**. The Y370H mutation does not affect the low-affinity nitrate transport activity in ZmNPF6.4. **C**. Kinetic study of ZmNPF6.4:Y370H. *ZmNPF6.4* and *ZmNPF6.4:Y370H*-injected oocytes (and water-injected controls) were incubated in a ^{15}N labeled nitrate solutions (25 µM to 30mM, pH 5.5) for 1 hour. Accumulated nitrate was quantified using an IRMS. In panel C, net nitrate uptake values were normalized by subtracting the mean of the water-injected control from the value of *ZmNPF6.4:Y370H*-injected oocytes. The nitrate uptake values from 25 µM to 250 µM are fitted with the Michaelis-Menten equation. Values from 400 µM to 30mM were fitted into a linear model using software Prism 6 (Graphpad Software, Inc., USA). Average values and standard errors of the mean were calculated from 9 replicate oocytes. Data presented represents equivalent results from two independent experiments obtained from oocytes of different frogs. Error bars indicate ± SEM, and asterisks denote significance from the water-injected controls (*P<0.05) using the unpaired one-way ANOVA analysis.

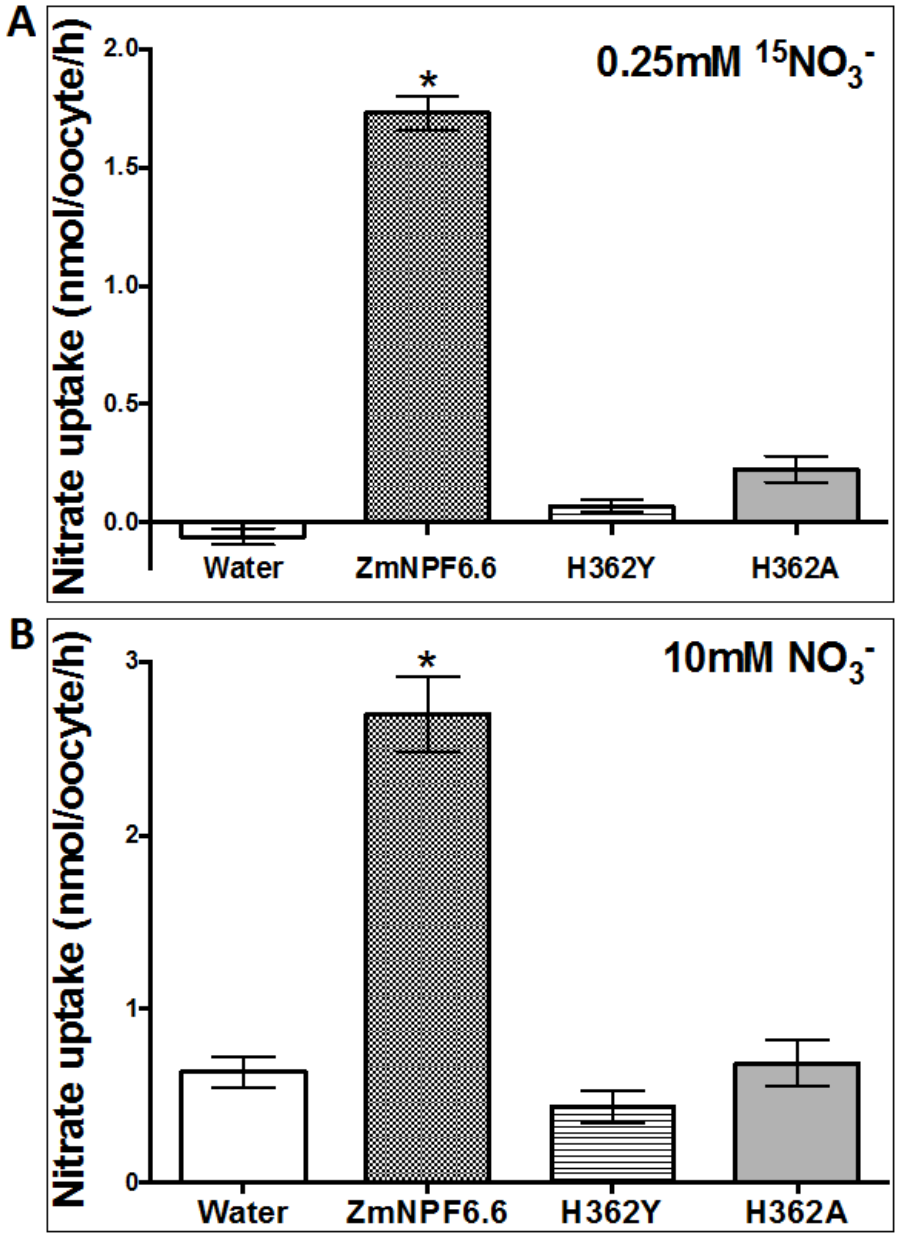

Figure 4.8. Nitrate uptake by ZmNPF6.6:H362Y

The H362Y and H362A mutation abolished the high-affinity (**A**) and low-affinity (**B**) nitrate transport activity of ZmNPF6.6. *ZmNPF6.6*, *ZmNPF6.6:H362Y*, *ZmNPF6.6:H362Y*A and water-injected oocytes were incubated in nitrate solution (250 µM or 10 mM, pH 5.5) for 1 hour. Accumulated nitrate was quantified by an IRMS. Average values and standard errors of the mean were calculated from 9 replicate oocytes and equivalent results were obtained from three repeat experiments. Error bars indicate ± SEM, and asterisks denote significance from the water-injected controls (*P<0.05) using the unpaired one-way ANOVA analysis.

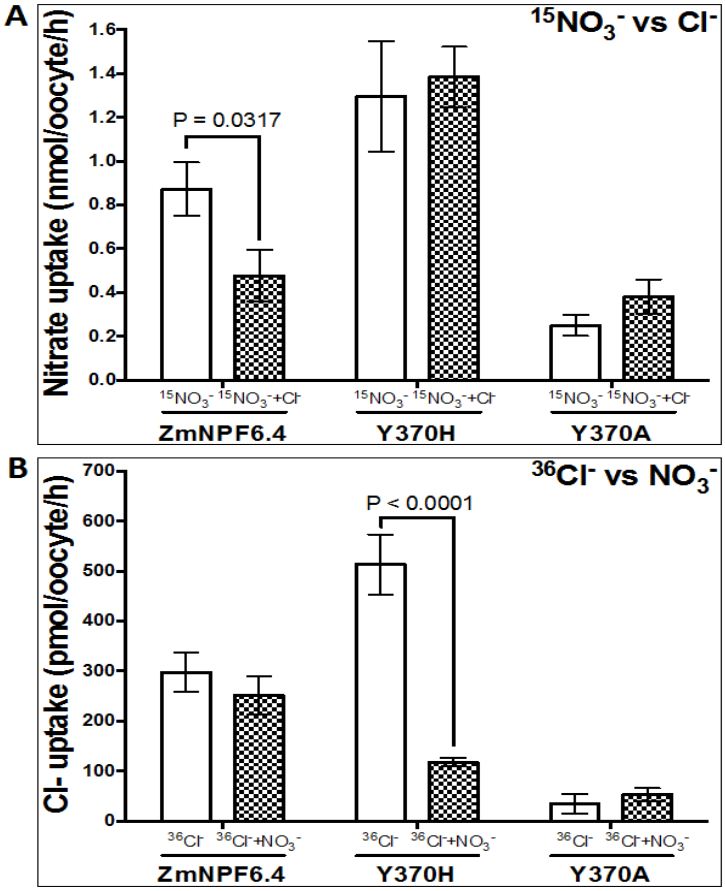

Figure 4.9. Competition between Nitrate and Chloride in ZmNPF6.4:Y370H-injected Oocytes.

A. ^{15}Nitrate/chloride competition flux experiment of ZmNPF6.4:Y370H. **B**. ^{36}Chloride/nitrate competition flux experiment of ZmNPF6.4:Y370H. The Y370H mutation abolished the chloride transport activity in the presence of equimolar concentrations of nitrate in ZmNPF6.4. In the $^{15}NO_3^-$/Cl$^-$ competition flux experiment (A), *ZmNPF6.4* and *ZmNPF6.4 Y370H*-injected oocytes (and water-injected control oocytes) were incubated in ^{15}N labeled nitrate solution supplemented with an equal concentration of chloride at pH 5.5 for 1 hour. Accumulated nitrate was quantified by an IRMS. For $^{36}Cl^-/NO_3^-$ competition experiments (B), *ZmNPF6.4* and *ZmNPF6.4:Y370H*-injected oocytes (and water-injected controls) were incubated in ^{36}Cl labeled chloride solution supplemented with equimolar concentrations of nitrate at pH 5.5 for 1 hour. A liquid scintillation analyzer was used to quantify accumulated chloride. Net uptake values were normalized by subtracting the mean of the water control value from the value of *ZmNPFs*-injected groups. Average values and standard errors of the mean were calculated from 8 replicate oocytes and equivalent results were obtained from three repeat experiments with oocytes derived from different frogs. Error bars indicate ± SEM, and asterisks denote significance from the water-injected controls (*P<0.05) using the unpaired one-way ANOVA analysis.

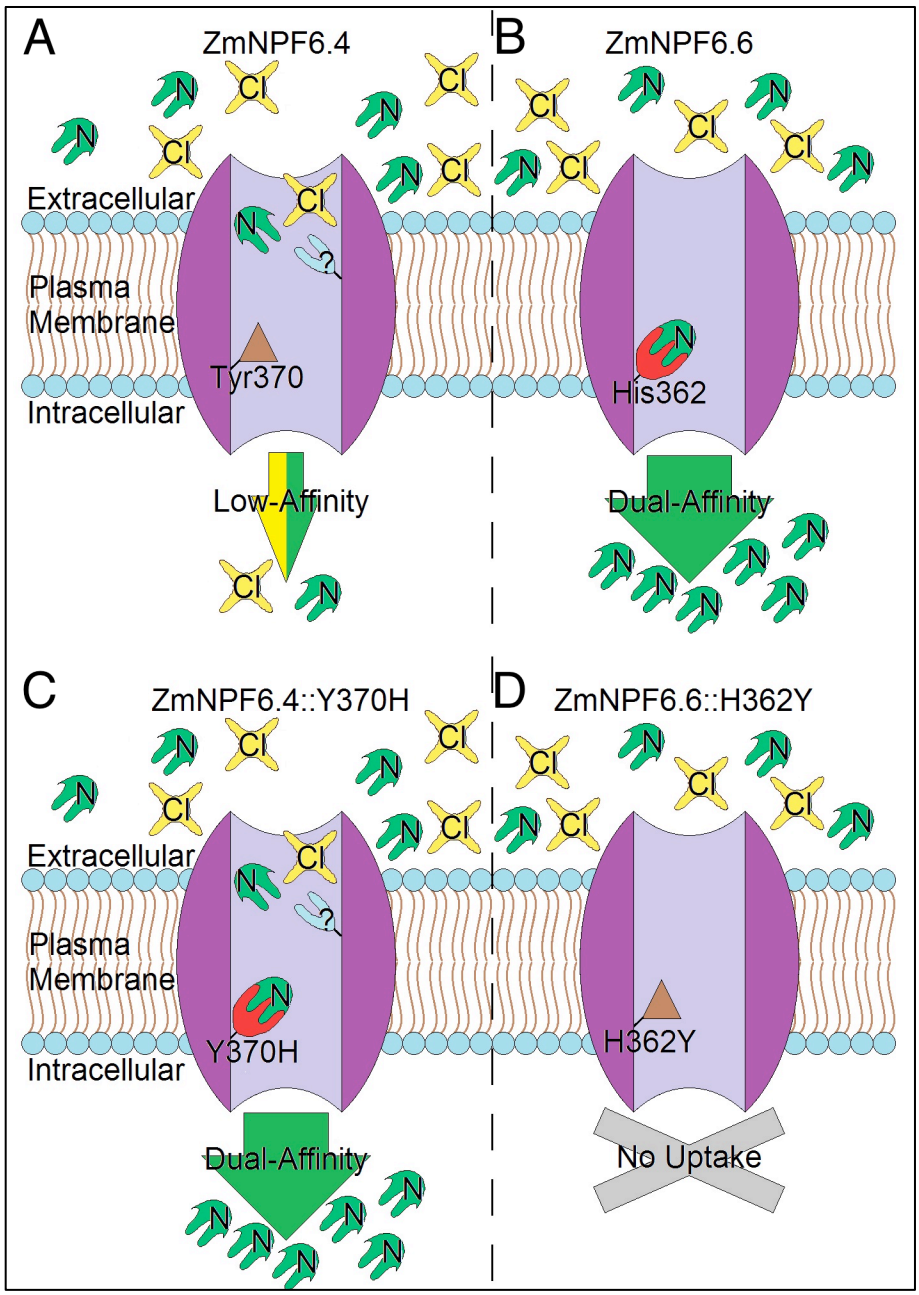

Figure 4.10. ZmNPF Activity Model

A. ZmNPF6.4 can transport nitrate and chloride in a low-affinity manner through a predicted binding site (indicated by the question mark). **B.** The His362 in ZmNPF6.6 has a higher affinity to nitrate over chloride, enabling the protein to selectively transport nitrate in a dual-affinity manner. **C.** The substitution of Y370H conferred ZmNPF6.4 a dual-affinity activity and nitrate selectivity. **D.** The H362Y substitution disrupts the function of ZmNPF6.6 since it does not harbor a second substrate binding site.

ZmNPF6.4 T106A Forward Primer	CCTCGGCCGCTACCTCGCGATCGCCATCTTCACC
ZmNPF6.4 T106A Reverse Primer	GGTGAAGATGGCGATCGCGAGGTAGCGGCCGAGG
ZmNPF6.4 T106D Forward Primer	CCTCGGCCGCTACCTCGATATCGCCATCTTCACC
ZmNPF6.4 T106D Reverse Primer	GGTGAAGATGGCGATATCGAGGTAGCGGCCGAGG
ZmNPF6.6 T104A Forward Primer	GGCCGCTACCTCGCCATCGCCATCTTC
ZmNPF6.6 T104A Reverse Primer	GAAGATGGCGATGGCGAGGTAGCGGCC
ZmNPF6.6 T104D Forward Primer	GGCCGCTACCTCGACATCGCCATCTTC
ZmNPF6.6 T104D Reverse Primer	GAAGATGGCGATGTCGAGGTAGCGGCC
AtNPF6.3 T101A Forward Primer	GGCAGGTACCTAGCGATTGCTATATTC
AtNPF6.3 T101A Reverse Primer	GAATATAGCAATCGCTAGGTACCTGCC
AtNPF6.3 T101D Forward Primer	GGCAGGTACCTAGATATTGCTATATTC
AtNPF6.3 T101D Reverse Primer	GAATATAGCAATATCTAGGTACCTGCC
ZmNPF6.4 Y370H Forward	GTTCTGGACGGTGCACGCGCAGATGAC
ZmNPF6.4 Y370H Reverse	GTCATCTGCGCGTGCACCGTCCAGAAC
ZmNPF6.4 Y370A Forward	GTTCTGGACGGTGGCCGCGCAGATGAC
ZmNPF6.4 Y370A Reverse	GTCATCTGCGCGGCCACCGTCCAGAAC
ZmNPF6.6 H362Y Forward	GTTCTGGACCATCTACGCGCAGATGAC
ZmNPF6.6 H362Y Reverse	GTCATCTGCGCGTAGATGGTCCAGAAC
ZmNPF6.6 H362A Forward	GTTCTGGACCATCGCCGCGCAGATGAC
ZmNPF6.6 H362A Reverse	GTCATCTGCGCGGCGATGGTCCAGAAC

Table 4.1. Primers used in Mutagenesis Studies

4.3 Materials and Methods

4.3.1 Mutagenesis PCR, cRNA transcription and injection

pCR8-ZmNPF6.4:T106A, *pCR8-ZmNPF6.4:T106D*, *pCR8-ZmNPF6.6:T104A*, *pCR8-ZmNPF6.6:T104D*, *pCR8-ZmNPF6.4:Y370H*, *pCR8-ZmNPF6.4:Y370A*, *pCR8-ZmNPF6.6:H362Y*, *pCR8-ZmNPF6.6:H362A* constructs were generated using Phusion polymerase (Thermo Scientific) alongside a point-directed mutagenesis PCR technique (mutagenic primers are listed in Table 4.1). For *pCR8-ZmNPF6.4* and *pCR8-ZmNPF6.6*, high GC contents required the addition of DMSO into the PCR reaction to a final concentration of 4% (v/v). The mutagenesis PCR products were sub-cloned into the *pGEMHE* vector and directly transformed into *E. coli* XL1 Blue strain. *pGEMHE-ZmNPF6.4* and *pGEMHE-ZmNPF6.6* mutant constructs were sequence verified and then linearized using restriction enzymes *Sph*1 and *Sbf*1, respectively. The linearized constructs were used as templates for *in vitro* cRNA synthesis using the mMESSAGE mMACHINE T7 kit (Ambion). Purified cRNA (using the lithium chloride precipitation method) was quantified and qualified by spectrophotometry (ND-1000 spectrophotometer, Nanodrop) and RNA electrophoresis.

Oocytes were injected with 46 nl (23 ng) of cRNA or 46 nl water using a Nanoinject II microinjector (Drummond Scientific) setting at the slow mode (23 nl/s) and incubated for 2 days in modified Ringers solution containing 96 mM NaCl, 2 mM KCl, 5 mM $MgCl_2$, 5 mM HEPES, 0.6 mM $CaCl_2$, 5% horse serum (Sigma), 1% penicillin-streptomycin (Sigma) and 50 mg/L tetracycline, pH 7.6, before experiments.

4.3.2 Chemical flux experiment

For the nitrate flux experiments, *Xenopus* oocytes were washed three times with basal solution (pH 7.5) and transferred to a ^{15}N containing nitrate solution (basal

solution supplemented with 0.25 mM or 10 mM $Na^{15}NO_3$ (10.34%, Sigma), pH 5.5). After one-hour incubation, oocytes were washed three times with ice-cold basal solution (pH 7.5) and dried individually in tin capsules at 60 °C for 3 days. The capsules were sealed and analyzed for the %N and the $^{14}N/^{15}N$ ratios using an isotope ratio mass spectrometer (Sercon 20-20) coupled to a front-end elemental analyzer (Sercon). In the kinetic study, oocytes were incubated in nitrate solutions with 12 different concentrations (25 μM, 50 μM, 100 μM, 150 μM, 250 μM, 400 μM, 1 mM, 2 mM, 5 mM, 10 mM, 20 mM and 30 mM) for one hour.

For chloride flux experiments, similar protocols were used as described in the nitrate flux experiments. Instead of 10 mM substrate, only 1mM NaCl was added into the uptake solution to achieve the high radioactive specific activity (~3810 Bq/ml). Before each experiment, radioactive $Na^{36}Cl$ (Amersham Biosciences) was added into uptake solutions to a concentration of 0.1% (v/v). After one hour incubation, each oocyte was washed three times with ice-cold basal solution (pH 7.5) and dissolved in 100 ml of 10% (w/v) SDS in a 5 ml scintillation vial. Incorporated radioactivity of each oocyte was quantified by a liquid scintillation analyzer (TRI-CARB 2100TR).

For substrate competition flux experiments, equal concentrations of unlabeled chloride (or nitrate) was added into ^{15}N nitrate solution (or ^{36}Cl chloride solution).

4.4 Discussion

It is well known that the phosphorylation status of Thr101 in AtNPF6.3 regulates its dual-affinity transport activity (Liu, 2003). Phosphorylation represses the low-affinity activity of the transporter while dephosphorylation renders the high-affinity system inactive (Liu, 2003). Phosphorylation status of Thr101 also influences the primary nitrate signaling capacity of AtNPF6.3 (Ho et al., 2009). The role of this regulatory motif has been further supported by structural evidence that indicated that phosphorylation may influence transporter dimerization, which is

considered an important component of the affinity switch mechanism (Sun et al., 2014). In a separate structural study of AtNPF6.3, Parker and Newstead (2014) suggested that phosphorylation of Thr101 alters the transporters structural flexibility within the membrane. This change is thought to influence activity rates.

Based on these results, the maize equivalent of AtNPF6.3, ZmNPF6.4 and ZmNPF6.6 showed little resemblance to the impact of phosphorylation status with the previously characterized Arabidopsis AtNPF6.3 model. In contrast, the most significant difference was the apparent influence on the low-affinity transport pathway instead of the high-affinity system. Both of the maize NPFs (ZmNPF6.4 and ZmNPF6.6) showed a reduction in low-affinity transport capacity when Thr104 or Thr106 was replaced with either alanine or aspartate, respectively (Figure 4.1C and Figure 4.2C). The replacement of threonine with alanine has been shown to prevent phosphorylation while inclusion of aspartate introduces a permanent phosphorylation status to the region (Liu, 2003). As a control, I repeated the mutations to Thr101 (T101A, T101D) in AtNPF6.3. Surprisingly, a similar response also extended to AtNPF6.3, where low-affinity transport was severely reduced in either of the two mutations (Figure 4.3C). There was no evidence of a loss of high-affinity activity with T101A as has been reported previously (Liu, 2003). At this stage it is reasonable to question whether the phosphorylation of Thr104 (or Thr101) is ultimately responsible for the affinity switch in the dual-affinity transporters ZmNPF6.6 (or AtNPF6.3). It is possible that experimental differences between studies may influence the results. The most likely variable is the status of the *Xenopus* oocytes expression system to promote phosphorylation of the expressed proteins. The use of PKA activators (8-bromoadenosine 3',5'-cyclic monophosphate, forskolin and 3-isobutyl-1-methylxanthine) or inhibitor (H89) have been found to influence transport activity by enhancing or reducing phosphorylation in *Xenopus* oocytes (Liu, 2003). Further analysis is required where an independent expression system is used (e.g. lipid

bilayer) as well as more detailed studies to investigate the extent of phosphorylation status of the transporters.

The publication of two structural models of AtNPF6.3 nominated His356 as a substrate binding/recognition site. His356 is proposed to bind nitrate through an electrostatic interaction in the pore region of the protein (Parker and Newstead, 2014; Sun et al., 2014). There is an equivalent His356 in ZmNPF6.6 (His 362) but a tyrosine (Tyr370) in ZmNPF6.4. Structural threading of both ZmNPF6.6 and ZmNPF6.4 against the apo model of AtNPF6.3, showed that both residues would face the central transport pore of the protein. This difference may relate to the functional characterization data of both proteins presented in Chapter 3. ZmNPF6.4 was shown to be a low-affinity non-selective nitrate and chloride transporter, while ZmNPF6.6 a dual-affinity nitrate specific transporter, This variation in the putative substrate binging site raises a question - does the histidine residue act as a selectivity filter as well as the dual-affinity determination site?

The transformation between a nitrate specific transporter and a non-selective nitrate and chloride transporter has previously been achieved through the introduction of a single amino acid substitution in the substrate selective filter of the Arabidopsis vacuole nitrate accumulator AtCLCa (Bergsdorf et al., 2009; Wege et al., 2010). Following this lead, a histidine was introduced at ZmNPF6.4:Tyr370 (Y370H). Surprisingly, a putative nitrate-binding site was artificially created which conferred not only the dual-affinity nitrate transport activity but also the nitrate specificity in ZmNPF6.4. Therefore based on the results with ZmNPF6.4, the histidine residue is important in both substrate specificity and transport affinity. It is interesting to note that most NPF nitrate transporters harbor a tyrosine at the equivalent site of AtNPF6.3 His356. It is possible similar mutagenesis experiments combined with transgenesis in plants could influence nitrate transport activity across a range of NPF proteins. Why a tyrosine in this location is common amongst

many of the NPF proteins is unknown. This question warrants further investigation.

The result with ZmNPF6.4 raises an interesting question about the mechanism of the low-affinity transport activity of the protein. In the absence of the histidine residue (Y370), it is unclear where on the protein nitrate binds or alternatively is nitrate binding actually required for low-affinity transport? To confirm this hypothesis, it will be necessary to determine the location of the substrate-binding site of ZmNPF6.4 as well as other low-affinity NPFs, possibly through a structural biology approach.

In contrast, modifications made to ZmNPF6.6 in this study has raised questions about the role of His362 as the sole nitrate binding site. Replacing His362 to tyrosine (H326Y) resulted in loss of ZmNPF6.6 activity in *Xenopus* oocytes (both high and low-affinity transport). Whether this mutation influenced protein stability in *Xenopus* is unknown and needs to be investigated. However, the data does suggest His362 is critical for its transport activity at both low and high concentrations.

Taken together, a ZmNPF activity model is proposed here (Figure 4.10). Since Tyr370 is unlikely to be the nitrate binding residue in ZmNPF6.4, we predict that ZmNPF6.4 may harbor a second substrate binding site which has similar affinity to nitrate and chloride. This predicted residue will allow ZmNPF6.4 transport both substrates in a low-affinity manner. Although ZmNPF6.6 can also transport chloride without the presence of nitrate, the strong electrostatic interaction between His362 and nitrate enabled ZmNPF6.6 to selectively transport nitrate in a dual-affinity manner. When the ZmNPF6.4::Tyr370 was substituted by a histidine, ZmNPF6.4 was conferred with a similar nitrate selectivity and dual-affinity activity as ZmNPF6.6. However, when ZmNPF6.6::His362 was substituted by a tyrosine, without a second substrate binding site, the function of ZmNPF6.6 was disrupted.

5 Functional Characterization of NRT2/NRT3 Nitrate Transporter System in Maize

5.1 Introduction

The class of NRT2 proteins are high-affinity proton-coupled nitrate transporters participating in various physiological processes, including root high-affinity nitrate transport, regulation of root morphology, abiotic and biotic stress responses and the loading of seed nitrate (Filleur et al., 2001; Remans et al., 2006; Chopin et al., 2007; Dechorgnat et al., 2012). NRT2 proteins belong to the major facilitator superfamily (MFS). They contain the signature MFS fold with 12 transmembrane domains collectively forming a central pore. Although NRT2's have similar structural resemblances to the NPF transporters, there is limited sequence homology between NRT2 and NPF family members. To date, several NRT2 members have been identified and functionally characterized in *Arabidopsis*, rice, barley and fungal species. In most cases it appears that both their functional activity and targeting to the plasma membrane requires the assistance of an ancillary protein called NRT3 (Quesada et al., 1994; Zhou et al., 2000; Wirth et al., 2007; Kotur et al., 2012). In Arabidopsis, this has been confirmed using chemical flux experiments, where nitrate transport only occurs when both *AtNRT2.1/AtNRT3.1* are co-injected into oocytes (Orsel et al., 2006; Kotur et al., 2012). There is no nitrate transport when either one is expressed alone. The method of interaction between NRT2 and NRT3 proteins is still poorly understood. However, there is evidence that suggests direct protein interactions occurring between NRT2 and NRT3 proteins from both membrane-based yeast-two-hybrid experiments and split-YFP experiments (Orsel et al., 2006; Kotur et al., 2012). It has been postulated that the post-translation interaction between NRT3 and NRT2 may enhance NRT2 plasma membrane targeting, a process that may be critical for

the fast modulation of nitrate uptake in response to the exogenous nitrate status (Wirth et al., 2007). A previous study has shown *ZmNRT2.1* in the model maize inbred Gaspe, is linked to nitrate acquisition at different stages of development and N status (Garnett et al., 2013). Little information is known about the functional activities of NRT2/NRT3 nitrate transport system in maize. In this chapter, maize (B73 genotype) homologs of the Arabidopsis NRT2.1 and NRT3.1 proteins were isolated and functional characterized.

5.2 Results

5.2.1 Molecular cloning of ZmNRT2.1 and ZmNRT3.1A

Based on the sequence alignments by Plett et al. (2010), two putative nitrate transporter genes, *ZmNRT2.1* (GRMZM2G010280_T01) and *ZmNRT3.1A* (GRMZM2G179294_T01) were cloned from the maize inbred B73. PCR primers (Table 5.1) were designed based on the sequence information obtained from MaizeSequence.org. The *ZmNRT2.1* loci is predicted to contain one exon and no introns, encoding a protein with 524 amino acids. The gene product of *ZmNRT2.1* shares 71% amino acid similarity with the Arabidopsis homolog AtNRT2.1 where it also contains 12 transmembrane domains (Figure 5.1A). Sequence analysis revealed that the amino acid sequence of the ZmNRT2.1 from B37 is different from the inbred Cecila used in the Quaggiotti's study (2003). In this study there is a 10 amino acid substitution of TMGRRRHAAH for ^{194}NMGGGATQLI in the fifth transmembrane domain.

ZmNRT3.1A contains two exons and one intron. The encoded protein of ZmNRT3.1A contains 203 amino acids and shares 44% amino acid sequence similarity with AtNRT3.1 (Figure 5.1B). Unlike the single transmembrane domain in AtNRT3.1 (Tsay et al., 2007), ZmNRT3.1A is predicted to contain two (TM1: 9-30; TM2: 177-196).

5.2.2 Sub-cellular localization of ZmNRT2.1 and ZmNRT3.1A

To explore the sub-cellular localization of the putative maize high-affinity nitrate transporter, yellow fluorescent protein was fused to the C-terminus of ZmNRT2.1 and bombarded into onion epidermal cells along with the plasma membrane marker construct *ECFP::Rop11*. As displayed in Figure 5.2A, ZmNRT2.1::YFP was localized to the cell periphery and overlapped with the ECFP marker. Onion epidermal cells contain large vacuoles, which makes it hard to distinguish the plasma membrane from other cell organelles. Plasmolysis was therefore induced by applying a high osmolality solution to better define its sub-cellular localization. Interestingly, YFP signal was absent from the Hechtian strands (stretched plasma membrane attached to cell wall) in the plasmolyzed cells, suggesting ZmNRT2.1 alone might be located on other cytoplasmic membranes or vesicles rather than strictly the plasma membrane.

Since it has been suggested that the proper membrane targeting of the NRT2 transporters requires the presence of NRT3 proteins, the potential mistargeting of ZmNRT2.1 observed here may be due to the lack of the maize NRT3 protein. To test this, *ZmNRT3.1A* was co-transformed into onion epidermal cells along with the *ZmNRT2.1* construct. In the presence of *ZmNRT3.1A*, YFP signal can be clearly detected on the Hechtian strands in the plasmolyzed onion epidermal cells, suggesting that ZmNRT2.1 is localized on the plasma membrane and that ZmNRT3.1A influenced its targeting to the PM. Unfortunately, *ZmNRT3.1A::YFP* transformed onion epidermal cells failed to show YFP signal. The sub-cellular localization of ZmNRT3.1A could not be determined.

5.2.3 Expression of ZmNRT2.1 and ZmNRT3.1A

According to the transcriptomic study of Sekhon et al (2011), both *ZmNRT2.1* and *ZmNRT3.1A* are exclusively expressed in the primary root. To begin defining the expression pattern of *ZmNRT2.1* and *ZmNRT3.1A*, primers were designed against

ZmNRT2.1 and *ZmNRT3.1A* and used in quantitative real-time PCR assays. Total RNA was collected from B73 maize seedlings grown on basal solution supplied with 2.5 mM NH_4NO_3 for 7 days and then shifted to a basal solution containing no nitrogen for 4 days. Samples were harvested on the fourth day and after 4 hours following re-supplementation of basal solution supplied with either 5 mM NO_3^-, NH_4^+, Cl^- or PO_4^{3-}.

A strong induction of *ZmNRT2.1* expression (~27-fold) was observed in roots when nitrogen was removed from the growth solution (Figure 5.3A). The expression level of *ZmNRT3.1A* in roots increased slightly by N-starvation treatment; however, this was not significantly different from the control group (Figure 5.3A). The induction of *NRT2/NRT3* by N starvation was previously documented in *Arabidopsis*, where N removal from the growth medium increased the transcript level of *AtNRT2.1* and *AtNRT3.1* by ~6.5 fold and ~2 fold, respectively, in nitrogen grown plants (Orsel et al., 2006).

Surprisingly, *ZmNRT2.1* expression was also induced by nitrate supplementation. As shown in Figure 5.3B, the nitrate treatment significantly increase the expression of *ZmNRT2.1*, by ~16 fold, which suggested a possible participation in the iHATS activity of nitrate uptake. Unexpectedly, chloride also deregulated the expression of *ZmNRT2.1* in roots to a similar level to the nitrate induced expression (Figure 5.3B). With all the treatments, ammonium was unable to induce expression of *ZmNRT2.1* (Figure 5.3B). The relative expression level of *ZmNRT2.1* in the shoot is extremely low, less than 1% of the total root expression levels (Figure 5.3A and B). The expression of *ZmNRT3.1A* was stable in both roots and shoots, displaying no apparent regulation by any of the treatments or tissues tested in this experiment (Figure 5.3C).

5.2.4 Chemical Flux Experiment of ZmNRT2.1 and ZmNRT3.1A

To determine the activity of the maize high-affinity nitrate transport system, ^{15}N-nitrate flux experiments were performed with *ZmNRT2.1, ZmNRT3.1A* cRNA-injected oocytes or with *ZmNRT2.1/3.1A* co-injected oocytes. Oocytes were incubated in ^{15}N labeled nitrate flux solution (250 μM, pH 5.5) for one hour and the accumulated ^{15}N label was measured using an IRMS. As seen from Figure 5.4, neither *ZmNRT2.1* nor *ZmNRT3.1A* individually injected oocytes accumulated nitrate. Only the *ZmNRT2.1*/*3.1A* co-injected oocytes were able to absorb nitrate compared with water-injected controls, suggesting the high-affinity nitrate uptake system in maize also requires the two components working together.

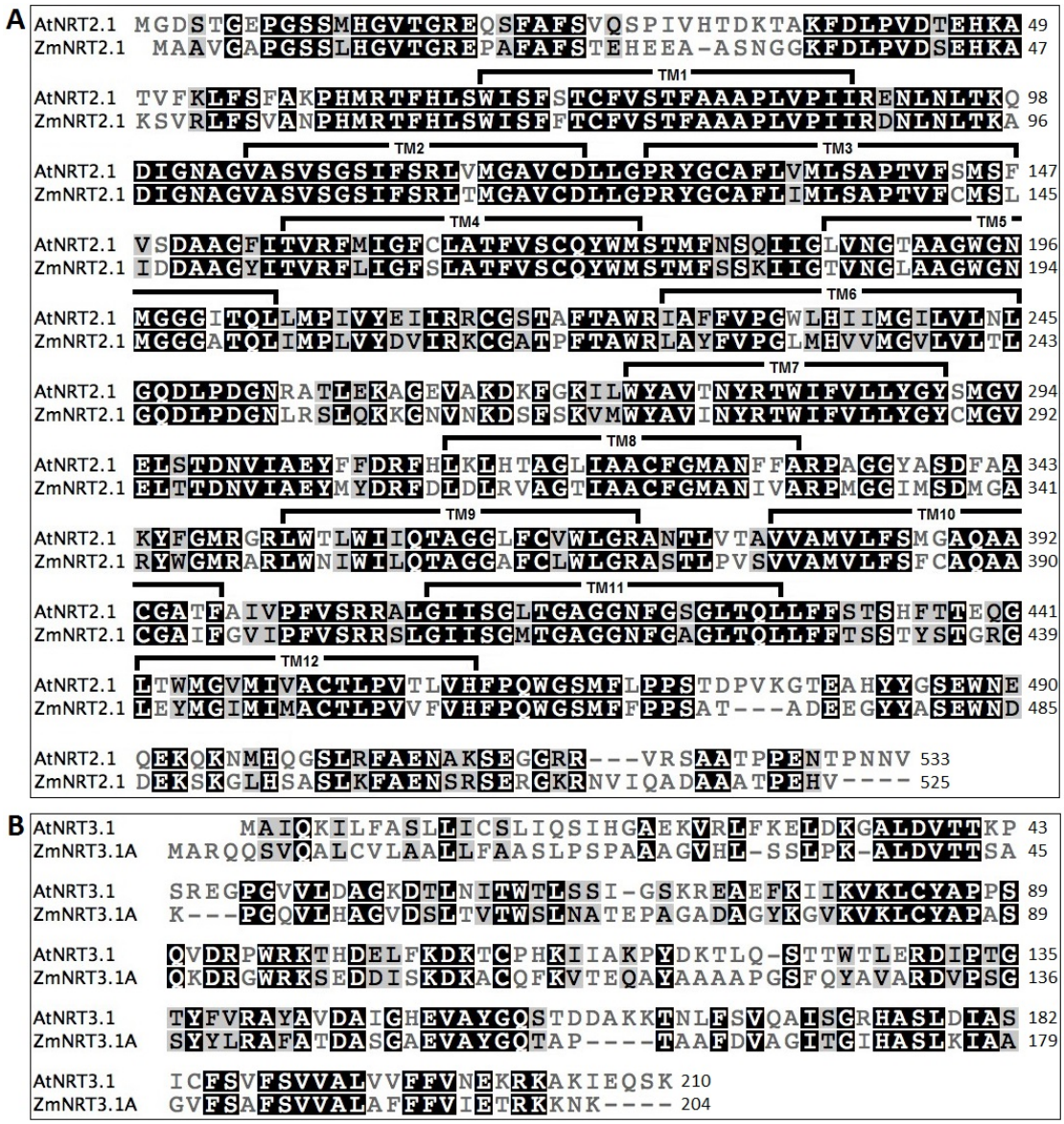

Figure 5.1. Amino Acid Sequence Alignments of AtNRT2.1/ZmNRT2.1 and AtNRT3.1/ZmNRT3.1A

Sequence alignment was performed using the Geneious alignment tool (Biomatters) with gap open penalty of 12, gap extension penalty of 3 and refinement iteration of 2. Identical residues are shaded black and conservative residues are shaded grey. The putative transmembrane domains (TM) of NRT2 transporters are underlined and numbered.

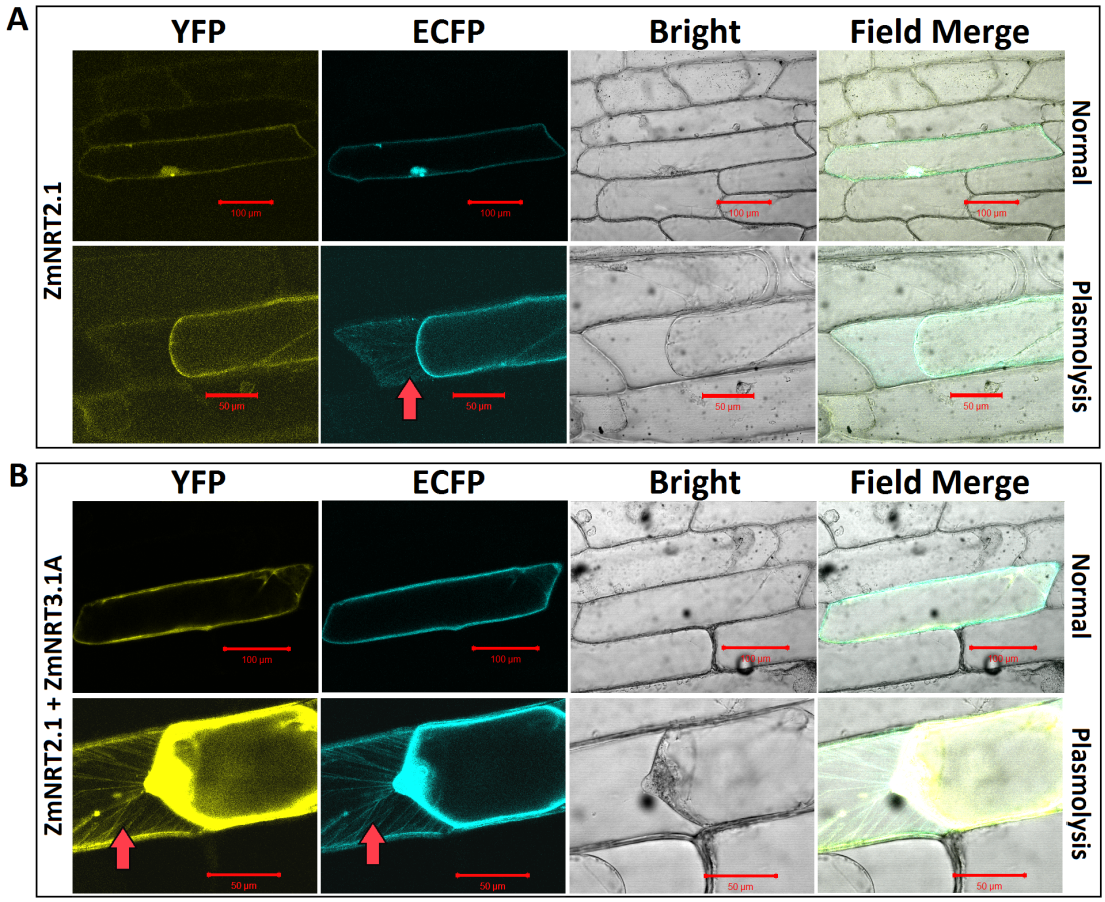

Figure 5.2. Sub-cellular localization of ZmNRT2.1/ZmNRT3.1A

A. *ZmNRT2.1:YFP* bombarded into Onion Epidermal cells. **B**. Co-bombardment of *ZmNRT2.1:YFP* and *ZmNRT3.1A* into Onion Epidermal cells. Onion epidermal cells were transformed with *ZmNRT-YFP* constructs using a biolistic PSD-1000/He particle delivery system. Note: localization of YFP signal (**B**) on Hechtian strands of plasmolysed tissues, indicated by red arrows. Images were taken using a LSM 5 PASCAL laser-scanning microscope (Zeiss) 12 hours after bombardment (bars = 100 µm or 50 µm).

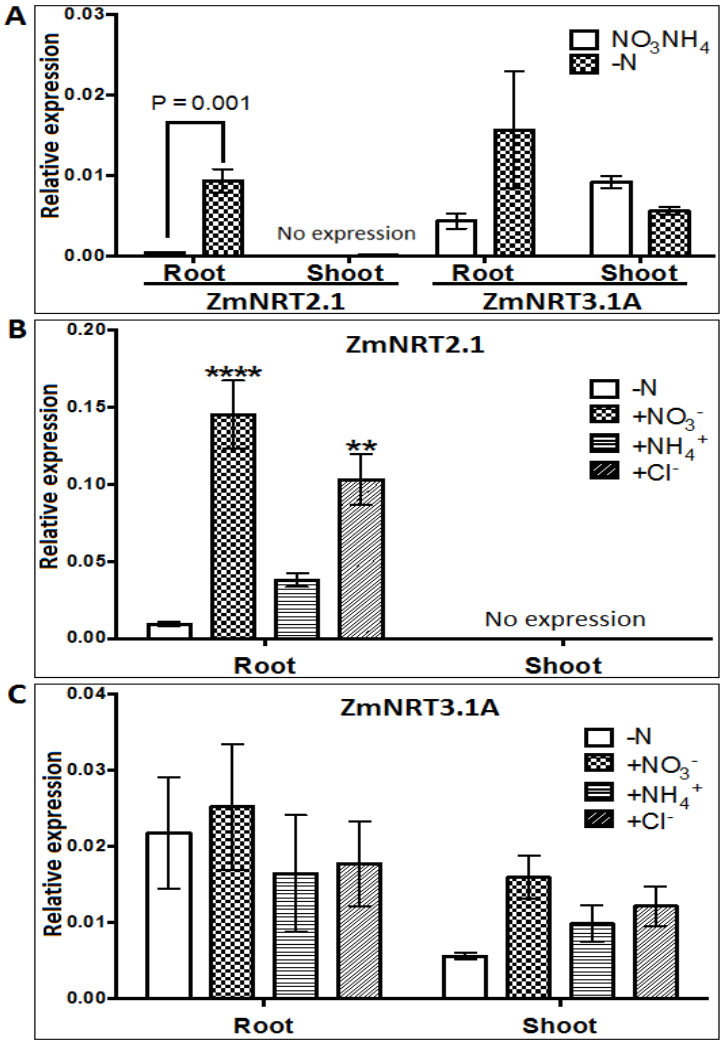

Figure 5.3. Expression of *ZmNRT2.1* and *ZmNRT3.1A* in Response to Nitrate, Ammonium and Chloride

B73 seedlings were grown in the growth basal solution supplied with 2.5 mM NH_4NO_3 for 7 days after germination. The solution was changed to the growth basal solution with no nitrogen for 4 days. After the starvation treatment, the seedlings were transferred to basal solution containing 5 mM nitrate, ammonium or chloride for 4 hours before harvest. Quantitative RT-PCR was performed using cDNA derived from total RNA of root and shoot tissues. **A**. The expression of *ZmNRT2.1* is induced by N-starvation. **B**. The expression of *ZmNRT2.1* is activated by nitrate and chloride in roots. **C**. The expression of *ZmNRT3.1A* is not regulated by nitrate, ammonium or chloride. Relative expression was normalized based on the maize *GaPDh*, *EF1A* and *Actin* genes. Similar results were obtained from three independent biological replications. Data points in each experiment represent means of 3 (n = 3) samples. Error bars indicate mean ± SEM, and asterisks denote significance (**P<0.005, ****P<0.00005) using the One-way ANOVA statistical analysis.

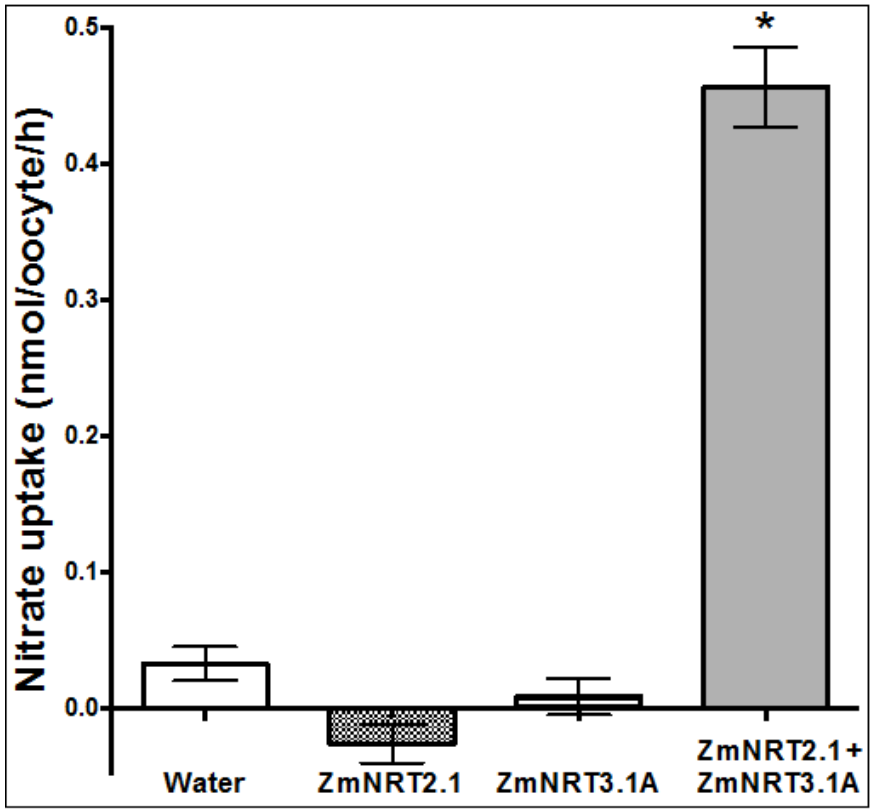

Figure 5.4. High-Affinity Nitrate Transport Activity of ZmNRT2.1 and ZmNRT3.1A

ZmNRT2.1, *ZmNRT3.1A*, *ZmNRT2.1/3.1A*-co-injected oocytes and water-injected oocytes were incubated in nitrate solution (250 µM, pH 5.5) for 1 hour. Accumulated nitrate was quantified by an IRMS. Average values and standard errors of the mean were calculated from 9 replicate oocytes and equivalent results were obtained from three repeat experiments with oocytes derived from different frogs. Error bars indicate mean ± SEM, and asterisks denote significance (*P<0.05) using the One-way ANOVA statistical analysis.

ZmNRT2.1 Clone Forward Primer	ATTGCCGGAACCTCAAGCAC
ZmNRT2.1Clone Reverse Primer	TCATGTCAACGGAGCACACG
ZmNRT2.1 C-terminal Reverse Primer	GACATGCTCCGGCGTGGC
ZmNRT3.1A Clone Forward Primer	CACAACCCCGAGCTCAGATCC
ZmNRT3.1A Clone Reverse Primer	GGGCAATATAATCCACTTTCGAGCA
ZmNRT3.1A C-terminal Reverse Primer	CTTGTTCTTCTTGCGGGTCTCG

Table 5.1. Primers used in Molecular Cloning

ZmNRT2.1 qPCR Forward Primer	CCATTGCCGGAACCTCAAGCA
ZmNRT2.1 qPCR Reverse Primer	CCCTGTGACTCCGTGCAGAGA
ZmNRT3.1A qPCR Forward Primer	GCGTGAAGGTGAAGCTGTGCT
ZmNRT3.1A qPCR Reverse Primer	TTGAACTGGCACGCCTTGTCC
ZmActin qPCR Forward Primer	CCAATTCCTGAAGATGAGTCT
ZmActin qPCR Reverse Primer	TGGTAGCCAACCAAAAACAGT
ZmGaPDh qPCR Forward Primer	GACAGCAGGTCGAGCATCTTC
ZmGaPDh qPCR Reverse Primer	GTCGACGACGCGGTTGCTGTA
ZmElF1 qPCR Forward Primer	GCCGCCAAGAAGAAATGATGC
ZmElF1 qPCR Reverse Primer	CGCCAAAAGGAGAAATACAAG

Table 5.2. Primers used in Quantitative Real Time PCR

5.3 Materials and Methods

5.3.1 Sequence Alignment and Phylogenetic Analysis

NRT2 and NRT3 protein nucleic and amino acid sequences were obtained from the Arabidopsis Information Resource and Maizesequence.org databases. All sequence alignments were conducted using the Geneious R7 software alignment tool (Biomatters) with gap open penalty of 12, gap extension penalty of 3 and refinement iteration of 2.

5.3.2 Seed Germination and Seedling Growth Conditions

Seeds of the maize inbred line B73 were scarified in aerated water for 4 hours. The seeds were then imbedded in wet diatomite rocks, covered with aluminum foil and incubated at 20 °C for 4 days to germinate. The germinated seeds were transferred to a hydroponic system filled with growth basal solution (0.5 mM $MgSO_4$, 0.5 mM KH_2PO_4, 25 µM H_3BO_3, 2 µM $MnSO_4$, 2 µM $ZnSO_4$, 0.5 µM $CuSO_4$, 0.5 µM Na_2MoO_4, 1.05 mM KCl, 0.1 mM Fe-EDTA, 0.1 mM FeEDDHA, 1.25 mM K_2SO_4, 0.25 mM $CaCl_2$, 1.75 mM $CaSO_4$, pH5.9) supplemented with 2.5 mM NH_4NO_3 and grown for 7 days with a 16 h/8 h light/dark regime at 20 °C.

5.3.3 RNA Extraction and Reverse Transcription

Maize root and shoot tissue were separated at the mesocotyl, ground in liquid nitrogen and stored at −80 °C. Total RNA was extracted from 100 mg tissue power using TRIzol reagent (Ambion) following the manufacturer's instructions. RNAs were quantified and qualified using a ND-1000 spectrophotometer (Nanodrop). 1 µg of total RNA from each sampled was used for cDNA synthesis using SuperScript III reverse transcriptase (Invitrogen) and the oligo dT primer, following the manufacturer's instructions.

5.3.4 Molecular Cloning

ZmNRT2.1 and *ZmNRT3.1A* full-length coding sequences were amplified from maize B73 cDNA using Platinum *Taq* DNA polymerase (Invitrogen). PCR products were subsequently inserted into pCR8/GW/TOPO vector (Invitrogen) and transformed into *E. coli* XL1-Blue strain (Stratagene). Primer details are listed in Table 5.1.

5.3.5 Sub-cellular Localization

0.25 µg of *ECFP::Rop11* plasmid and 0.25 µg of *pBS-35S-ZmNRTs-YFP* plasmid were coated onto 1.5 mg of gold microcarriers (Bio-Rad, 0.6 µm diameter, pre-washed by 70% (v/v) ethanol and suspended in 50 µl of 50% (v/v) glycerol). Before bombardment, the onion epidermal cells were incubated on a bombardment media (1 pack of Murashige and Skoog basal medium with vitamins (*Phyto*Technology Laboratories), 500 mg/L tryptone, 120 g/L sucrose and 4 g/L gelrite, pH adjusted to 5.85) to induce osmotic stress for 4 hours. The DNA coated gold microcarriers were bombarded into onion epidermal cells using a biolistic PSD-1000/He particle delivery system with an 1100 psi rupture disc (Bio-Rad). The transformed onion epidermal peels were transferred to a ne bombardment media where sucrose levels were reduced to 30 g/L. The bombarded tissue was incubated for 12-24 hours in the dark before visualization. Images were obtained using a LSM 5 PASCAL laser scanning microscope (Zeiss) with two excitation wavelengths, 458 nm and 514, using an argon laser combined with two bandpass filters, 470-500 nm and 570-590 nm, for ECFP and YFP respectively. Where required, plasma membrane localization was confirmed using a plasmolysis treatment by treating the epidermal peels with 0.75 M mannitol for 15 mins (Campos-Soriano et al., 2011).

5.3.6 ZmNRT2.1 and ZmNRT3.1A Gene Expression

Maize seedlings were grown as described in Chapter 2.3.2. After 7 days, seedlings were removed from the NH_4NO_3 solution and rinsed with RO water before transferring to a nitrogen free basal solution for 4 days to induce a nitrogen starvation treatment. The seedlings were transferred to a re-supply solution (basal solution supplemented with 5 mM NO_3^-, NH_4^+ or Cl^-) for 4 hours before harvest. Harvested samples were immediately frozen in liquid nitrogen and stored at -80°C. RNA extraction and reverse transcription were conducted as described in Section 5.3.3.

qPCR reactions contained 1 µl of synthesized cDNA and 4 µM of forward and reverse primers made up to 20 µl with SYBR Green real-time PCR master mix (Lifetechnology). Reactions were performed in a QuantStudio 12K flex real-time PCR system (Lifetechnology) with an initial denaturation of 95°C for 20 s, followed by 40 cycles of (95°C for 1 s and 55°C for 20 s). One additional melting curve step was added at the end of qPCR reaction to ensure the quality of reaction. qPCR primers of *ZmNRT2.1*, *ZmNRT3.1A* and 3 endogenous reference genes, *ZmActin*, *ZmElF1* and *ZmGaPDh* were designed using Primer 3 software and primer efficiency were tested with threshold of 90% (Table 5.2). Relative expression levels of each gene were calculated using the equation $2^{-\Delta Ct}$, where ΔCt is the sample Ct subtracted by the geometric mean of the Ct of the 3 reference genes.

5.3.7 Chemical Flux Experiment

ZmNRT2.1 and *ZmNRT3.1A* coding sequences were sub-cloned into a *Xenopus laevis* oocyte expression vector, *pGEMHE* (Liman et al., 1992), using the LR clonase II (Invitrogen) following the manufacturer's instructions. *pGEMHE-ZmNRT2.1* and *pGEMHE-ZmNRT3.1A* were linearized by restriction enzyme digestion with *Sbf*I and *Sph*I, respectively. The linearized constructs were used as templates for *in vitro* cRNA synthesis using the mMESSAGE mMACHINE T7 kit (Ambion). Purified

cRNA (using the lithium chloride precipitation method) were quantified and qualified by spectrophotometry (ND-1000 spectrophotometer, Nanodrop) and RNA electrophoresis.

Oocytes were injected with 46 nl (23 ng) of cRNA or 46 nl water using a Nanoinject II microinjector (Drummond Scientific) setting on the slow mode (23 nl/s) and incubated for 2 days in the modified Ringers solution before each experiment. For the nitrate flux experiments, oocytes were washed three times with basal solution (pH 7.5) buffer and then transferred to ^{15}N labeled nitrate solution (basal solution supplemented with 0.25 mM $Na^{15}NO_3$ (10%, Sigma), pH 5.5). After a one-hour incubation period, oocytes were washed three times with ice-cold basal solution (pH 7.5) and dried individually in tin capsules at 60°C for 3 days. The capsules were sealed and analyzed for the %N and the $^{14}N/^{15}N$ ratios using an isotope ratio mass spectrometer (Sercon 20-20) coupled to a front-end elemental analyzer (Sercon).

5.4 Discussion

AtNRT2.1 has been suggested to act as a high-affinity nitrate transporter as well as a nitrate sensor regulating root morphology according to the external nitrogen status (Little et al., 2005; Remans et al., 2006). Under N-limitation, such as a nitrogen-free or low-nitrogen nutrient solution, *AtNRT2.1* expression is often observed to be upregulated (Orsel et al., 2006; Remans et al., 2006). At the same time lateral root elongation is stimulated, which is considered an important adaptive response linked to external nitrogen status. In maize, there was a similar expression pattern with *ZmNRT2.1*, which showed a 27-fold increase in transcript levels when plants were transferred from a 2.5 mM NH_4NO_3 growth medium to a nitrogen-free medium. Interestingly, *ZmNRT2.1* expression in roots was also found to be nitrate inducible, a phenotype consistent with previous results obtained from other experiments using maize genotypes across varying nitrogen induction periods (Quaggiotti et al., 2003; Santi et al., 2003; Trevisan et al., 2008). The strong

transcriptional regulation of *ZmNRT2.1* by nitrate may not necessarily be directly correlated with NRT2.1 protein abundance and activity. Wirth et al., (2007) observed little correlation between *AtNRT2.1* transcription levels and changes in the encoded protein. Ultimately, post-translational regulation may play an important role in transport activity such as nitrate uptake through iHATS. At this stage the analysis of ZmNRT2.1 activity in maize is preliminary and not conclusive. Future work is required to detail the functional activities of the protein using heterologous expression systems (*Xenopus* oocytes) and ultimately using reverse genetic approaches to examine the impact of the protein in net nitrate uptake and redistribution within the plant.

When co-expressed with ZmNRT3.1A, ZmNRT2.1 was able to transport nitrate into *Xenopus* oocytes. Whether ZmNRT2.1 also has a chloride transport activity as observed with ZmNPF6.4 and ZmNPF6.6 still needs to be determined. The fact that chloride enhances expression of ZmNRT2.1 in root tissues suggests a transport related activity may also exist. From this study, it would appear ZmNRT2.1 activity also requires the presence of ZmNRT3.1A. ZmNRT3.1 was required for both plasma membrane localization of ZmNRT2.1 and for nitrate transport activity while expressing in *Xenopus* oocytes. As an ancillary protein, ZmNRT3.1A along cannot transport nitrate or target to plasma membrane. These are consistent with the NRT2/NRT3 relationships observed in other higher plants. However, with the techniques used in this study, whether there is a direct protein-protein interaction between ZmNRT2.1 and ZmNRT3.1A have yet to be determined. Other techniques such as the yeast two-hybrid split-ubiquitin assay and split-YFP assay would help to elucidate this question. Unlike the Arabidopsis NRT3 genes (Okamoto et al., 2006), the expression of *ZmNRT3.1A* was not regulated by nitrate. Whether there is a post-transcriptional or post-translational regulation by ZmNRT3.1 requires further studies.

6 Conclusion and Future Directions

Maize is an important agricultural commodity grown around the globe for its consistent yield capacity and qualities as an animal and human food resource. Understanding the mechanisms maize uses to manage their nitrogen requirements across a developmental lifecycle will ultimately help target pre-breeding programs towards the development of improved N use efficiencies. An important component in maintaining nitrogen supply is the mechanisms involved in the uptake of nitrogen into roots and its redistribution between cells and organelles. In this study, the functional activities of a select group of the maize NPF and NRT2 nitrate transporter families were investigated. Both classes have been shown to be important in nitrate transport in model species, for example Arabidopsis, but also in crop species including barley and rice (Krapp et al., 2014). The aim of this research is to begin the process of translating previous research findings on the molecular control of nitrate transport from model plant species, to that of agriculturally relevant plants such as maize.

As a first step, homologs of key NPF and NRT2/NRT3 family members were cloned based on published phylogenetic studies and transcriptomic data sets (Plett et al., 2010; Sekhon et al., 2011; Léran et al., 2014). The sequences of three maize homologs of the Arabidopsis dual-affinity nitrate transceptor, AtNPF6.3 (AtNRT1.1 or CHL1), one maize homolog of the low-affinity nitrate transporters, AtNPF7.2/7.3, and two maize homologs of the high-affinity transporter, AtNRT2.1 and AtNRT3.1, were identified and cloned from root cDNA of the sequenced maize inbred, B73. Based on amino acid derived phylogenetic relationships, *AtNPF6* candidate genes in maize were identified as *ZmNPF6.4*, *ZmNPF6.5*, *ZmNPF6.6* and *ZmNPF7.10* (Plett et al., 2010; Léran et al., 2014). Homologs of *AtNRT2.1* and *AtNRT3.1* were identified as *ZmNRT2.1* and *ZmNRT3.1A*, respectively (Plett et al.,

2010). Across the maize NPF6 homologs, each contained significant conservation of key residues contained in AtNPF6.3, including the proposed affinity switch residue Thr101, the proton-coupling motif ExxER and the proposed structural salt bridge residues, Lys164 and Glu476 (Parker and Newstead, 2014; Sun et al., 2014). ZmNPF7.10 showed strong sequence similarity with its Arabidopsis homologs *AtNPF7.2* and *AtNPF7.3*, but was found to lack the 7th transmembrane domain, a region, which harbors a proposed nitrate-binding site. The lack of the 7th transmembrane domain most likely made this transporter dysfunctional (Parker and Newstead, 2014; Sun et al., 2014). The ZmNRT2.1 homolog showed about 71% amino acid identity with AtNRT2.1 while ZmNRT3.1 was less conserved with only ~44% amino acid identity. ZmNRT3.1 is predicted to have two transmembrane domains while AtNRT3.1 is presumed to only have one. Using an onion peel epidermal cell expression system, YFP fusions to the C-terminus of ZmNPF6.4, ZmNPF6.5 and ZmNPF6.6 revealed putative targeting to the plasma membrane. In similar experiments, YFP tagged ZmNRT2.1 also showed a preferential targeting to the plasma membrane but only when it was co-bombarded with its 'chaperone-like' protein ZmNRT3.1. The interaction between ZmNRT2.1 and ZmNRT3.1 is consistent with observations from other plant species including Arabidopsis, rice, barley and fungal species (Zhou et al., 2000; Tong et al., 2005; Wirth et al., 2007; Yan et al., 2011; Kotur et al., 2012).

In hydroponically grown maize plants, both *ZmNPF6.4* and *ZmNPF6.6* were expressed in both root and shoot tissues at varying levels. In contrast, both *ZmNPF6.5* and *ZmNPF7.10* showed no evidence of RNA expression in either tissue under the conditions used. *ZmNPF6.4* expression was constitutive across both root and shoot tissues and showed no change when nitrate supply was varied. In contrast, *ZmNPF6.6* was predominantly expressed in roots, with very low expression in shoot tissues and it was strongly induced by nitrate re-supply, showing a 30-fold induction within 2 hours of supply. This form of nitrate induction is similar to that previously observed with *AtNPF6.3* (Tsay et al., 1993).

For the high-affinity transporter, *ZmNRT2.1* expression was confined to root tissues showing induction during N starvation or in response to transient N re-supply. In contrast, the expression pattern of ZmNRT3.1 varied little in the presence or absence of N in the nutrient media.

NPF and NRT2 activities in *Xenopus* oocytes

Each of the maize NPF cDNAs were tested in *Xenopus* oocytes for their ability to accumulate ^{15}N-nitrate. Only *ZmNPF6.4* and *ZmNPF6.6*-injected oocytes accumulated nitrate above the water-injected controls. The transport activity of both proteins was further defined using a combination of chemical flux and electrophysiology experiments. These experiments indicated, both proteins were pH dependent, responding to acidic conditions in line with their proton/nitrate symporter properties. ZmNRT6.4 behaved strictly as a low-affinity nitrate transporter while ZmNRT6.6 displayed a dual-affinity nitrate transport activity. The ability to transport nitrate at both low and high concentrations makes ZmNPF6.6 one of three characterized dual-affinity nitrate transporters identified in plants (AtNPF6.3, MtNPF6.8 and ZmNPF6.6) (Liu et al., 1999; Morère-Le Paven et al., 2011). This result further supports the putative role of selected NPF6-like proteins as multi-functional transporters adaptable to changes in external nitrate concentrations.

An interesting finding from this work was the identification that both ZmNPF6.4 and ZmNPF6.6 were also able to transport chloride, albeit at a different capacity and substrate specificity to that of nitrate. ZmNPF6.4 was non-selective for both nitrate and chloride, while ZmNPF6.6 was highly selective for nitrate over chloride. The differences between ZmNPF6.4 and ZmNPF6.6 may relate to a specific physiological function within the plant. For example, nitrate inducible ZmNPF6.6 could be responsible for root iHATS/iLATS nitrate uptake or alternatively function as a nitrate sensor during the primary nitrate response like that of AtNPF6.3 (Ho et al., 2009). The low-affinity transport capacity of ZmNPF6.4 suggests a role for the

constitutive LATS nitrate (or chloride) transport that has previously been observed in maize roots (Hole et al., 1997; White and Broadley, 2001; Garnett et al., 2013). At the same time, ZmNPF6.6 could use nitrate as an effective competitor of chloride transport when chloride is abundant, for example in saline affected soils. Elevated levels of nitrate are known to outcompete chloride uptake under field-based situations (Xu et al., 2000). Chloride transport at the plasma membrane of plant cells involves multiple mechanisms and numerous channel activities such as OR channels, S and F-type channels, stretch activated and hyperpolarization activated channels (White and Broadley, 2001). In particular, a plasma membrane H^+/Cl^- symporter has been documented in plant (*Sinapis alba*) root-hair cells using electrophysiology approach (Felle, 1994). However there is no molecular identity of this chloride channel/transporter. The data presented here would suggest that either ZmNPF6.4 or ZmNPF6.6 are possible candidates for this role.

Both ZmNPF6.4 and ZmNPF6.6 could also be linked to the control of stomata opening. Proton-coupled anion (nitrate and chloride) transport at the plasma membrane of guard cells has been proposed but no definitive genetic identity has yet been linked to either activity (Assmann and Wang, 2001; Chen and Blatt, 2010). Interestingly, Guo et al, (2003) using a mutant based approach and GFP targeting, showed that AtNPF6.3 (AtNRT1.1) was active in guard cells and that loss of function reduced nitrate content of guard cells and stomata aperture. As nitrate accumulates in guard cells during opening, it is probable that a NPF transporter is active, possibly for osmotic adjustment to facilitate water flow into the cell. The membrane potential of the guard cell plasma membrane would favor the activity of a NPF related H^+-symport process. It is clear, further studies are required to identify if either ZmNPF6.4 or ZmNPF6.6 are located in guard cells and whether their nitrate or chloride transport activities are related to stomata opening.

Dual Affinity

The different functional characteristics of ZmNPF6.4 and ZmNPF6.6 were partially explained by the analysis of their substrate binding/recognition residue, the equivalent AtNPF6.3:His356 in ZmNPF6.4 (Tyr370) and ZmNPF6.6 (His362), respectively. AtNPF6.3:His356 has been suggested as a putative residue required for nitrate binding in the central pore of the protein (Parker and Newstead, 2014; Sun et al., 2014). In AtNPF6.3, its replacement with alanine disrupted transport activity. When amino acid sequences in this region were compared amongst the maize homologs, ZmNPF6.4 like many other NPF homologs, contained a tyrosine residue instead of suggested nitrate binding histidine residue. By replacing Tyr370 in ZmNPF6.4 with His370, low-affinity transport activity was converted to a dual-affinity system. The change also resulted in enhanced nitrate specificity over that of chloride. The fact that ZmNPF6.4 in its native state transports nitrate, would suggest that it and other low-affinity NPFs with a tyrosine residue in this location must bind nitrate at a different location than that predicted for AtNPF6.3:His356. Alternatively there may not be a substrate-binding site required for low-affinity nitrate transport activity. To test this hypothesis, further crystal structures and directed mutagenic studies are required to define the substrate binding site of the low-affinity NPF transporters such as ZmNPF6.4.

Changes to the conserved Thr101 (found in AtNPF6.3) in both maize NPF homologs (ZmNPF6.4 and ZmNPF6.6) resulted in a general disruption of the low-affinity transport pathway. This change was opposite to what was expected. For example, the inclusion of aspartate in Thr101 has been shown to abolish high-affinity transport with minimal impact on the low-affinity system (Liu, 2003). Surprisingly, when the same experiment was conducted with AtNPF6.3 in this study, a change in the low affinity transport pathway occurred. It is unclear why these experiments differ from those previously published. It may be a reflection of the heterologous expression system and the potential variability in the capacity of oocytes to phosphorylate heterologous expressed proteins. Although the *Xenopus*

oocyte is a versatile heterologous expression system, it has one major disadvantage caused by batch-to-batch variation in activity and quality that can occur between frog harvests. Although manageable with repeated experimentation, direct comparisons with previously published work can vary if significant care is not taken. For example, performing nitrate flux experiments with oocytes derived from frogs in different ages resulted in nearly a 3-fold variation in the amount of measured nitrate uptake (Figure 3.1A and Figure 4.8B). Without a specific antibody to quantify the actual protein abundance and location in the oocyte, this variation is difficult to normalize across experiments and individual studies. Furthermore, the endogenous currents introduced by oocyte native transporters and channels can be problematic in voltage-clamp electrophysiological experiments (Schroeder, 1994). The use of secondary technologies such as giant liposomes would offer a refined approach where transport protein activity can be measured in the absence of endogenous transport activity (Schneider et al., 2010; Collins and Gordon, 2013; Scalise et al., 2013).

High-Affinity Nitrate Transport

A preliminarily study of the maize NRT2/NRT3 high-affinity nitrate transport system was conducted. Similar to observations in Arabidopsis (Kotur et al., 2012), the maize NRT2.1 homolog also required a NRT3 protein to function and be targeted to the plasma membrane. *ZmNRT2.1/3.1A* co-injected oocytes were able to accumulate nitrate while single injections of either *ZmNRT2.1* or *ZmNRT3.1A* failed to elicit nitrate uptake. Co-injection was also required to observe YFP::ZmNRT2.1 signal at the plasma membrane of onion epidermal cells. Future experiments are required to verify if a direct protein-protein interaction occurs between ZmNRT2.1 and ZmNRT3.1A and the impact on net nitrate uptake when this transporter is silenced. Its dynamic expression profile across a developmental time scale in response to N supply (Garnett et al., 2013) suggests it is an important protein for the uptake of nitrate into maize roots.

Defining Nitrate Transporter Activity in Plants

New research is required to define the *in planta* function of ZmNPF6.4, ZmNPF6.6 and ZmNRT2.1/ZmNRT3.1A. To do this, mutant plant lines for each of the transporters will be required. The recent development of genome editing technologies based on zinc finger nucleases (ZFNs), transcription activator-like effector nucleases (TALENs) or clustered regularly interspaced short palindromic repeats (CRISPR)/CRISPR-associated (Cas) systems (Wu et al., 2009; Liang et al., 2014; Char et al., 2015) offers a promising way forward to generate site selected mutants to better understand their physiological relevance to nitrate transport. Furthermore, more detailed investigations across a broad range of maize inbreeds and hybrids will help to identify natural selections of NPF6 and NRT2 proteins which are required for N transport and redistribution.

Future Directions

In conclusion, my PhD research functionally characterized two maize NPF nitrate transporters, ZmNPF6.4 and ZmNPF6.6, and two members from the maize NRT2/NRT3 high-affinity nitrate uptake system, ZmNRT2.1 and ZmNRT3.1A. Unfortunately, there are still many unresolved questions about their individual roles in nitrate transport and potentially nitrate signaling. Hopefully future experiments, including the analysis of *ZmNPF6.4/6.6* or *ZmNRT2.1/3.1A* knockout maize lines, targeted mutagenesis of key residues within NPF genes and further structural studies of maize NPF proteins will help advance our understanding of these important transport proteins. Furthermore, there are large number of uncharacterized NPF and NRT members in maize. A thorough understanding of their roles in nitrate transport will also be required.

7 Bibliography

Alboresi A, Gestin C, Leydecker MT, Bedu M, Meyer C, Truong HN (2005) Nitrate, a signal relieving seed dormancy in *Arabidopsis*. Plant, Cell & Environment **28:** 500-512

Almagro A, Lin SH, Tsay YF (2008) Characterization of the Arabidopsis nitrate transporter NRT1.6 reveals a role of nitrate in early embryo development. The Plant Cell **20:** 3289-3299

Arnold K, Bordoli L, Kopp J, Schwede T (2006) The SWISS-MODEL workspace: a web-based environment for protein structure homology modelling. Bioinformatics **22:** 195-201

Assmann SM, Wang X-Q (2001) From milliseconds to millions of years: guard cells and environmental responses. Current Opinion in Plant Biology **4:** 421-428

Bergsdorf E-Y, Zdebik AA, Jentsch TJ (2009) Residues important for nitrate/proton coupling in plant and mammalian CLC transporters. Journal of Biological Chemistry **284:** 11184-11193

Biasini M, Bienert S, Waterhouse A, Arnold K, Studer G, Schmidt T, Kiefer F, Cassarino TG, Bertoni M, Bordoli L, Schwede T (2014) SWISS-MODEL: modelling protein tertiary and quaternary structure using evolutionary information. Nucleic Acids Research **42:** W252-W258

Bouguyon E, Brun F, Meynard D, Kubeš M, Pervent M, Leran S, Lacombe B, Krouk G, Guiderdoni E, Zažímalová E, Hoyerová K, Nacry P, Gojon A

(2015) Multiple mechanisms of nitrate sensing by Arabidopsis nitrate transceptor NRT1.1. Nature Plants **1:** 15015

Campos-Soriano L, Gómez-Ariza J, Bonfante P, San Segundo B (2011) A rice calcium-dependent protein kinase is expressed in cortical root cells during the presymbiotic phase of the arbuscular mycorrhizal symbiosis. BMC Plant Biology **11:** 90

Celine M, Isabelle Q, Andre G, Bertrand H (2001) The challenge of remobilisation in plant nitrogen economy. A survey of physio-agronomic and molecular approaches. Annals of Applied Biology **138:** 69-81

Char SN, Unger-Wallace E, Frame B, Briggs SA, Main M, Spalding MH, Vollbrecht E, Wang K, Yang B (2015) Heritable site-specific mutagenesis using TALENs in maize. Plant Biotechnology Journal **13:** 1002-1010

Chen C-Z, Lv X-F, Li J-Y, Yi H-Y, Gong J-M (2012) Arabidopsis NRT1.5 is another essential component in regulation of nitrate reallocation and stress tolerance. Plant Physiology **159:** 1582-1590

Chen Z-H, Blatt MR (2010) Membrane Transport in Guard Cells. *In* eLS. John Wiley & Sons, Ltd

Chiu C-C, Lin C-S, Hsia A-P, Su R-C, Lin H-L, Tsay Y-F (2004) Mutation of a nitrate transporter, AtNRT1:4, results in a reduced petiole nitrate content and altered leaf development. Plant & Cell Physiology **45:** 1139

Chopin F, Orsel M, Dorbe M-F, Chardon F, Truong H-N, Miller AJ, Krapp A, Daniel-Vedele F (2007) The Arabidopsis ATNRT2.7 nitrate transporter controls nitrate content in seeds. The Plant Cell **19:** 1590-1602

Collins MD, Gordon SE (2013) Giant liposome preparation for imaging and patch-clamp electrophysiology. Journal of Visualized Experiments **76:** e50227

Cosgrove DJ, Hedrich R (1991) Stretch-activated chloride, potassium, and calcium channels coexisting in plasma membranes of guard cells of Vicia faba L. Planta **186:** 143-153

Crawford NM, Glass ADM (1998) Molecular and physiological aspects of nitrate uptake in plants. Trends in Plant Science **3:** 389-395

David LC, Dechorgnat J, Berquin P, Routaboul JM, Debeaujon I, Daniel-Vedele F, Ferrario-Méry S (2014) Proanthocyanidin oxidation of Arabidopsis seeds is altered in mutant of the high-affinity nitrate transporter NRT2.7. Journal of Experimental Botany **65:** 885-893

De Angeli A, Monachello D, Ephritikhine G, Frachisse JM, Thomine S, Gambale F, Barbier-Brygoo H (2006) The nitrate/proton antiporter AtCLCa mediates nitrate accumulation in plant vacuoles. Nature **442:** 939-942

Dechorgnat J, Nguyen CT, Armengaud P, Jossier M, Diatloff E, Filleur S, Daniel-Vedele F (2011) From the soil to the seeds: the long journey of nitrate in plants. Journal of Experimental Botany **62:** 1349-1359

Dechorgnat J, Patrit O, Krapp A, Fagard M, Daniel-Vedele F (2012) Characterization of the Nrt2.6 gene in Arabidopsis thaliana: A link with plant response to biotic and abiotic stress. PLoS ONE **7:** e42491

Downs GS, Bi Y-M, Colasanti J, Wu W, Chen X, Zhu T, Rothstein SJ, Lukens LN (2013) A developmental transcriptional network for maize defines coexpression modules. Plant Physiology **161:** 1830-1843

Eveland AL, Goldshmidt A, Pautler M, Morohashi K, Liseron-Monfils C, Lewis MW, Kumari S, Hiraga S, Yang F, Unger-Wallace E, Olson A, Hake S, Vollbrecht E, Grotewold E, Ware D, Jackson D (2014) Regulatory modules controlling maize inflorescence architecture. Genome Research **24:** 431-443

Fan S-C, Lin C-S, Hsu P-K, Lin S-H, Tsay Y-F (2009) The Arabidopsis nitrate transporter NRT1.7, expressed in phloem, is responsible for source-to-sink remobilization of nitrate. The Plant Cell **21:** 2750-2761

FAO (2012). *In*. Food and Agriculture Organization of the United Nations

Felle HH (1994) The H+/Cl- symporter in root-hair cells of Sinapis-Alba. Plant Physiology **106:** 1131-1136

Filleur S, Dorbe M-F, Cerezo M, Orsel M, Granier F, Gojon A, Daniel-Vedele F (2001) An Arabidopsis T-DNA mutant affected in Nrt2 genes is impaired in nitrate uptake. FEBS Letters **489:** 220-224

Frommer WB (1995) Heterologous expression of genes in bacterial, fungal, animal, and plant cells. Annual Review of Plant Physiology and Plant Molecular Biology **46:** 419-444

Garnett T, Conn V, Plett D, Conn S, Zanghellini J, Mackenzie N, Enju A, Francis K, Holtham L, Roessner U, Boughton B, Bacic A, Shirley N, Rafalski A, Dhugga K, Tester M, Kaiser BN (2013) The response of the maize nitrate

transport system to nitrogen demand and supply across the lifecycle. New Phytologist **198:** 82-94

Giles J (2005) Nitrogen study fertilizes fears of pollution. Nature **433:** 791-791

Glass AD, Kotur Z (2013) A reevaluation of the role of Arabidopsis NRT1.1 in high-affinity nitrate transport. Plant Physiol **163:** 1103-1106

Glass ADM (2009) Nitrate uptake by plant roots. Botany **87:** 659-659

Guex N, Peitsch MC, Schwede T (2009) Automated comparative protein structure modeling with SWISS-MODEL and Swiss-PdbViewer: a historical perspective. Electrophoresis **30:** S162-S173

Guo F, Young J, Crawford NM (2003) The nitrate transporter AtNRT1.1 (CHL1) functions in stomatal opening and contributes to drought susceptibility in arabidopsis. The Plant Cell **15:** 107-117

Guo F-Q, Wang R, Chen M, Crawford NM (2001) The Arabidopsis dual-affinity nitrate transporter gene AtNRT1.1 (CHL1) Is activated and functions in nascent organ development during vegetative and reproductive growth. The Plant Cell **13:** 1761-1777

Guo FQ, Young J, Crawford NM (2003) The nitrate transporter AtNRT1.1 (CHL1) functions in stomatal opening and cotribute to drought susceptibiity in arabidopsis. THE PLANT CELL **15:** 107-117

Ho C-H, Lin S-H, Hu H-C, Tsay Y-F (2009) CHL1 functions as a nitrate sensor in plants. Cell **138:** 1184-1194

Ho CH, Lin SH, Hu HC, Tsay YF (2009) CHL1 Functions as a Nitrate Sensor in Plants. Cell **138:** 1184-1194

Hole DJ, Emran AM, Drew MC (1997) Influx and efflux kinetcs of ammonium transport in maize roots. Maydica. **42 (4):** 347-354

Hsu PK, Tsay YF (2013) Two phloem nitrate transporters, NRT1.11 and NRT1.12, are important for redistributing xylem-borne nitrate to enhance plant growth. Plant Physiology **163:** 844-856

Huang N, Chiang C, Crawford NM, Tsay Y (1996) CHL1 encodes a component of the low-affinity nitrate uptake system in arabidopsis and shows cell type-specific expression in roots. The Plant Cell **8:** 2183-2191

Huang NC, Liu KH, Lo HJ, Tsay YF (1999) Cloning and functional characterization of an Arabidopsis nitrate transporter gene that encodes a constitutive component of low-affinity uptake. The Plant Cell **11:** 1381-1392

IITA (2009) Maize. *In*. International Institute of Tropical Agriculture

Jackson RB, Caldwell MM (1993) The scale of nutrient heterogeneity around individual plants and its quantification with geostatistics. Ecology **74:** 612-614

Kanno Y, Hanada A, Chiba Y, Ichikawa T, Nakazawa M, Matsui M, Koshiba T, Kamiya Y, Seo M (2012) Identification of an abscisic acid transporter by functional screening using the receptor complex as a sensor. Proceedings of the National Academy of Sciences of the United States of America **109:** 9653-9658

Kiba T, Feria-Bourrellier AB, Lafouge F, Lezhneva L, Boutet-Mercey S, Orsel M, Brehaut V, Miller A, Daniel-Vedele F, Sakakibara H, Krapp A (2012) The Arabidopsis nitrate transporter NRT2.4 plays a double role in roots and shoots of nitrogen-starved plants. The Plant Cell **24:** 245-258

Kichey T, Hirel B, Heumez E, Dubois Fdr, Le Gouis J (2007) In winter wheat (Triticum aestivum L.), post-anthesis nitrogen uptake and remobilisation to the grain correlates with agronomic traits and nitrogen physiological markers. Field Crops Research **102:** 22-32

Kiefer F, Arnold K, Künzli M, Bordoli L, Schwede T (2009) The SWISS-MODEL Repository and associated resources. Nucleic Acids Research **37:** D387-D392

Kotur Z, Mackenzie N, Ramesh S, Tyerman SD, Kaiser BN, Glass ADM (2012) Nitrate transport capacity of the Arabidopsis thaliana NRT2 family members and their interactions with AtNAR2.1. New Phytologist **194:** 724-731

Krapp A, David LC, Chardin C, Girin T, Marmagne A, Leprince A-S, Chaillou S, Ferrario-Méry S, Meyer C, Daniel-Vedele F (2014) Nitrate transport and signalling in Arabidopsis. Journal of Experimental Botany **65:** 789-798

Krouk G, Lacombe B, Bielach A, Perrine-Walker F, Malinska K, Mounier E, Hoyerova K, Tillard P, Leon S, Ljung K, Zazimalova E, Benkova E, Nacry P, Gojon A (2010) Nitrate-Regulated Auxin Transport by NRT1.1 Defines a Mechanism for Nutrient Sensing in Plants. Developmental Cell **18:** 927-937

Kucera B, Cohn MA, Leubner-Metzger G (2005) Plant hormone interactions during seed dormancy release and germination. Seed Science Research **15:** 281-307

Léran S, Forde B, Gassmann W, Geiger D, Gojon A, Gong J-M, Halkier BA, Harris JM, Hedrich R, Limami AM, Rentsch D, Varala K, Seo M, Tsay Y-F, Zhang M, Coruzzi G, Lacombe B, Boyer J-C, Chiurazzi M, Crawford N, Daniel-Vedele F, David L, Dickstein R, Fernandez E (2014) A unified nomenclature of NITRATE TRANSPORTER 1/PEPTIDE TRANSPORTER family members in plants. Trends in Plant Science **19:** 5-9

Léran S, Garg B, Boursiac Y, Corratgé-Faillie C, Brachet C, Tillard P, Gojon A, Lacombe B (2015) AtNPF5.5, a nitrate transporter affecting nitrogen accumulation in Arabidopsis embryo. Scientific reports **5:** 7962

Li J-F, Li L, Sheen J (2010) Protocol: a rapid and economical procedure for purification of plasmid or plant DNA with diverse applications in plant biology. Plant Methods **6:** 1

Li J-Y, Fu Y-L, Pike SM, Bao J, Tian W, Zhang Y, Chen C-Z, Zhang Y, Li H-M, Huang J, Li L-G, Schroeder JI, Gassmann W, Gong J-M (2010) The Arabidopsis nitrate transporter NRT1.8 functions in nitrate removal from the xylem sap and mediates cadmium tolerance. The Plant Cell **22:** 1633-1646

Li W, Wang Y, Okamoto M, Crawford NM, Siddiqi MY, Glass ADM (2007) Dissection of the AtNRT2.1:AtNRT2.2 inducible high-affinity nitrate transporter gene cluster. Plant Physiology **143:** 425-433

Liang Z, Zhang K, Chen K, Gao C (2014) Targeted mutagenesis in Zea mays using TALENs and the CRISPR/Cas system. Journal of Genetics and Genomics **41:** 63-68

Liman ER, Tytgat J, Hess P (1992) Subunit stoichiometry of a mammalian K + channel determined by construction of multimeric cDNAs. Neuron **9:** 861-871

Lin S-H, Kuo H-F, Canivenc Gv, Lin C-S, Lepetit M, Hsu P-K, Tillard P, Lin H-L, Wang Y-Y, Tsai C-B, Gojon A, Tsay Y-F (2008) Mutation of the Arabidopsis NRT1.5 nitrate transporter causes defective root-to-shoot nitrate transport. The Plant Cell **20:** 2514-2528

Little DY, Rao H, Oliva S, Daniel-Vedele F, Krapp A, Malamy JE, Haselkorn R (2005) The putative high-affinity nitrate transporter NRT2.1 represses lateral root initiation in response to nutritional cues. Proceedings of the National Academy of Sciences of the United States of America **102:** 13693-13698

Liu J, Han L, Chen F, Bao J, Zhang F, Mi G (2008) Microarray analysis reveals early responsive genes possibly involved in localized nitrate stimulation of lateral root development in maize (Zea mays L.). Plant Science **175:** 272-282

Liu K-H (2003) Switching between the two action modes of the dual-affinity nitrate transporter CHL1 by phosphorylation. The EMBO Journal **22:** 1005-1013

Liu KH, Huang CY, Tsay YF (1999) CHL1 is a dual-affinity nitrate transporter of Arabidopsis involved in multiple phases of nitrate uptake. The Plant Cell **11:** 865-874

Martinoia E, Heck U, Wiemken A (1981) Vacuoles as storage compartments for nitrate in barley leaves. Nature **289:** 292-294

Matilla AJ, María del Carmen R-G, Matilla-Vázquez MA (2009) Seed dormancy and ABA signaling: The breakthrough goes on. Plant Signaling & Behavior **4:** 1035-1048

Miller AJ, Fan X, Orsel M, Smith SJ, Wells DM (2007) Nitrate transport and signalling. Journal of Experimental Botany **58:** 2297-2306

Miller AJ, Smith SJ (1996) Nitrate transport and compartmentation in cereal root cells. Journal of Experimental Botany **47:** 843-854

Miller AJ, Smith SJ (2008) Cytosolic nitrate ion homeostasis: Could it have a role in sensing nitrogen status? Annals of Botany **101:** 485-489

Molendijk AJ, Ruperti B, Singh MK, Dovzhenko A, Ditengou FA, Milia M, Westphal L, Rosahl S, Soellick T-R, Uhrig J, Weingarten L, Huber M, Palme K (2008) A cysteine-rich receptor-like kinase NCRK and a pathogen-induced protein kinase RBK1 are Rop GTPase interactors. The Plant Journal **53:** 909-923

Moose S, Below FE (2009) Biotechnology approaches to improving maize nitrogen use efficiency. *In* Biotechnology in Agriculture and Forestey, Vol 63. Springer Berlin Heidelberg, Berlin, Heidelberg, pp 65-77

Morère-Le Paven M-C, Frugier F, Legros C, Limami AM, Viau L, Hamon A, Vandecasteele C, Pellizzaro A, Bourdin C, Laffont C, Lapied B, Lepetit M (2011) Characterization of a dual-affinity nitrate transporter MtNRT1.3 in the model legume Medicago truncatula. Journal of Experimental Botany **62:** 5595-5605

Nazoa P, Vidmar JJ, Tranbarger TJ, Mouline K, Damiani I, Tillard P, Zhuo D, Glass ADM, Touraine B (2003) Regulation of the nitrate transporter gene AtNRT2.1 in Arabidopsis thaliana : responses to nitrate, amino acids and developmental stage. Plant Molecular Biology **52:** 689-703

Nolan C (2012) The dark knight rises. *In*,

Okamoto M, Kumar A, Li W, Wang Y, Siddiqi MY, Crawford NM, Glass ADM (2006) High-affinity nitrate transport in roots of Arabidopsis depends on expression of the NAR2-like gene AtNRT3.1. Plant Physiology **140:** 1036-1046

Orsel M, Chopin F, Leleu O, Smith SJ, Krapp A, Daniel-Vedele F, Miller AJ (2006) Characterization of a two-component high-affinity nitrate uptake system in Arabidopsis. Physiology and protein-protein interaction. Plant Physiology **142:** 1304-1317

Parker JL, Newstead S (2014) Molecular basis of nitrate uptake by the plant nitrate transporter NRT1.1. Nature **507:** 68-72

Pellizzaro A, Clochard T, Cukier C, Bourdin C, Juchaux M, Montrichard F, Thany S, Raymond V, Planchet E, Limami AM, Morère-Le Paven M-C (2014) The nitrate transporter MtNPF6.8 (MtNRT1.3) transports abscisic

acid and mediates nitrate regulation of primary root growth in Medicago truncatula. Plant Physiology **166:** 2152-2165

Plett D, Toubia J, Garnett T, Tester M, Kaiser BN, Baumann U (2010) Dichotomy in the NRT gene families of dicots and grass species. PLOS ONE **5:** e15289

Preuss CP, Huang CY, Tyerman SD (2011) Proton-coupled high-affinity phosphate transport revealed from heterologous characterization in Xenopus of barley-root plasma membrane transporter, HvPHT1;1. Plant, Cell & Environment **34:** 681-689

Provart N, Si Y, Li P, Patel R, Nelson T, Wang L, Reidel EJ, Sun Q, Brutnell TP, Myers CR, Gandotra N, Kebrom TH, Tausta SL, Ponnala L, Turgeon R, Liu P (2010) The developmental dynamics of the maize leaf transcriptome. Nature Genetics **42:** 1060-1067

Quaggiotti S, Ruperti B, Borsa P, Destro T, Malagoli M (2003) Expression of a putative high-affinity NO3- transporter and of an H+-ATPase in relation to whole plant nitrate transport physiology in two maize genotypes differently responsive to low nitrogen availability. Journal of Experimental Botany **54:** 1023-1031

Quesada A, Galván A, Fernández E (1994) Identification of nitrate transporter genes in Chlamydomonas reinhardtii. The Plant journal : for Cell and Molecular Biology **5:** 407-419

Ramos C (1996) Effect of agricultural practices on the nitrogen losses to the environment. Fertilizer Research **43:** 183-189

Remans T, Nacry P, Pervent M, Filleur S, Diatloff E, Mounier E, Tillard P, Forde BG, Gojon A (2006) The Arabidopsis NRT1.1 transporter participates in the signaling pathway triggering root colonization of nitrate-rich patches. Proceedings of the National Academy of Sciences of the United States of America **103:** 19206-19211

Remans T, Nacry P, Pervent M, Girin T, Tillard P, Lepetit M, Gojon A (2006) A central role for the nitrate transporter NRT2.1 in the integrated morphological and physiological responses of the root system to nitrogen limitation in Arabidopsis. Plant Physiology **140:** 909-921

Rossato L, Laine P, Ourry A (2001) Nitrogen storage and remobilization in Brassica napus L. during the growth cycle: nitrogen fluxes within the plant and changes in soluble protein patterns. Journal of Experimental Botany **52:** 1655-1663

Santi S, Locci G, Monte R, Pinton R, Varanini Z (2003) Induction of nitrate uptake in maize roots: expression of a putative high-affinity nitrate transporter and plasma membrane H+-ATPase isoforms. Journal of Experimental Botany **54:** 1851-1864

Scalise M, Pochini L, Giangregorio N, Tonazzi A, Indiveri C (2013) Proteoliposomes as tool for assaying membrane transporter functions and interactions with xenobiotics. Pharmaceutics **5:** 472-497

Schiltz S, Munier-Jolain N, Jeudy C, Burstin J, Salon C (2005) Dynamics of exogenous nitrogen partitioning and nitrogen remobilization from vegetative organs in pea revealed by 15N in vivo labeling throughout seed filling. Plant Physiology **137:** 1463-1473

Schneider B, Junge F, Shirokov VA, Durst F, Schwarz D, Dötsch V, Bernhard F (2010) Membrane protein expression in cell-free systems. Methods in Molecular Biology **601:** 165-186

Schroeder JI (1994) Heterologous expression and functional analysis of higher plant transport proteins in Xenopus oocytes. Methods **6:** 70-81

Segonzac C, Boyer J-C, Ipotesi E, Szponarski W, Tillard P, Touraine B, Sommerer N, Rossignol M, Gibrat R (2007) Nitrate efflux at the root plasma membrane: identification of an Arabidopsis excretion transporter. The Plant Cell **19:** 3760-3777

Sekhon RS, Lin H, Childs KL, Hansey CN, Robin Buell C, de Leon N, Kaeppler SM (2011) Genome‐wide atlas of transcription during maize development. The Plant Journal **66:** 553-563

Siddiqi MY, Glass ADM, Ruth TJ, Rufty TW (1990) Studies of the uptake of nitrate in barley: I. Kinetics of 13NO3− influx. Plant Physiology **93:** 1426-1432

Simpson RJ, Lambers H (1983) Nitrogen redistribution during grain growth in wheat (Triticum aestivum L.): IV. Development of a quantitative model of the translocation of nitrogen to the grain. Plant Physiology **71:** 7-14

Stulen I, Pere-Soba M, De Kok LJ, van der Eerden L (1998) Impact of gaseous nitrogen deposition on plant functioning. New Phytologist **139:** 61-70

Subramanian C, Woo J, Cai X, Xu X, Servick S, Johnson CH, Nebenführ A, Von Arnim AG (2006) A suite of tools and application notes for in vivo protein interaction assays using bioluminescence resonance energy transfer (BRET). The Plant Journal **48:** 138-152

Sun J, Bankston JR, Payandeh J, Hinds TR, Zagotta WN, Zheng N (2014) Crystal structure of the plant dual-affinity nitrate transporter NRT1.1. Nature **507:** 73-77

Tischner R, Kaiser W (2007) Nitrate assimilation in plants. *In* Biology of the Nitrogen Cycle. Elsevier, pp 283-301

Tong Y, Zhou JJ, Li Z, Miller AJ (2005) A two‐component high‐affinity nitrate uptake system in barley. The Plant Journal **41:** 442-450

Trevisan S, Borsa P, Botton A, Varotto S, Malagoli M, Ruperti B, Quaggiotti S (2008) Expression of two maize putative nitrate transporters in response to nitrate and sugar availability. Plant Biology **10:** 462-475

Tsay Y-F, Chiu C-C, Tsai C-B, Ho C-H, Hsu P-K (2007) Nitrate transporters and peptide transporters. FEBS Letters **581:** 2290-2300

Tsay Y-F, Schroeder JI, Feldmann KA, Crawford NM (1993) The herbicide sensitivity gene CHL1 of arabidopsis encodes a nitrate-inducible nitrate transporter. Cell **72:** 705-713

USDA (2012) Average U.S. farm prices of selected fertilizers. *In*,

Wang L, Czedik-Eysenberg A, Mertz RA, Si Y, Tohge T, Nunes-Nesi A, Arrivault S, Dedow LK, Bryant DW, Zhou W, Xu J, Weissmann S, Studer A, Li P, Zhang C, LaRue T, Shao Y, Ding Z, Sun Q, Patel RV, Turgeon R, Zhu X, Provart NJ, Mockler TC, Fernie AR, Stitt M, Liu P, Brutnell TP (2014) Comparative analyses of C4 and C3 photosynthesis in developing leaves of maize and rice. Nature Biotechnology **32:** 1158-1165

Wang Y-Y, Hsu P-K, Tsay Y-F (2012) Uptake, allocation and signaling of nitrate. Trends in Plant Science **17:** 624

Wang Y-Y, Tsay Y-F (2011) Arabidopsis nitrate transporter NRT1.9 is important in phloem nitrate transport. The Plant Cell **23:** 1945-1957

Wege S, Jossier M, Filleur S, Thomine S, Barbier‐Brygoo H, Gambale F, De Angeli A (2010) The proline 160 in the selectivity filter of the Arabidopsis NO3−/H+ exchanger AtCLCa is essential for nitrate accumulation in planta. The Plant Journal **63:** 861-869

White PJ, Broadley MR (2001) Chloride in Soils and its Uptake and Movement within the Plant: A Review. Annals of Botany **88:** 967-988

Winter D, Vinegar B, Nahal H, Ammar R, Wilson GV, Provart NJ (2007) An "Electronic Fluorescent Pictograph" browser for exploring and analyzing large-scale biological data sets. PLOS ONE **2:** e718

Wirth J, Chopin F, Santoni V, Viennois G, Tillard P, Krapp A, Lejay L, Daniel-Vedele F, Gojon A (2007) Regulation of root nitrate uptake at the NRT2.1 protein level in Arabidopsis thaliana. Journal of Biological Chemistry **282:** 23541-23552

Wu Y-Y, Moehle EA, Shukla VK, Urnov FD, DeKelver RC, Doyon Y, McCaskill D, Blakeslee B, Greenwalt SA, Zhang L, Choi VM, Hinkley SJ, Arnold NL, Rebar EJ, Rock JM, Butler HJ, Meng X, Gopalan S, Mitchell JC, Miller JC, Simpson MA, Zhifang G, Worden SE, Gregory PD, Katibah GE (2009) Precise genome modification in the crop species Zea mays using zinc-finger nucleases. Nature **459:** 437-441

Xiang D, Venglat P, Tibiche C, Yang H, Risseeuw E, Cao Y, Babic V, Cloutier M, Keller W, Wang E, Selvaraj G, Datla R (2011) Genome-wide analysis reveals gene expression and metabolic network dynamics during embryo development in Arabidopsis. Plant Physiology **156:** 346-356

Xu GH, Fan XR, Miller AJ (2012) Plant nitrogen assimilation and use efficiency. Annual Review of Plant Biology **63:** 153-182

Xu GH, Magen H, Tarchitzky J, Kafkafi U (2000) Advances in chloride nutrition of plants. Advances in Agronomy **68:** 97-150

Yan M, Fan X, Feng H, Miller AJ, Shen Q, Xu G (2011) Rice OsNAR2.1 interacts with OsNRT2.1, OsNRT2.2 and OsNRT2.3a nitrate transporters to provide uptake over high and low concentration ranges. Plant, Cell & Environment **34:** 1360-1372

Yang Y, Hammes UZ, Taylor CG, Schachtman DP, Nielsen E (2006) High-affinity auxin transport by the AUX1 influx carrier protein. Current Biology **16:** 1123-1127

Zhou J-J, Theodoulou FL, Muldin I, Ingemarsson Br, Miller AJ (1998) Cloning and functional characterization of a Brassica napus transporter that is able to transport nitrate and histidine. Journal of Biological Chemistry **273:** 12017-12023

Zhou J-J, Trueman LJ, Boorer KJ, Theodoulou FL, Forde BG, Miller AJ (2000) A high affinity fungal nitrate carrier with two transport mechanisms. Journal of Biological Chemistry **275:** 39894-39899

Zhou JJ, Fernandez E, Galvan A, Miller AJ (2000) A high affinity nitrate transport system from Chlamydomonas requires two gene products. FEBS Letters **466:** 225-227